Physik-Department
Technische Universität München
Institut für Theoretische Physik
Lehrstuhl Univ.-Prof. Dr. Andrzej J. Buras

QCD and QED Anomalous Dimension Matrix for Weak Decays at NNLO

Martin Gorbahn

Technische Universität München
Physik-Department
James-Franck-Straße
85748 Garching
Germany
Email: mgorbahn@ph.tum.de

Physik-Department
Technische Universität München
Institut für Theoretische Physik
Lehrstuhl Univ.-Prof. Dr. Andrzej J. Buras

QCD and QED Anomalous Dimension Matrix for Weak Decays at NNLO

Martin Gorbahn

Vollständiger Abdruck der von der Fakultät für Physik der Technischen Universität München zur Erlangung des akademischen Grades eines

Doktors der Naturwissenschaften (Dr. rer. nat.)

genehmigten Dissertation.

Vorsitzender:		Univ.-Prof. Dr. Stephan Paul
Prüfer der Dissertation:	1.	Univ.-Prof. Dr. Andrzej J. Buras
	2.	Univ.-Prof. Dr. Manfred Lindner

Die Dissertation wurde am 16.10.2003 bei der Technischen Universität München eingereicht und durch die Fakultät für Physik am 28.10.2003 angenommen.

Contents

Chapter 1

Introduction

The standard model is a renormalizable quantum gauge field theory which describes the electromagnetic, weak, and strong interactions of the known fundamental matter-building blocks of quarks and leptons. And it does it with extreme success. The electroweak sector of the standard model has been tested up to the quantum level in the Large Electron Positron Collider, the Stanford Linear Accelerator, and the Fermi National Accelerator Laboratory. Thus the gauge sector of the standard model is well tested and the spontaneous symmetry breaking via the Higgs mechanism is strongly favored.

In spite of its tremendous success the common belief is that the standard model is not the final answer. This is due to the persisting of many fundamental problems in high energy and astroparticle physics. So we do not understand why the light quarks and, which is maybe even more severe, why the neutrinos are so light compared to the weak scale, namely the scale associated with the breaking of the standard model gauge group. In addition we do not understand why the breaking scale of the standard model is many orders of magnitude smaller than the Planck scale, the scale where the gravitational coupling becomes strong. Furthermore our current description of physics will break down at the Planck scale when we can not anymore neglect the contribution of gravity, since up to now no renormalizable quantum field theory of gravity has been found.

Hence it is generally believed that there is new physics, even if we have not seen it yet. The standard model is then thought to be just an effective theory and deviations are expected to occur as suppressed higher dimensional operators. To find deviations of the standard model or to test new physics it is then a good strategy to study processes which are forbidden on the classical level of the standard model. Such processes would only be induced radiatively and new physics effects could give contributions of similar size. Flavour violating neutral interactions will induce processes of the above mentioned type.

While the gauge sector of the standard model has been tested precisely, the flavour sector has not reached this precision yet. The first generation of flavour precision experiments leave still relatively large uncertainties in the mixing parameters of the flavour sector. On the other hand, the standard model seems to consistently describe the flavor sector up to the measured precision, and we might have to wait for the second generation of hadronic machines to find deviations from the standard model.

To keep up with this increasing experimental precision, and thus to falsify the standard model or its extension, high precision is needed on the theoretical side, too. This thesis will be concerned with higher order corrections to weak B meson decays, where the B quantum number, associated with the b-quark, is changed by a unit of one.

The study of weak B decays lies at the heart of the flavor physics program. First, the B meson is, apart from the Υ, the heaviest bound state, and thus allows for rich phenomenology in its decays. Second, there is the possibility of large charge-parity (CP) violating asymmetries, since, contrary to K and D decays, the CP violating phase is not accompanied by a strong CKM suppressing parameter. Third, the heaviness of the b quark mass m_b compared to the typical hadron binding energy Λ_{QCD} allows for theoretical methods which take the hadronic uncertainties systematically into account.

The last feature facilitates the study of inclusive B decays like $B \to X_s\gamma$. Here the decay rate is the sum of the decays of a B meson into a photon and an hadronic state of strangeness -1. The heaviness of m_b implies that the total decay rate is well approximated by the partonic decay rate, while non-perturbative corrections can be added systematically.

The inclusive radiative B decay $B \to X_s\gamma$ places very important constraints on models of physics beyond the Standard Model (SM). The present experimental world average for the branching fraction is [1–5]

$$\mathrm{BR}(B \to X_s\gamma)_{\mathrm{exp}} = (3.34 \pm 0.38) \times 10^{-4}\,, \tag{1.1}$$

while the most recent SM prediction is [6, 7]

$$\mathrm{BR}(B \to X_s\gamma)_{\mathrm{th}} = (3.70 \pm 0.30) \times 10^{-4}\,. \tag{1.2}$$

The experimental error is rapidly approaching the level of accuracy of the theoretical prediction. The main limiting factor on the theoretical side resides in the perturbative QCD calculation and is related to the ambiguity in the definition of the charm quark mass in some two-loop diagrams containing the charm quark [6]. To improve significantly the present Next-to-Leading-Order (NLO) QCD calculation, one would need to include one more order in the strong coupling expansion, and compute at least the dominant NNLO effects: a very challenging enterprise, which seems to have already captured the imagination of some theorists [8].

The present calculation of the branching ratio of $B \to X_s\gamma$ consists of several parts that are worth recalling. Perturbative QCD effects play an important role, due to the presence of large logarithms $L = \ln(m_b/M_W)$, that can be resummed using the formalism of the operator product expansion and renormalization group techniques. The main components of the NLO calculation, which aims at resumming all the next-to-leading $O(\alpha_s^n L^{n-1})$ logarithms, have been established more than six years ago. They are *i*) the $O(\alpha_s)$ corrections to the relevant Wilson coefficients [9–13], *ii*) the $O(\alpha_s)$ matrix elements of the corresponding dimension-five and six operators [14–21], and *iii*) the $O(\alpha_s^2)$ Anomalous Dimension Matrix

(ADM) describing the mixing of physical dimension-five and six operators [22–26]. After the $O(\alpha_s)$ matrix elements of some suppressed operators have been computed last year [7], the NLO calculation is now formally complete. Higher order electroweak [27–31] and non-perturbative effects [32–37] amount to a few percent in the total rate and seem to be well under control.

Nearly all the ingredients of the NLO QCD calculation involve a considerable degree of technical sophistication and have been performed independently by at least two groups, sometimes using different methods. However, the most complex part of the whole enterprise, the calculation of the two-loop dimension-five [25] and of the three-loop dimension-six [26] $O(\alpha_s^2)$ ADM, has never been checked by a different group. One of the main results of this thesis is to present an independent calculation of the $O(\alpha_s^2)$ ADM governing the $b \to s\gamma$ and $b \to sg$ transitions. In addition we will make a first step to the calculation of the complete $O(\alpha_s^3)$ ADM relevant for a complete Next-to-Next-to-Leading-Order (NNLO) QCD calculation by computing the three-loop self-mixing of the dimension-six operators.

The rare semileptonic decay $B \to X_s \ell^+\ell^-$ represents, for new physics searches, a route complementary to the radiative ones. The rare semileptonic transitions $b \to s\ell^+\ell^-$ have been observed for the first time by Belle and BaBar in 2001-2002 in the exclusive mode $B \to K\ell^+\ell^-$ [38, 39], and we now also have a measurement of the inclusive branching fraction [40,41]. A precise measurement of the inclusive channel $B \to X_s\ell^+\ell^-$ is particularly relevant because it is amenable to a clean theoretical description, especially in the region of low leptonic invariant mass, $m_{\ell\ell}^2 = m_b^2\,\hat{s}$, below the charm resonances, $0.05 \leq \hat{s} \leq 0.25$.

Because of the presence of large logarithms already at zeroth order in α_s, a precise calculation of the $B \to X_s\ell^+\ell^-$ rate involves the resummation of formally next-to-next-to-leading $O(\alpha_s^n L^{n-2})$ logarithms. The NNLO QCD calculation of $B \to X_s\ell^+\ell^-$ has required the computation of *i*) the $O(\alpha_s)$ corrections to the corresponding Wilson coefficients [13] and *ii*) the associated matrix elements at $O(\alpha_s)$ [42–45]. Moreover, it involves *iii*) the $O(\alpha_s^2)$ ADM, but the operator basis must be enlarged to include the semileptonic operators characteristic of the $b \to s\ell^+\ell^-$ transition. The only potentially relevant NNLO terms still missing at low $\hat{s}$ have to do with the three-loop ADM of the operators in the low-energy effective Hamiltonian, and with the two-loop matrix element of one of them, $Q_9 = e^2/g_s^2\,\bar{s}_L\gamma_\mu b_L \sum_\ell \bar{\ell}\gamma^\mu\ell$.

On the other hand, electroweak effects in $b \to s\ell^+\ell^-$ have never been discussed in the literature. As shown in the case of radiative decays [27–31], they may be as important as the higher order QCD effects.

In this thesis we will *i*) calculate the relevant three-loop ADM [46, 47] and take advantage of existing calculations of $O(\alpha_s^2)$ corrections to semileptonic quark decays and thus complete the NNLO calculation for $B \to X_s\ell^+\ell^-$ *ii*) study the electroweak effects in this decay and calculating the dominant $O(\alpha)$ contributions to the running *iii*) update the SM prediction of the branching ratio.

We have so far emphasized the inclusive modes, as they are amenable to a cleaner theoretical description. However, one should not underestimate the importance of the exclusive B meson decays like $B \to K^*\gamma$ [48, 49], $B \to K^*\ell^+\ell^-$ [38, 39], $B \to \rho\gamma$ [48–51] and $B \to \rho\ell^+\ell^-$. A thorough study of the exclusive channels can yield useful additional information in testing the flavor sector of the SM. These processes have received a lot of theoretical interest in recent years and their accurate description will also benefit from a firm understanding of higher order perturbative corrections.

The ADM we have computed can also be used in analyses of new physics models, provided they do not introduce new operators with respect to the SM. This applies, for example, to the case of two Higgs doublet models [6,12,52–54], and to some supersymmetric scenarios with minimal flavor violation, see for instance [54–58]. On the other hand, in left-right-symmetric models [54,59,60] and in the general minimal supersymmetric SM [61], additional operators with different chirality structures arise. In many cases one can exploit the chiral invariance of QCD and use the same ADM, but in general an extended basis is required.

This work is organized as follows. In the first chapter we will concentrate on the foundations of effective field theory methods for weak decays. We will start with an introduction to the field theoretical concepts needed in such calculations, in particular we will concentrate on the renormalization of QCD and QED. Next the concept of effective field theory is introduced and the QCD and QED renormalization of the effective operators is discussed in detail. Having the renormalization constants at hand we can discuss the resummation of the large logarithms which arise in weak decays. We will derive the equation which governs a scheme change for a NNLO QCD calculation and hereby prove the scheme independence up to this order.

The methods how to calculate the three-loop operator mixing are discussed in the following chapter. We will discuss how the ultraviolet divergencies are extracted, and sketch how the calculation was implemented in a computer algebra code. Next the ADM is presented for our chosen operator basis. We then show how to transform the results to different bases, in particular to the one used in [22, 23].

In the final chapter we will apply our calculated results. As a simple application we will compute the magic numbers needed for a NNLO analysis of non-leptonic B decays. In the next section the ingredients for a complete NLO QCD calculation of $B \to X_s\gamma$ are collected and a final formula is given. The relevant NNLO contributions to $B \to X_s\ell^+\ell^-$ are collected in the next section, together with the dominating $O(\alpha)$ electroweak effects.

Chapter 2

Foundations

2.1 Field Theories

Our current description of the physics of elementary particles is based on the concepts of quantum field theories. These theories consistently incorporate both special relativity and quantum mechanics. Furthermore it is commonly thought that any theory which incorporates the two above mentioned principles will at low energy have the form of a quantum field theory [62]. The standard model, which gives our current description of the phenomena of elementary particles, is the current milestone which has passed many tests of theory and experiment.

It is clear that we cannot summarize the whole development here. Instead we would like to give a brief introduction to the aspects relevant to our work. In particular we would like to focus on quantum chromodynamics (QCD).

All theories which describe the fundamental interactions can be given in terms of a Lagrangian density. For scalar fields it reads

$$\mathcal{L} = \mathcal{L}\left(\phi_i(x), \partial_\mu \phi_i(x), x\right) \,, \tag{2.1}$$

where the ϕ_i are the field operators. The total action is defined by the integral:

$$S\left(\phi_i\right) = \int d^4x \mathcal{L}\left(\phi_i(x), \partial_\mu \phi_i(x), x\right). \tag{2.2}$$

The correlation of field operators of Green's function

$$G_n(x_1, \ldots, x_n) = \langle 0|T\phi(x_1)\cdots\phi(x_n)|0\rangle \tag{2.3}$$

can be computed in terms of the functional integral

$$G_n(x_1, \ldots, x_n) = N^{-1} \int (d\phi) e^{iS(\phi)} \phi(x_i) \ldots \phi(x_j), \tag{2.4}$$

where the normalization factor is:

$$N = \int (d\phi) e^{iS(\phi)}. \tag{2.5}$$

The $\phi(x)$ on the right hand side of the equation represents the classical field. The integration is over the value of $\phi(x)$ at every space-time point.

2.1.1 Gauge Theories

Gauge theories are defined as theories which are locally invariant under a particular gauge symmetry. The local symmetry transformation has the form of a Lie group transformation. Thus the gauge theory may be thought of as a direct product of space time and a Lie group.

In the case of QCD the gauge group is the group of special unitary 3 by 3 matrices, namely $SU(3)$. The quarks are in the fundamental representation and the action of the group is:

$$\psi_i(x) \to \psi_i'(x) = U_{ij}(x)\psi_j(x), \qquad U_{ij} = e^{-iT^a\delta^a(x)}. \tag{2.6}$$

The T^a are the 8 generators of the Lie group in the fundamental representation. They span the corresponding Lie algebra and fulfill the following commutation relations:

$$\left[T^a, T^b\right] = f^{abc}T^c \,. \tag{2.7}$$

The f^{abc} are called structure constants and form the Lie algebra of the adjoint representation.

In gauge theories the partial derivative has to be replaced by the covariant derivative

$$\partial_\mu \psi_i \to D_{\mu ij}\psi_j = \left(\partial_\mu \delta_{ij} + igT^a_{ij}G^a_\mu\right)\psi_j \tag{2.8}$$

to retain the gauge symmetry. Hereby the gluon field G^a_μ comes naturally into play and the interaction with the quark is given by the gauge invariant Fermionic part of the QCD Lagrangian:

$$\mathcal{L}_{\text{fermi}} = \psi_i \left(i\not{D}_{ij} - m\delta_{ij}\right)\psi_j \,. \tag{2.9}$$

Here m is the quark mass.

The contribution of the gauge field to the QCD Lagrangian

$$\mathcal{L}_{\text{gauge}} = -\frac{1}{4}G^a_{\mu\nu}G^{a\mu\nu} \tag{2.10}$$

is given in terms of the gluon field strength tensor

$$G^a_{\mu\nu} = \partial_\mu G^a_\nu - \partial_\nu G^a_\mu + gf^{abc}G^b_\mu G^c_\nu. \tag{2.11}$$

The total gauge invariant Lagrangian for one quark field is thus given by:

$$\mathcal{L}_{\text{inv}} = \mathcal{L}_{\text{fermi}} + \mathcal{L}_{\text{gauge}} \,. \tag{2.12}$$

2.1.2 Quantization of Gauge Fields

In the case of gauge theories the functional integral (2.4) includes an infinite amount of field configurations which are related by gauge invariance to one another. Furthermore the gauge variant two-point correlation function vanishes, which would be disasterous for formulating perturbation theory, if we sum over all gauge configurations. To avoid this overcounting a particular gauge configuration can be chosen. This has been done in the functional formalism by Faddeev and Popov [63].

We would like to sketch the idea of the Faddeev-Popov quantization. First we choose the gauge condition to be of the form $F_a(G, x) = f_a(x)$ and consider the Green's function of a gauge invariant operator. In this case the functional integral of Eq. (2.4) would give the same result for any particular gauge configuration. Hence we write

$$\langle 0|TX|0\rangle = N_{\text{gauge}}^{-1} \int (dG)(d\psi)(d\bar{\psi})Xe^{iS_{inv}}\Delta(G)\prod_{x,a}\delta(F_a(x)-f_a(x)), \tag{2.13}$$

where the integral of all gauge transformations is separated from the integral of the gauge configuration which satisfies the given gauge condition. Thus the normalization is given by:

$$N_{\text{gauge}} = \int (dG)(d\psi)(d\bar{\psi})e^{iS_{inv}}\Delta(G)\prod_{x,a}\delta(F_a(x)-f_a(x)). \tag{2.14}$$

The factor $\Delta(G)$ is a Jacobian that arises in transforming the fields to the one which satisfies the gauge transformation times the set of gauge transformations. It is a determinant and can be written as the integral

$$\Delta(G) = \int d\eta^a d\bar{\eta}^a e^{i\mathcal{L}_{\text{gauge}-\text{compensating}}} \tag{2.15}$$

over anticommuting scalar fields η and $\bar{\eta}$, the Faddeev-Popov ghosts.

In the case where $F_a = \partial_\mu G^{a\mu}$ the gauge-compensating Lagrangian is up to a divergence

$$\mathcal{L}_{\text{ghost}} = \partial_\mu\bar{\eta}^a\left(\partial^\mu\eta_a + gf_{abc}\eta_b G^{c\mu}\right), \tag{2.16}$$

while the gauge-fixing part is

$$\mathcal{L}_{\text{gauge}-\text{fixing}} = -\frac{1}{2\xi}\left(\partial_\mu G^{a\mu}\right)^2/,. \tag{2.17}$$

The complete QCD Lagrangian for one quark is then given by:

$$\mathcal{L}_{\text{QCD}} = \mathcal{L}_{\text{inv}} + \mathcal{L}_{\text{ghost}} + \mathcal{L}_{\text{gauge}-\text{fixing}}. \tag{2.18}$$

This definition leaves gauge-invariant Green's functions invariant, while gauge variant Green's functions will give different results, and in particular might depend on the gauge-fixing parameter ξ. This last feature makes the Faddeev-Popov quantization so important in perturbation theory, because the two point correlation function does not vanish anymore if we use the Lagrangian (2.18).

2.1.3 Renormalization

It is well known that in the calculation of Green's function divergencies do arise. These divergencies can be regularized by discretizing the action, this is by evaluating the functional integral (2.4) on a lattice. The divergencies will now occur in the limit when the lattice spacing $a \to 0$ goes to zero.

Basic Idea of Renormalization and Regularization

The basic idea of renormalization is to reabsorb the divergencies, which occur in the limit of a vanishing regulator, in a redefinition of the action. For example the Fermionic Lagrangian[1] (2.9)

$$\mathcal{L}^{(0)}_{\text{kineticfermi}} = i\bar{\psi}_{0i}\left(\not{\partial}\,\delta_{ij} + g_0 T^a_{ij}\not{G}^a_0\right)\psi_{0j} - m_0\bar{\psi}_{0i}\psi_{0i} \tag{2.19}$$

is written in terms of the unrenormalized or bare fields ψ_0, G_0 and masses and couplings m_0, g_0. These unrenormalized parameters have an explicit regulator dependence, being chosen such that the resulting Green functions are finite.

If we reexpress the bare Lagrangian (2.19) in terms of renormalized fields, masses and couplings by defining

$$\psi_0 = Z_\psi^{(1/2)}\psi, \qquad m_0 = Z_m m, \qquad G_0 = Z_G^{(1/2)}G, \qquad g_0 = Z_g g \tag{2.20}$$

we can split the resulting Lagrangian

$$\mathcal{L}_{\text{kineticfermi}} = Z_\psi\bar{\psi}_i i\not{\partial}\,\psi_i + Z_g Z_G Z_\psi \psi_i i g T^a_{ij}\not{G}^a\psi_j - Z_\psi Z_m m\bar{\psi}_i\psi_i \tag{2.21}$$

in a sum of one that resembles the bare Lagrangian, except that the bare parameters are now replaced by the renormalized ones, and a counterterm Lagrangian

$$\begin{aligned}\mathcal{L}_{\text{fermi}} &= i\bar{\psi}_i\left(\not{\partial}\,\delta_{ij} + gT^a_{ij}\not{G}^a\right)\psi_j - m\bar{\psi}_i\psi_i \\ &+ (Z_\psi - 1)\,\bar{\psi}_i i\not{\partial}\,\psi_i + (Z_g Z_G Z_\psi - 1)\, i g\psi_i T^a_{ij}\not{G}^a\psi_j \\ &- (Z_\psi Z_m - 1)\, m\bar{\psi}_i\psi_i\,.\end{aligned} \tag{2.22}$$

The last form is particularly well suited for the use of perturbation theory. The $\bar{\psi}\,(i\not{\partial} - m)\,\psi$ part is treated as the free Lagrangian, while $\psi_i T^a_{ij}\not{G}^a\psi_j$ and the counterterms are treated as interactions. The Z factors will hereby be expanded in powers of the coupling constant g.

Perturbation theory and Renormalization

Yet the use of a lattice as a regulator of our theory is impractical if we want to apply perturbation theory. Symmetries like translation and Lorentz invariance are violated using this regulator. The standard regularization method for perturbative calculation is dimensional regularization, which we will exclusively use in this work.

In perturbation theory the short distance divergencies arise in form of integrals over loop momenta. For example there are linear divergent integrals in four dimensional space time, which would be finite in a two dimensional theory. The idea of dimensional regularization is to perform the integration in d dimensions. The integrals are analytic in d and the

[1] The actual implementation of Fermions on a lattice leads to many difficulties, like the Fermion doubling problem.

original divergencies are rediscovered for $d \to 4$. The pole of the integral can be expanded in a Laurent series using the parameter

$$\epsilon = \frac{4-d}{2}. \tag{2.23}$$

As the unrenormalized Lagrangian is now defined in d dimensions the unrenormalized coupling constant becomes a dimensionfull parameter. By keeping the renormalized coupling constant dimensionless a scale μ appears:

$$g_0 = Z_g g \mu^\epsilon. \tag{2.24}$$

Renormalizing the QCDxQED Lagrangian

In this work we are concerned with the calculation of QCD and QED corrections to weak decays. The Lagrangian for a massive quark of electromagnetic charge Q_ψ reads:

$$\begin{aligned}
\mathcal{L}_{\mathrm{QCD}\times\mathrm{QED}} = & \bar{\psi}_{0i}\left(i\partial\!\!\!/ - m_0\right)\psi_{0i} + g_0\bar{\psi}_{0i}T^a_{ij}G\!\!\!/^a_0\psi_{0j} + g_0\bar{\psi}_{0i}Q_\psi A\!\!\!/_0\psi_{0i} \\
& -\frac{1}{4}\left(\partial_\mu G^a_{0\nu} - \partial_\nu G^a_{0\mu}\right)\left(\partial^\mu G^{a\nu}_0 - \partial_\nu G^{a\mu}_0\right) - \frac{1}{2\xi_0}\left(\partial^\mu G^a_{0\mu}\right)^2 \\
& -\frac{1}{4}\left(\partial_\mu A_{0\nu} - \partial_\nu A_{0\mu}\right)\left(\partial^\mu A^\nu_0 - \partial_\nu A^\mu_0\right) - \frac{1}{2\xi_{A0}}\left(\partial^\mu A_{0\mu}\right)^2 \\
& -\frac{g}{2}f^{abc}\left(\partial_\mu G^a_{0\nu} - \partial_\nu G^a_{0\mu}\right)G^{b\mu}_0 G^{c\nu}_0 - \frac{g^2}{4}f^{abe}f^{cde}G^a_{0\mu}G^b_{0\nu}G^{c\mu}_0 G^{d\nu}_0 \\
& +\bar{\eta}^a_0\partial^\mu\partial_\mu\eta^a_0 + gf^{abc}\left(\partial^\mu\bar{\eta}^a\right)\eta^b G^c_{0\mu}.
\end{aligned} \tag{2.25}$$

Here A denotes the photon, the gauge field associated with the $U(1)$ symmetry. The ghost fields associated with the $U(1)$ gauge field fixing decouples from the theory.

The renormalization of this QCD×QED Lagrangian containing a massive quark proceeds as usual. First, we introduce the renormalized fields and variables via

$$\begin{aligned}
G^a_{\mu,0} &= Z_G^{1/2}G^a_\mu\,, & \eta^a_0 &= Z_\eta^{1/2}\eta^a\,, & \psi_0 &= Z_\psi^{1/2}\psi\,, \\
g_0 &= Z_g g\,, & m_0 &= Z_{m_b}m\,, & \xi_0 &= \xi\,, \\
A_{\mu,0} &= Z_A^{1/2}A_\mu\,, & e_0 &= Z_e e\,, & \xi_{A0} &= \xi_A\,.
\end{aligned} \tag{2.26}$$

The gauge-parameters ξ and ξ_A are kept unrenormalized. This is legitimate, because the non-renormalization of the gauge-parameter is guaranteed by the usual Slavnov-Taylor identity. In the calculation of the renormalization constants we use an expansion in external momenta. Such an expansion will in general produce spurious infrared (IR) divergencies. The above mentioned Slavnov-Taylor identity is unaffected by the IR regularization adopted for the Yang-Mills theory. On the other hand the IR rearrangement we apply in our calculation requires the introduction of the gauge-variant subtraction

$$(Z_M - 1)Z_G G^a_\mu G^{a\mu}, \tag{2.27}$$

which can be interpreted as a counterterm for a fictitious gluon mass M.

The renormalization constants Z can be expanded in powers of the electromagnetic and strong coupling constant

$$\begin{aligned} Z &= 1 + \sum_{j=1}^{\infty}\sum_{k=1}^{\infty}\left(\frac{g}{4\pi}\right)^{2k}\left(\frac{e}{4\pi}\right)^{2j} Z^{(k|j)} \\ &= 1 + \sum_{k=1}^{\infty}\left(\frac{g}{4\pi}\right)^{2k} Z^{(k)} + \left(\frac{e}{4\pi}\right)^{2} Z^{(e)} + \left(\frac{e}{4\pi}\right)^{2}\left(\frac{g}{4\pi}\right)^{2} Z^{(es)} + \dots , \end{aligned} \tag{2.28}$$

where we only keep e^2 and e^2g^2 contributions in the electricmagnetic coupling constant. One can further expand the Z factors in their ϵ poles:

$$\begin{aligned} Z^{(k)} &= \sum_{l=0}^{k}\frac{1}{\epsilon^l}Z^{(k,l)} \qquad Z^{(e)} = \frac{1}{\epsilon}Z^{(e,1)} \\ Z^{(es)} &= \frac{1}{\epsilon}Z^{(es,1)} + \frac{1}{\epsilon^2}Z^{(es,2)} . \end{aligned} \tag{2.29}$$

There is some arbitrariness in the definition of the Z factors. This is be fixed by the choice of a renormalization scheme. For example in minimal subtraction scheme or MS scheme only the pole parts are subtracted. Another useful scheme is the modified minimal subtraction or $\overline{\mathrm{MS}}$ scheme [64]. Here the parameter μ is redefined

$$\mu \to \mu\left(\frac{e^{\gamma_E}}{4\pi}\right)^{(1/2)} . \tag{2.30}$$

before the minimal subtraction is performed. Using the above notation, the $\overline{\mathrm{MS}}$ renormalization constants at one-loop order take the following form

$$\begin{aligned} Z_G^{(1,1)} &= \left(\frac{13}{6} - \frac{1}{2}\xi\right) C_A - \frac{2}{3}N_f , \\ Z_u^{(1,1)} &= \left(\frac{3}{4} - \frac{1}{4}\xi\right) C_A , \\ Z_q^{(1,1)} &= -\xi C_F , \\ Z_g^{(1,1)} &= -\frac{11}{6}C_A + \frac{1}{3}N_f , \\ Z_{m_b}^{(1,1)} &= -3C_F , \\ Z_M^{(1,1)} &= \left(-\frac{29}{24} - \frac{1}{8}\xi\right) C_A - \frac{2}{3}N_f , \end{aligned} \tag{2.31}$$

where $C_A = 3$ and $C_F = 4/3$ are the quadratic Casimir operators of $SU(3)$. As usual N_f stands for the number of active quark flavours. Our result for $Z_M^{(1,1)}$ agrees with the expression given in [65].

At the two-loop level the poles of the $\overline{\mathrm{MS}}$ renormalization constants are given by

$$
\begin{aligned}
Z_G^{(2,1)} &= \left(\frac{59}{16} - \frac{11}{16}\xi - \frac{1}{8}\xi^2\right) C_A^2 - C_F N_f - \frac{5}{4} C_A N_f \,, \\
Z_u^{(2,1)} &= \left(\frac{95}{96} + \frac{1}{32}\xi\right) C_A^2 - \frac{5}{24} C_A N_f \,, \\
Z_q^{(2,1)} &= \frac{3}{4} C_F^2 - \left(\frac{25}{8} + \xi + \frac{1}{8}\xi^2\right) C_F C_A + \frac{1}{2} C_F N_f \,, \\
Z_g^{(2,1)} &= -\frac{17}{6} C_A^2 + \frac{1}{2} C_F N_f + \frac{5}{6} C_A N_f \,, \\
Z_{m_b}^{(2,1)} &= -\frac{3}{4} C_F^2 - \frac{97}{12} C_F C_A + \frac{5}{6} C_F N_f \,, \\
Z_M^{(2,1)} &= \left(-\frac{383}{192} - \frac{7}{64}\xi - \frac{3}{32}\xi^2\right) C_A^2 + \left(\frac{1}{2} + \frac{1}{4}\xi\right) C_F N_f + \left(\frac{5}{12} - \frac{5}{16}\xi\right) C_A N_f \,,
\end{aligned} \tag{2.32}
$$

and

$$
\begin{aligned}
Z_G^{(2,2)} &= \left(-\frac{13}{8} - \frac{17}{24}\xi + \frac{3}{16}\xi^2\right) C_A^2 + \left(\frac{1}{2} + \frac{1}{3}\xi\right) C_A N_f \,, \\
Z_u^{(2,2)} &= \left(-\frac{35}{32} + \frac{3}{32}\xi^2\right) C_A^2 + \frac{1}{4} C_A N_f \,, \\
Z_q^{(2,2)} &= \frac{1}{2}\xi^2 C_F^2 + \left(\frac{3}{4}\xi + \frac{1}{4}\xi^2\right) C_F C_A \,, \\
Z_g^{(2,2)} &= \frac{121}{24} C_A^2 - \frac{11}{6} C_A N_f + \frac{1}{6} N_f^2 \,, \\
Z_{m_b}^{(2,2)} &= \frac{9}{2} C_F^2 + \frac{11}{2} C_F C_A - C_F N_f \,, \\
Z_M^{(2,2)} &= \left(\frac{1211}{384} + \frac{59}{192}\xi + \frac{5}{128}\xi^2\right) C_A^2 - \frac{1}{2}\xi C_F N_f + \left(\frac{7}{12} - \frac{1}{24}\xi\right) C_A N_f - \frac{2}{3} N_f^2 \,.
\end{aligned} \tag{2.33}
$$

Except for $Z_M^{(2,1)}$ and $Z_M^{(2,2)}$, which have never been given explicitly, our renormalization constants agree with the results in the literature [66], if one bears in mind that the original papers contain some typing errors. We have also calculated the three-loop renormalization constants [67–70], but we do not report them here, as they are not needed in our calculation.

2.1.4 Renormalization Group Equation

The splitting of the unrenormalized Lagrangian in the free, the interacting, and the counterterm Lagrangian introduces an arbitrariness in the definition of the renormalized parameters. The counterterm has to cancel the divergencies of a graph, but a finite subtraction is still possible. Such a finite renormalization would be a change in renormalization prescription. For example a finite change of m and g in (2.22) can be absorbed in a redefinition of

Z_m and Z_g. The invariance of the theory under such finite renormalizations is traditionally called renormalization group.

A particularly useful change of the renormalization scheme is the one related to a redefinition of μ. For example the scheme change from MS to $\overline{\text{MS}}$ is just a change of μ by

$$\mu \to \mu \left(\frac{e^{\gamma_E}}{4\pi}\right)^{(1/2)} . \tag{2.34}$$

The infinitesimal change of μ will result in a change of the renormalized parameters, so that all resulting physical quantities are invariant. The equations which govern this change of the renormalized parameters are called renormalization group equations.

The differential equations are derived from Eq. (2.28). Here one uses the fact that the unrenormalized quantities are μ independent. For the coupling constant we find

$$\mu\frac{dg}{d\mu} = \beta\left(g(\mu), e(\mu), \epsilon\right), \qquad \mu\frac{de}{d\mu} = \beta_e\left(e(\mu), g(\mu), \epsilon\right), \tag{2.35}$$

where the β functions are given

$$\begin{aligned}
\beta\left(g(\mu), e(\mu), \epsilon\right) &= -\epsilon g - Z_g^{-1}\mu\left(\frac{d}{d\mu}Z_g\right)g \equiv -\epsilon g - \beta\left(g(\mu), e(\mu)\right) , \\
\beta_e\left(e(\mu), g(\mu), \epsilon\right) &= -\epsilon e - Z_e^{-1}\mu\left(\frac{d}{d\mu}Z_e\right)e \equiv -\epsilon e - \beta_e\left(e(\mu), g(\mu)\right) .
\end{aligned} \tag{2.36}$$

In an mass independent scheme like the $\overline{\text{MS}}$ scheme the only explicit mass dependence of the counterterms resides in the couplings. For the beta function of the strong coupling we can then write

$$\begin{aligned}
\beta(g, e) &= -\beta_0\frac{g^3}{(4\pi)^2} - \beta_1\frac{g^5}{(4\pi)^4} - \beta_2\frac{g^7}{(4\pi)^6} - \beta_{se}\frac{g^3e^2}{(4\pi)^4} + \ldots \\
&= 2Z_g^{(1,1)}\frac{g^3}{(4\pi)^2} + 4Z_g^{(2,1)}\frac{g^5}{(4\pi)^4} + 6Z_g^{(3,1)}\frac{g^7}{(4\pi)^6} + 4Z_g^{(es,1)}\frac{g^3e^2}{(4\pi)^4} + \ldots .
\end{aligned} \tag{2.37}$$

Using the same argument and Eq. (2.35) similar formulas can be derived for the anomalous dimensions, which govern the renormalization group evolution

$$\gamma_m = Z_m^{-1}\mu\left(\frac{d}{d\mu}Z_m\right), \qquad \gamma_\psi = Z_\psi^{-1}\mu\left(\frac{d}{d\mu}Z_\psi\right) \tag{2.38}$$

of the mass and the quark field.

2.2 Effective Field Theories

Weak decays are usually characterized by two different scales. In the case of B decays we have $M_W \gg m_b$. In this context large logarithms occur, which will render a straightforward perturbative calculation unreliable. In effective field theories the effects of the heavy particles can systematically be incorporated in a so-called matching calculation. The large logarithms can then be resummed using renormalization group equations for the effective theory.

The Appelquist-Carrazone decoupling theorem [71] lies at the heart of the effective field theories. It states that in many classes of theories the contribution of heavy particles to Green's functions can be absorbed into the renormalization constants of a Lagrangian which consists only out of light fields. Corrections are smaller by a power of momenta divided by a heavy mass.

If we work with a mass independent scheme like the $\overline{\text{MS}}$ scheme we have to put the decoupling theorem by hand in effective field theory [72, 73]. This is done via matching of a high scale Lagrangian on a low scale one.

At high scales our theory is described by a Lagrangian, which contains a set of heavy χ and light ϕ fields. It can be split into a part, which contains only the light fields, and one that contains the rest:

$$\mathcal{L}_{\text{full}} = \mathcal{L}_H(\chi, \phi) + \mathcal{L}(\phi). \tag{2.39}$$

When we now go to a scale μ smaller than the the mass scale of the heavy fields our theory will be described by an effective Lagrangian

$$\mathcal{L}_{\text{eff}} = \mathcal{L}(\phi) + \delta\mathcal{L}(\phi) \tag{2.40}$$

in terms of the light fields. The matching corrections are encoded in the "correcting" Lagrangian $\delta\mathcal{L}(\phi)$ and can be calculated at the high scale $M_H \sim M_\chi$ using perturbation theory. This is done by requiring that all one light-particle irreducible graphs with external light particles are the same in the full and in the effective theory. The resulting contribution to the correction Lagrangian is analytic in p/M_χ in the region relevant for the low energy theory. Thus it can be expanded in terms of decreasing importance and matched on the low energy effective theory.

In the following we will calculate the renormalization group equations for the "correcting" Lagrangian. We will apply perturbation theory using the Lagrangian of the light fields $\mathcal{L}(\phi)$ and renormalize the composite operators of $\delta\mathcal{L}(\phi)$.

2.2.1 Effective Hamiltonian for $|\Delta B| = 1$ Decays

We want to apply this formalism to $|\Delta B| = 1$ decays. We work in the framework of an effective low-energy theory with five active quarks, three active leptons, photons and gluons, obtained by integrating out heavy degrees of freedom characterized by a mass scale

$M \geq M_W$. In the leading order of the weak coupling the effective off-shell Lagrangian relevant for the $b \to s\gamma$, $b \to sg$ and $b \to s\ell^+\ell^-$ transition at a scale μ is given by

$$\mathcal{L}_{\text{eff}} = \mathcal{L}_{\text{QCD}\times\text{QED}}(u, d, s, c, b, e, \mu, \tau) + \frac{4G_F}{\sqrt{2}} V_{ts}^* V_{tb} \sum_{i=1}^{32} C_i(\mu)\, Q_i \,. \tag{2.41}$$

Here the first term is the conventional QCD-QED Lagrangian[2] for the light SM particles. In the second term V_{ij} denotes the elements of the CKM matrix and $C_i(\mu)$ are the Wilson coefficients of the corresponding operators Q_i built out of the light fields.

In our case it is useful to divide the local operators Q_i entering the effective Lagrangian into five different classes: *i*) physical operators, *ii*) gauge-invariant operators that vanish by use of the QCD$\times$QED equations of motion (EOM), *iii*) gauge-variant EOM-vanishing operators, and *iv*) so-called evanescent operators that vanish algebraically in four dimensions. In principle, one could also encounter *v*) non-physical counterterms that can be written as a Becchi-Rouet-Stora-Tyutin (BRST) variation of some other operators, so-called BRST-exact operators. However, they turn out to be unnecessary in the case of the $O(\alpha_s^2)$ mixing of the operators Q_i considered below. See also [25].

Neglecting the mass of the strange quark, the physical operators [74–78] can consist out of the four quark operators, the magnetic moment type operators, and the semileptonic operators.

The four quark operators can be subclassifed into the current-current type operators

$$\begin{aligned} Q_1 &= (\bar{s}_L \gamma_\mu T^a c_L)(\bar{c}_L \gamma^\mu T^a b_L) \,, \\ Q_2 &= (\bar{s}_L \gamma_\mu c_L)(\bar{c}_L \gamma^\mu b_L) \,, \end{aligned} \tag{2.42}$$

where q_L and q_R are the chiral quark fields. Notice that, since QCD is flavour-blind and up and charm quarks have the same electromagnetic charge, it is not necessary for our purposes to consider the analogues of Q_1 and Q_2 involving the up instead of the charm quark. The QCD penguin operators are

$$\begin{aligned} Q_3 &= (\bar{s}_L \gamma_\mu b_L) \sum\nolimits_q (\bar{q} \gamma^\mu q) \,, \\ Q_4 &= (\bar{s}_L \gamma_\mu T^a b_L) \sum\nolimits_q (\bar{q} \gamma^\mu T^a q) \,, \\ Q_5 &= (\bar{s}_L \gamma_\mu \gamma_\nu \gamma_\rho b_L) \sum\nolimits_q (\bar{q} \gamma^\mu \gamma^\nu \gamma^\rho q) \,, \\ Q_6 &= (\bar{s}_L \gamma_\mu \gamma_\nu \gamma_\rho T^a b_L) \sum\nolimits_q (\bar{q} \gamma^\mu \gamma^\nu \gamma^\rho T^a q) \,, \end{aligned} \tag{2.43}$$

where the sum over q and ℓ extends over all light quark and lepton fields, respectively. The electroweak penguin operators arise first at $O(\alpha)$ and have to be taken into account

[2] In principle the QCD-QED Lagriangian will also recieve matching corrections at higher loop order. These can be avoided by using a physical renormalization scheme for say the gluon wavefunction renormalization [13]

if QED corrections are considered. They are

$$
\begin{aligned}
Q_3^Q &= (\bar{s}_L \gamma_\mu b_L) \sum\nolimits_q Q_q (\bar{q}\gamma^\mu q)\,, \\
Q_4^Q &= (\bar{s}_L \gamma_\mu T^a b_L) \sum\nolimits_q Q_q (\bar{q}\gamma^\mu T^a q)\,, \\
Q_5^Q &= (\bar{s}_L \gamma_\mu \gamma_\nu \gamma_\rho b_L) \sum\nolimits_q Q_q (\bar{q}\gamma^\mu \gamma^\nu \gamma^\rho q)\,, \\
Q_6^Q &= (\bar{s}_L \gamma_\mu \gamma_\nu \gamma_\rho T^a b_L) \sum\nolimits_q Q_q (\bar{q}\gamma^\mu \gamma^\nu \gamma^\rho T^a q)\,,
\end{aligned}
\tag{2.44}
$$

where Q_q is the electromagnetic charge of the quark q.

The magnetic moment type operators Q_7 and Q_8 are

$$
\begin{aligned}
Q_7 &= \frac{e}{g^2} m_b (\bar{s}_L \sigma^{\mu\nu} b_R) F_{\mu\nu}\,, \\
Q_8 &= \frac{1}{g} m_b (\bar{s}_L \sigma^{\mu\nu} T^a b_R) G^a_{\mu\nu}\,,
\end{aligned}
\tag{2.45}
$$

where e (g) is the electromagnetic (strong) coupling constant, $F_{\mu\nu}$ ($G^a_{\mu\nu}$) is the electromagnetic (gluonic) field strength tensor, and T^a are the colour matrices normalized so that $\mathrm{Tr}(T^a T^b) = \delta^{ab}/2$.

The semileptonic operators Q_9 and Q_{10}, relevant for the $b \to s\ell^+\ell^-$ transition are given by:

$$
\begin{aligned}
Q_9 &= \frac{e^2}{g^2} (\bar{s}_L \gamma_\mu b_L) \sum\nolimits_\ell (\bar{\ell}\gamma^\mu \ell)\,, \\
Q_{10} &= \frac{e^2}{g^2} (\bar{s}_L \gamma_\mu b_L) \sum\nolimits_\ell (\bar{\ell}\gamma^\mu \gamma_5 \ell)\,.
\end{aligned}
\tag{2.46}
$$

We have defined Q_1–Q_6 and Q_3^Q–Q_6^Q in such a way that problems connected with the treatment of γ_5 in $n = 4 - 2\epsilon$ dimensions do not arise [24]. Consequently, we are allowed to consistently use fully anticommuting γ_5 in dimensional regularization throughout the calculation.

The gauge-invariant EOM-vanishing operators can be chosen to be [12, 13]

$$\begin{aligned}
Q_{11} &= \frac{e}{g^2}\bar{s}_L\gamma^\mu b_L\partial^\nu F_{\mu\nu} + \frac{e^2}{g^2}(\bar{s}_L\gamma_\mu b_L)\sum\nolimits_f Q_f(\bar{f}\gamma^\mu f)\,,\\
Q_{12} &= \frac{1}{g}\bar{s}_L\gamma^\mu T^a b_L D^\nu G^a_{\mu\nu} + Q_4\,,\\
Q_{13} &= \frac{1}{g^2}m_b\bar{s}_L \not{D}\not{D} b_R\,,\\
Q_{14} &= \frac{i}{g^2}\bar{s}_L \not{D}\not{D}\not{D} b_L\,,\\
Q_{15} &= \frac{ie}{g^2}\left[\bar{s}_L \overleftarrow{\not{D}}\sigma^{\mu\nu}b_L F_{\mu\nu} - F_{\mu\nu}\bar{s}_L\sigma^{\mu\nu}\not{D}b_L\right] + Q_7\,,\\
Q_{16} &= \frac{i}{g}\left[\bar{s}_L \overleftarrow{\not{D}}\sigma^{\mu\nu}T^a b_L G^a_{\mu\nu} - G^a_{\mu\nu}\bar{s}_L T^a\sigma^{\mu\nu}\not{D}b_L\right] + Q_8\,,
\end{aligned} \tag{2.47}$$

where the sum over f runs over all light Fermion fields, while D_μ and $\overleftarrow{D}_\mu$ denotes the covariant derivative of the gauge group $SU(3)_C \times U(1)_Q$ acting on the fields to the right and left, respectively. Notice that the set of operators Q_1–Q_{16} closes off-shell under QCD renormalization, up to evanescent operators [13, 74–78]. In order to remove the divergences of all possible one-particle irreducible (1PI) Green's functions with single insertion of Q_1–Q_{10} we also have to introduce the following gauge-variant EOM-vanishing operators

$$\begin{aligned}
Q_{17} &= \frac{i}{g}m_b\bar{s}_L\left[\overleftarrow{\not{D}}\not{G} - \not{G}\not{D}\right]b_R\,,\\
Q_{18} &= i\left[\bar{s}_L\left(\overleftarrow{\not{D}}\not{G}\not{G} - \not{G}\not{G}\not{D}\right)b_L - im_b\bar{s}_L\not{G}\not{G}b_R\right]\,,\\
Q_{19} &= \frac{1}{g}\left[\bar{s}_L\left(\overleftarrow{\not{D}}\overleftarrow{\not{D}}\not{G} + \not{G}\not{D}\not{D}\right)b_L + im_b\bar{s}_L\not{G}\not{D}b_R\right]\,,\\
Q_{20} &= i\left[\bar{s}_L\left(\overleftarrow{\not{D}}G^a_\mu G^{a\mu} - G^a_\mu G^{a\mu}\not{D}\right)b_L - im_b\bar{s}_L G^a_\mu G^{a\mu}b_R\right]\,,\\
Q_{21} &= \frac{1}{g}\left[\bar{s}_L\left(\overleftarrow{\not{D}}\overleftarrow{D}_\mu G^\mu + G_\mu D^\mu\not{D}\right)b_L + im_b\bar{s}_L G_\mu D^\mu b_R\right]\,,\\
Q_{22} &= \frac{1}{g}\left[\bar{s}_L\left(\overleftarrow{\not{D}}T^a + T^a\not{D}\right)b_L + im_b\bar{s}_L T^a b_R\right]\partial^\mu G^a_\mu\,,\\
Q_{23} &= \frac{1}{g}\left[\bar{s}_L\overleftarrow{\not{D}}\not{G}\not{D}b_L + im_b\bar{s}_L\overleftarrow{\not{D}}\not{G}b_R\right]\,,\\
Q_{24} &= d^{abc}\left[\bar{s}_L\left(\overleftarrow{\not{D}}T^a - T^a\not{D}\right)b_L - im_b\bar{s}_L T^a b_R\right]G^b_\mu G^{c\mu}\,,
\end{aligned} \tag{2.48}$$

where G^a_μ denotes the gluon field, and we have used the abbreviations $G_\mu = G^a_\mu T^a$ and $d^{abc} = 2\mathrm{Tr}(\{T^a, T^b\}T^c)$.

In contrast to the case of the two-loop mixing of the magnetic operators considered in [25, 46], it is a priori not clear if BRST-exact operators do arise as counterterms of Q_1–Q_6 on the three-loop level. Since the BRST variation raises both ghost number and mass dimension by one unit, it is evident that any BRST-exact operator that potentially could mix with Q_1–Q_6 has to be a BRST variation of a dimension-five operator containing a single anti-ghost field. The only possibility for the latter operator having the correct chirality structure is given in the R_ξ gauge by [77]

$$\begin{aligned} B_1 &= s\left[\frac{1}{g}\left(\partial_{\mu_1}\bar{\eta}^a\right)\left(\bar{s}_L\gamma^{\mu_1}T^a b_L\right)\right] \\ &= -\frac{1}{g}\left[\frac{1}{\xi}\partial_{\mu_1}\partial^{\mu_2}G^a_{\mu_2} + gf^{abc}\left(\partial_{\mu_1}\bar{\eta}^b\right)\eta^c\right]\left(\bar{s}_L\gamma^{\mu_1}T^a b_L\right)\,, \end{aligned} \tag{2.49}$$

where s denotes the BRST operator.

It is important to remark that the EOM-vanishing operators introduced in Eqs. (2.47) and (2.48) arise as counterterms independently of what kind of IR regularization is adopted in the computation. However, if the regularization respects the underlying symmetry, and all the diagrams are calculated without expansion in the external momenta, non-physical operators have vanishing matrix elements [79, 80]. In this case the EOM-vanishing operators given in Eqs. (2.47) and (2.48) play no role in the calculation of the mixing of physical operators. If the gauge symmetry is broken, this is no longer the case, as diagrams with insertions of non-physical operators will generally have non-vanishing projection on the physical operators. Since our IR regularization implies a massive gluon propagator, non-physical counterterms play a crucial role at intermediate stages of the calculation.

2.2.2 Evanescent Operators

In order to remove the divergences of all possible 1PI Green's functions with single insertion of Q_1–Q_6 we have to introduce some evanescent operators $\vec{E}$ as well. At the one-loop level one encounters four evanescent operators, which can be chosen to be [24, 26]

$$\begin{aligned} E_1^{(1)} &= (\bar{s}_L\gamma_{\mu_1\mu_2\mu_3}T^a c_L)(\bar{c}_L\gamma^{\mu_1\mu_2\mu_3}T^a b_L) - 16Q_1\,, \\ E_2^{(1)} &= (\bar{s}_L\gamma_{\mu_1\mu_2\mu_3}c_L)(\bar{c}_L\gamma^{\mu_1\mu_2\mu_3}b_L) - 16Q_2\,, \\ E_3^{(1)} &= (\bar{s}_L\gamma_{\mu_1\mu_2\mu_3\mu_4\mu_5}b_L)\textstyle\sum_q(\bar{q}\gamma^{\mu_1\mu_2\mu_3\mu_4\mu_5}q) + 64Q_3 - 20Q_5\,, \\ E_4^{(1)} &= (\bar{s}_L\gamma_{\mu_1\mu_2\mu_3\mu_4\mu_5}T^a b_L)\textstyle\sum_q(\bar{q}\gamma^{\mu_1\mu_2\mu_3\mu_4\mu_5}T^a q) + 64Q_4 - 20Q_6\,, \end{aligned} \tag{2.50}$$

where we have used the abbreviations $\gamma_{\mu_1\cdots\mu_n} = \gamma_{\mu_1}\cdots\gamma_{\mu_n}$, $\gamma^{\mu_1\cdots\mu_n} = \gamma^{\mu_1}\cdots\gamma^{\mu_n}$. At the two-loop level four more evanescent operators arise that can be defined as [24, 26]

$$\begin{aligned}
E_1^{(2)} &= (\bar{s}_L\gamma_{\mu_1\mu_2\mu_3\mu_4\mu_5}T^a c_L)(\bar{c}_L\gamma^{\mu_1\mu_2\mu_3\mu_4\mu_5}T^a b_L) - 256Q_1 - 20E_1^{(1)}\,,\\
E_2^{(2)} &= (\bar{s}_L\gamma_{\mu_1\mu_2\mu_3\mu_4\mu_5}c_L)(\bar{c}_L\gamma^{\mu_1\mu_2\mu_3\mu_4\mu_5}b_L) - 256Q_2 - 20E_2^{(1)}\,,\\
E_3^{(2)} &= (\bar{s}_L\gamma_{\mu_1\mu_2\mu_3\mu_4\mu_5\mu_6\mu_7}b_L){\textstyle\sum_q}(\bar{q}\gamma^{\mu_1\mu_2\mu_3\mu_4\mu_5\mu_6\mu_7}q) + 1280Q_3 - 336Q_5\,,\\
E_4^{(2)} &= (\bar{s}_L\gamma_{\mu_1\mu_2\mu_3\mu_4\mu_5\mu_6\mu_7}T^a b_L){\textstyle\sum_q}(\bar{q}\gamma^{\mu_1\mu_2\mu_3\mu_4\mu_5\mu_6\mu_7}T^a q) + 1280Q_4 - 336Q_6\,.
\end{aligned} \tag{2.51}$$

Finally, at the three-loop level another four evanescent operators are needed. We define them in the following way:

$$\begin{aligned}
E_1^{(3)} &= (\bar{s}_L\gamma_{\mu_1\mu_2\mu_3\mu_4\mu_5\mu_6\mu_7}T^a c_L)(\bar{c}_L\gamma^{\mu_1\mu_2\mu_3\mu_4\mu_5\mu_6\mu_7}T^a b_L) - 4096Q_1 - 336E_1^{(1)}\,,\\
E_2^{(3)} &= (\bar{s}_L\gamma_{\mu_1\mu_2\mu_3\mu_4\mu_5\mu_6\mu_7}c_L)(\bar{c}_L\gamma^{\mu_1\mu_2\mu_3\mu_4\mu_5\mu_6\mu_7}b_L) - 4096Q_2 - 336E_2^{(1)}\,,\\
E_3^{(3)} &= (\bar{s}_L\gamma_{\mu_1\mu_2\mu_3\mu_4\mu_5\mu_6\mu_7\mu_8\mu_9}b_L){\textstyle\sum_q}(\bar{q}\gamma^{\mu_1\mu_2\mu_3\mu_4\mu_5\mu_6\mu_7\mu_8\mu_9}q) + 21504Q_3 - 5440Q_5\,,\\
E_4^{(3)} &= (\bar{s}_L\gamma_{\mu_1\mu_2\mu_3\mu_4\mu_5\mu_6\mu_7\mu_8\mu_9}T^a b_L){\textstyle\sum_q}(\bar{q}\gamma^{\mu_1\mu_2\mu_3\mu_4\mu_5\mu_6\mu_7\mu_8\mu_9}T^a q) + 21504Q_4 - 5440Q_6\,.
\end{aligned} \tag{2.52}$$

Needless to say that the above choice of evanescent operators $E_1^{(3)}$–$E_4^{(3)}$ is not unique, in the sense that their particular structure can be changed quite a lot without affecting the three-loop anomalous dimensions of the four-quark operators Q_1–Q_6. For instance, adding any multiple of ϵ times any physical operator to them, leaves the anomalous dimensions up to $O(\alpha_s^3)$ unchanged. This is contrary to what happens if such a redefinition is applied to the one- and two-loop evanescent operators as given in Eqs. (2.50) and (2.51). However, the evanescent operators $E_1^{(3)}$–$E_4^{(3)}$ become more important at the four-loop level.

For the renormalization of the electroweak penguin operators Q_3^Q–Q_6^Q one encounters at the one-loop level two evanescent operators, which can be chosen to be

$$\begin{aligned}
E_3^{Q(1)} &= (\bar{s}_L\gamma_{\mu_1\mu_2\mu_3\mu_4\mu_5}b_L){\textstyle\sum_q}Q_q(\bar{q}\gamma^{\mu_1\mu_2\mu_3\mu_4\mu_5}q) + 64Q_3^Q - 20Q_5^Q\,,\\
E_4^{Q(1)} &= (\bar{s}_L\gamma_{\mu_1\mu_2\mu_3\mu_4\mu_5}T^a b_L){\textstyle\sum_q}Q_q(\bar{q}\gamma^{\mu_1\mu_2\mu_3\mu_4\mu_5}T^a q) + 64Q_4^Q - 20Q_6^Q\,.
\end{aligned} \tag{2.53}$$

At the two-loop level two more evanescent operators arise, which we choose to be

$$\begin{aligned}
E_3^{Q(2)} &= (\bar{s}_L\gamma_{\mu_1\mu_2\mu_3\mu_4\mu_5\mu_6\mu_7}b_L){\textstyle\sum_q}Q_q(\bar{q}\gamma^{\mu_1\mu_2\mu_3\mu_4\mu_5\mu_6\mu_7}q) + 1280Q_3^Q - 336Q_5^Q\,,\\
E_4^{Q(2)} &= (\bar{s}_L\gamma_{\mu_1\mu_2\mu_3\mu_4\mu_5\mu_6\mu_7}T^a b_L){\textstyle\sum_q}Q_q(\bar{q}\gamma^{\mu_1\mu_2\mu_3\mu_4\mu_5\mu_6\mu_7}T^a q) + 1280Q_4^Q - 336Q_6^Q\,.
\end{aligned} \tag{2.54}$$

Finally to apply the QED one-loop renormalization of the semileptonic operators Q_9 and Q_{10} we introduce the follwing two evanescent operators:

$$\begin{aligned}
E_1^{L(1)} &= \frac{1}{6}(\bar{s}_L\gamma_{\mu_1\mu_2\mu_3}b_L){\textstyle\sum_l}(\bar{l}\gamma^{\mu_1\mu_2\mu_3}l) + Q_{10} - \frac{5}{3}Q_9\\
E_2^{L(1)} &= (\bar{s}_L\gamma_{\mu_1\mu_2\mu_3}b_L){\textstyle\sum_l}(\bar{l}\gamma^{\mu_1\mu_2\mu_3\gamma_5}l) + \frac{5}{3}(\bar{s}_L\gamma_{\mu_1\mu_2\mu_3}b_L){\textstyle\sum_l}(\bar{l}\gamma^{\mu_1\mu_2\mu_3}l) - \frac{32}{3}Q_9\,.
\end{aligned} \tag{2.55}$$

2.2.3 Renormalizing Composite Operators

Our aim is to study the renormalization properties of the physical operators Q_1–Q_{10} introduced in Eqs. (2.42–2.46). Upon renormalization, the bare Wilson coefficients $C_{i,B}(\mu)$ of Eq. (2.41) transform as

$$C_{i,B}(\mu) = Z_{ji} C_j(\mu)\,, \tag{2.56}$$

where the renormalization constants Z_{ij} can be expanded in powers of $\alpha_s = \frac{g^2}{4\pi}$ and $\alpha = \frac{e^2}{4\pi}$ as

$$\begin{aligned} Z_{ij} &= \delta_{ij} + \sum_{k=1}^{\infty} \left(\frac{\alpha_s}{4\pi}\right)^k Z_{ij}^{(k)} + \frac{\alpha}{4\pi} Z_{ij}^{(e)} + \frac{\alpha_s \alpha}{16\pi^2} Z_{ij}^{(es)} \\ Z_{ij}^{(k)} &= \sum_{l=0}^{k} \frac{1}{\epsilon^l} Z_{ij}^{(k,l)}, \qquad Z_{ij}^{(e)} = \sum_{l=0}^{1} \frac{1}{\epsilon^l} Z_{ij}^{(e,l)}, \qquad Z_{ij}^{(es)} = \sum_{l=0}^{2} \frac{1}{\epsilon^l} Z_{ij}^{(es,l)}\,. \end{aligned} \tag{2.57}$$

Following the standard $\overline{\text{MS}}$ scheme prescription, Z_{ij} is given by pure $1/\epsilon^l$ poles, except when i corresponds to an evanescent operator, while j does not. In the latter case, the renormalization constant is finite, to make sure that the matrix elements of the evanescent operators vanish in four dimensions [81–83]. The calculation of an effective amplitude $\mathcal{A}_{\text{eff}}$, also involves the matrix element $\langle Q_i \rangle \equiv \langle F|Q_i(\mu)|I\rangle$ of the operator Q_i between an initial state I and a final state F, which is renormalized by the usual coupling, mass, and wave function renormalization factor characteristic of the operator $Q_i \to Z(Q_i)$. The renormalized effective amplitude is therefore given by

$$\mathcal{A}_{\text{eff}} = Z_{ji} C_j(\mu) \langle Z(Q_i) \rangle_R\,, \tag{2.58}$$

where $\langle Z(Q_i)\rangle_R$ denotes the matrix element of the operator $Z(Q_i)$ after performing coupling, mass and wave function renormalization. Clearly, it is also possible to define the operator renormalization constant $\overline{Z}_{ij}$ from the relation between unrenormalized and amputated Green's functions via $\langle Z(Q_i)\rangle_R = \overline{Z}_{ij}\langle Q_j\rangle_B$. In this case, one simply has $\overline{Z}_{ij} = Z_{ij}^{-1}$. In general $Z(Q_i)$ will not be proportional to Q_i. For example, in many of the EOM-vanishing operator introduced in Eqs. (2.47) and (2.48) one has two different terms, only one of which has a factor of m_b. Correspondingly, the m_b renormalization of the operator is

$$Z_{m_b}(Q_i) = Q_i + (Z_{m_b} - 1) Q_i'\,, \tag{2.59}$$

where Z_{m_b} denotes the mass renormalization constant of the bottom quark, and Q_i' is the part of Q_i proportional to m_b. Another important example in the case of QED corrections are the pengiun operators (2.43–2.44), where the renormalization will depend on the flavour of the particular insertion.

The product on the right-hand side of Eq. (2.58) must be finite by definition at any given order in α_s and α. Therefore, requiring the cancellation of UV divergences we can

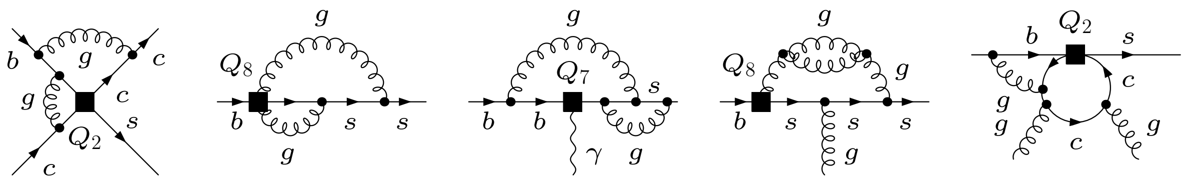

Figure 2.1: Some of the two-loop 1PI diagrams we had to calculate in order to find the $O(\alpha_s^2)$ mixing of the complete set of operators Q_1–Q_{32}.

extract $Z_{ij}^{(k)}$ order by order. The result, up to third order in α_s and to order α and $\alpha\alpha_s$, reads

$$\begin{aligned}
Z_{ij}^{(1)}\langle Q_j\rangle_R^{(0)} &= -\langle Z(Q_i)\rangle_R^{(1)}\,, \\
Z_{ij}^{(2)}\langle Q_j\rangle_R^{(0)} &= -\langle Z(Q_i)\rangle_R^{(2)} - Z_{ij}^{(1)}\langle Z(Q_j)\rangle_R^{(1)}\,, \\
Z_{ij}^{(3)}\langle Q_j\rangle_R^{(0)} &= -\langle Z(Q_i)\rangle_R^{(3)} - Z_{ij}^{(1)}\langle Z(Q_j)\rangle_R^{(2)} - Z_{ij}^{(2)}\langle Z(Q_j)\rangle_R^{(1)}\,, \\
Z_{ij}^{(e)}\langle Q_j\rangle_R^{(0)} &= -\langle Z(Q_i)\rangle_R^{(e)}\,, \\
Z_{ij}^{(es)}\langle Q_j\rangle_R^{(0)} &= -\langle Z(Q_i)\rangle_R^{(es)} - Z_{ij}^{(e)}\langle Z(Q_j)\rangle_R^{(1)} - Z_{ij}^{(1)}\langle Z(Q_j)\rangle_R^{(e)}\,,
\end{aligned} \tag{2.60}$$

where the superscript (k) always stands for the k-th order contribution in α_s, while (e) and (es) denote the contribution in α and $\alpha\alpha_s$ respectively.

If we leave aside the complication that in general $Z(Q_i)$ will not be proportional to Q_i, and write symbolically $\langle Z(Q_i)\rangle_R = Z_i\langle Q_i\rangle_B$, the above relations can be rewritten in terms of bare quantities. Up to the considered order we obtain

$$\begin{aligned}
Z_{ij}^{(1)}\langle Q_j\rangle_B^{(0)} &= -\langle Q_i\rangle_B^{(1)} - Z_i^{(1)}\langle Q_i\rangle_B^{(0)}\,, \\
Z_{ij}^{(2)}\langle Q_j\rangle_B^{(0)} &= -\langle Q_i\rangle_B^{(2)} - Z_{ij}^{(1)}\langle Q_j\rangle_B^{(1)} - Z_i^{(1)}\langle Q_i\rangle_B^{(1)} \\
&\quad - Z_{ij}^{(1)}Z_j^{(1)}\langle Q_j\rangle_B^{(0)} - Z_i^{(2)}\langle Q_i\rangle_B^{(0)}\,, \\
Z_{ij}^{(3)}\langle Q_j\rangle_B^{(0)} &= -\langle Q_i\rangle_B^{(3)} - Z_{ij}^{(1)}\langle Q_j\rangle_B^{(2)} - Z_i^{(1)}\langle Q_i\rangle_B^{(2)} \\
&\quad - Z_{ij}^{(2)}\langle Q_j\rangle_B^{(1)} - Z_{ij}^{(1)}Z_j^{(1)}\langle Q_j\rangle_B^{(1)} - Z_i^{(2)}\langle Q_i\rangle_B^{(1)} \\
&\quad - Z_{ij}^{(2)}Z_j^{(1)}\langle Q_j\rangle_B^{(0)} - Z_{ij}^{(1)}Z_j^{(2)}\langle Q_j\rangle_B^{(0)} - Z_i^{(3)}\langle Q_i\rangle_B^{(0)}\,. \\
Z_{ij}^{(e)}\langle Q_j\rangle_B^{(0)} &= -\langle Q_i\rangle_B^{(e)} - Z_i^{(e)}\langle Q_i\rangle_B^{(0)}\,, \\
Z_{ij}^{(es)}\langle Q_j\rangle_B^{(0)} &= -\langle Q_i\rangle_B^{(es)} - Z_{ij}^{(e)}\langle Q_j\rangle_B^{(1)} - Z_{ij}^{(1)}\langle Q_j\rangle_B^{(e)} \\
&\quad - Z_i^{(e)}\langle Q_i\rangle_B^{(1)} - Z_i^{(1)}\langle Q_i\rangle_B^{(e)} \\
&\quad - Z_{ij}^{(e)}Z_j^{(1)}\langle Q_j\rangle_B^{(0)} - Z_{ij}^{(0)}Z_j^{(e)}\langle Q_j\rangle_B^{(0)} - Z_i^{(es)}\langle Q_i\rangle_B^{(0)}\,.
\end{aligned} \tag{2.61}$$

The first line in Eqs. (2.61) recalls the familiar result that the one-loop renormalization matrix is given by the UV divergences of the one-loop matrix elements, after performing

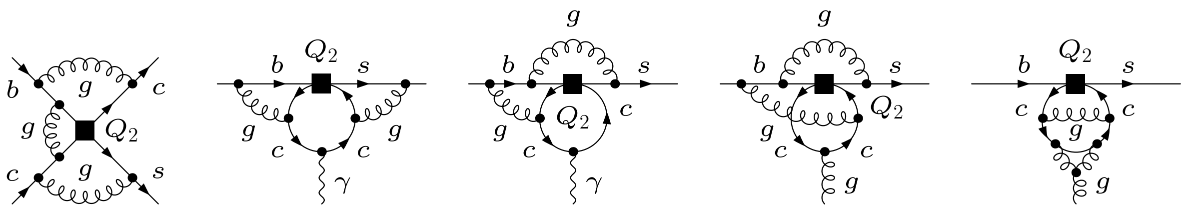

Figure 2.2: Some of the three-loop 1PI diagrams we had to calculate in order to find the mixing of the four-quark operators Q_1–Q_6 into Q_1–Q_6 and Q_7–Q_{10} at $O(\alpha_s^3)$.

wave function and possibly coupling and mass renormalization. For example, in the case of the operators Q_1–Q_6 in QCD, one has $Z_i = Z_q^2$ with Z_q denoting the wave function renormalization constant of the quark fields, and Eqs. (2.61) take a particularly simple form, which upon expansion in α_s reproduces the classical results derived more than ten years ago [81].

For a given set of operators and knowing the QCD and QED renormalization constants, the solution of the above systems of linear equations requires the calculation of a sufficient number of Green's functions for different external fields with single insertions of the operators Q_i. In our case, in order to determine the complete $Z_{ij}^{(k)}$ of all the operators introduced in Section 2.2.1 and 2.2.2, it is sufficient to calculate the $O(\alpha_s^k)$ matrix elements of Q_1–Q_{32} for the $b \to sc\bar{c}$, $b \to sd\bar{d}$, $b \to s$, $b \to s\gamma$, $b \to sg$ and $b \to sgg$ transition — see Fig. 2.1. As we are interested in a subset of the three-loop ADM, the mixing of Q_1–Q_6 into Q_1–Q_6 and Q_7–Q_{10}, we have actually calculated only the three-loop $b \to sc\bar{c}$, $b \to s\gamma$, and $b \to sg$ amplitudes involving insertions of Q_1–Q_6 (see Fig. 2.2). We have calculated the complete off-shell amplitudes up to terms proportional to external momenta squared. By using the EOM it is therefore straightforward to extract the mixing into Q_1–Q_6 and Q_7–Q_{10}. Notice that the results for the $Z_{ij}^{(k)}$ cannot depend on the considered Green's functions and that the pole parts need to have the structure of the complete set of local operators Q_1–Q_{32}. Both features represent a powerful consistency check of the computation of the renormalization constants $Z_{ij}^{(k)}$.

The normalization of the physical operators adopted in Section 2.2.1 has been chosen [13] in such a way that the power of α_s in Z_{ij} is equal to the number of loops of the contributing diagrams. For instance, without the factor $1/g^2$ in Q_7–Q_{10}, as in the standard normalization adopted in [6, 7, 45], both one- and two-loop diagrams contribute to the $O(\alpha_s)$ mixing matrix, because of the $O(\alpha_s)$ two-loop mixing of four-quark into magnetic operators. This choice simplifies both the implementation of the renormalization program and the resummation of large logarithms, since the redefinition enables one to proceed for $b \to s\ell^+\ell^-$ in the same way as in the $b \to s\gamma$ and $b \to sg$ case.

In a mass independent renormalization scheme $Z_{ij}^{(k)}$ is μ-independent. This allows to check the renormalization of two- and three-loop matrix elements. The right-hand sides of the Eqs. (2.60) and (2.61) receive contributions from irreducible two- and three-loop diagrams as well as one- and two-loop counterterms. The μ-dependence is different in each case and governed by the n-loop factor $(\mu^{2\epsilon})^n$. The UV structure of the k-th term is therefore given by

$$Z_{ij}^{(k)} \langle Q_j \rangle_B^{(0)} = \sum_{n=0}^{k} \sum_{l=1}^{n} \left(\mu^{2\epsilon}\right)^n \frac{1}{\epsilon^l} M^{(n,l)}\,, \tag{2.62}$$

where $M^{(n,l)}$ denotes the $1/\epsilon^l$ pole of the sum of all n-loop contributions. Expanding in powers of ϵ we find the following set of equations which have to be fulfilled to get a μ-independent $Z_{ij}^{(k)}$ up to three-loop order:

$$\begin{aligned} 3M^{(3,2)} + 2M^{(2,2)} + M^{(1,2)} &= 0\,, \\ 3M^{(3,3)} + 2M^{(2,3)} + M^{(1,3)} &= 0\,, \\ 9M^{(3,3)} + 4M^{(2,3)} + M^{(1,3)} &= 0\,. \end{aligned} \tag{2.63}$$

This system of equations provides us with a powerful check of the renormalization of two- as well as three-loop diagrams. Notice that the locality of UV divergences also places some constraints on the renormalization matrix itself. We will return to this point later on.

2.2.4 Renormalization Constants and Anomalous Dimensions

The anomalous dimensions γ_{ij} defined by

$$\mu \frac{d}{d\mu} C_i(\mu) = \gamma_{ji} C_j(\mu) \tag{2.64}$$

can be expressed in terms of the entries of the renormalization matrix Z_{ij} as follows

$$\gamma_{ij} = Z_{ik}\, \mu \frac{d}{d\mu} Z_{kj}^{-1}\,. \tag{2.65}$$

In a mass independent renormalization scheme the only μ-dependence of Z_{ij} resides in the coupling constant. In consequence, we might rewrite Eq. (2.65) as

$$\gamma_{ij} = 2\beta(\epsilon, \alpha_s, \alpha) Z_{ik} \frac{d}{d\alpha_s} Z_{kj}^{-1} + 2\beta_e(\epsilon, \alpha_s, \alpha) Z_{ik} \frac{d}{d\alpha} Z_{kj}^{-1}\,, \tag{2.66}$$

where $\beta(\epsilon, \alpha_s, \alpha)$ and $\beta(\epsilon, \alpha_s, \alpha)$ is related to the β functions via

$$\beta(\epsilon, \alpha_s, \alpha) = \alpha_s\big(-\epsilon + \beta(\alpha_s, \alpha)\big) \tag{2.67}$$

$$\beta_e(\epsilon, \alpha_s, \alpha) = \alpha\big(-\epsilon + \beta_e(\alpha_s, \alpha)\big)\,. \tag{2.68}$$

The finite parts of Eq. (2.66) in the limit of ϵ going to zero give the anomalous dimensions. Expanding the anomalous dimensions and the β function in powers of α_s and α as

$$\begin{aligned}
\hat{\gamma} &= \sum_{k=1}^{\infty}\left(\frac{\alpha_s}{4\pi}\right)^k \hat{\gamma}^{(k-1)} + \frac{\alpha}{4\pi}\hat{\gamma}_e^{(0)} + \frac{\alpha_s\alpha}{16\pi^2}\hat{\gamma}_{es}^{(0)} \\
\beta(\alpha_s,\alpha) &= -\sum_{k=1}^{\infty}\left(\frac{\alpha_s}{4\pi}\right)^k \beta_{k-1} - \frac{\alpha_s\alpha}{16\pi^2}\beta_{es} \\
\beta_e(\alpha_s,\alpha) &= -\sum_{k=1}^{\infty}\left(\frac{\alpha}{4\pi}\right)^k \beta_{e_{k-1}} - \frac{\alpha_s\alpha}{16\pi^2}\beta_{e_{es}}\,,
\end{aligned} \tag{2.69}$$

we find in accordance with [65] up to third order in α_s and up to order α and $\alpha\alpha_s$:

$$\begin{aligned}
\hat{\gamma}^{(0)} &= 2\hat{Z}^{(1,1)}\,, \\
\hat{\gamma}^{(1)} &= 4\hat{Z}^{(2,1)} - 2\hat{Z}^{(1,1)}\hat{Z}^{(1,0)} - 2\hat{Z}^{(1,0)}\hat{Z}^{(1,1)} + 2\beta_0\hat{Z}^{(1,0)}\,, \\
\hat{\gamma}^{(2)} &= 6\hat{Z}^{(3,1)} - 4\hat{Z}^{(2,1)}\hat{Z}^{(1,0)} - 2\hat{Z}^{(1,1)}\hat{Z}^{(2,0)} - 4\hat{Z}^{(2,0)}\hat{Z}^{(1,1)} - 2\hat{Z}^{(1,0)}\hat{Z}^{(2,1)}\,, \\
&\quad + 2\hat{Z}^{(1,1)}\hat{Z}^{(1,0)}\hat{Z}^{(1,0)} + 2\hat{Z}^{(1,0)}\hat{Z}^{(1,1)}\hat{Z}^{(1,0)} + 2\hat{Z}^{(1,0)}\hat{Z}^{(1,0)}\hat{Z}^{(1,1)} \\
&\quad + 2\beta_1\hat{Z}^{(1,0)} + 4\beta_0\hat{Z}^{(2,0)} - 2\beta_0\hat{Z}^{(1,0)}\hat{Z}^{(1,0)}\,, \\
\hat{\gamma}_e^{(0)} &= 2\hat{Z}^{(1,1)}\,, \\
\hat{\gamma}_{es}^{(1)} &= 4\hat{Z}^{(es,1)} - 2\hat{Z}^{(1,1)}\hat{Z}^{(e,0)} - 2\hat{Z}^{(1,0)}\hat{Z}^{(e,1)} \\
&\quad - 2\hat{Z}^{(e,1)}\hat{Z}^{(1,0)} - 2\hat{Z}^{(e,0)}\hat{Z}^{(1,1)} + 2\beta_0\hat{Z}^{(e,0)} + 2\beta_{e_0}\hat{Z}^{(1,0)}\,.
\end{aligned} \tag{2.70}$$

On the other hand the pole parts of Eq. (2.66) must vanish. From this condition one obtains relations between single, double and triple $1/\epsilon$ poles of the Z_{ij}, which constitute a useful check of the calculation. In agreement with [65] we find

$$\begin{aligned}
\hat{Z}^{(2,2)} &= \frac{1}{2}\hat{Z}^{(1,1)}\hat{Z}^{(1,1)} - \frac{1}{2}\beta_0\hat{Z}^{(1,1)}\,, \\
\hat{Z}^{(3,3)} &= \frac{1}{6}\hat{Z}^{(1,1)}\hat{Z}^{(1,1)}\hat{Z}^{(1,1)} - \frac{1}{2}\beta_0\hat{Z}^{(1,1)}\hat{Z}^{(1,1)} + \frac{1}{3}\beta_0^2\hat{Z}^{(1,1)}\,, \\
\hat{Z}^{(3,2)} &= \frac{2}{3}\hat{Z}^{(2,1)}\hat{Z}^{(1,1)} + \frac{1}{3}\hat{Z}^{(1,1)}\hat{Z}^{(2,1)} - \frac{1}{3}\hat{Z}^{(1,1)}\hat{Z}^{(1,0)}\hat{Z}^{(1,1)} - \frac{1}{6}\hat{Z}^{(1,0)}\hat{Z}^{(1,1)}\hat{Z}^{(1,1)} \\
&\quad - \frac{1}{3}\beta_1\hat{Z}^{(1,1)} - \frac{2}{3}\beta_0\hat{Z}^{(2,1)} + \frac{1}{6}\beta_0\hat{Z}^{(1,0)}\hat{Z}^{(1,1)}\,, \\
\hat{Z}^{(es,2)} &= 0\,.
\end{aligned} \tag{2.71}$$

2.3 Summation of the Logarithms

2.3.1 The Evolution Matrix

The effective Hamiltonian for non-leptonic $|\Delta F| = 1$ decays has the following generic structure [84]:

$$\mathcal{H}_{\text{eff}} = -\frac{4G_F}{\sqrt{2}} V_{\text{CKM}} \vec{Q}^T \vec{C}(\mu) \,. \tag{2.72}$$

Here G_F denotes the Fermi constant and $\vec{Q}^T$ is a row vector containing the relevant local operators Q_i, which in the case considered here include the current-current operators Q_1 and Q_2, and the QCD penguin operators Q_3–Q_6. The decay amplitude for a decay of a meson M into a final state F is simply given by $\langle F|\mathcal{H}_{\text{eff}}|M\rangle$.

We want to investigate the renormalization scale dependence of the effective Hamiltonian, in particular the NNLO QCD contributions, which until now have not been completely studied in the literature. We will, therefore, postpone the discussion of QED contributions to the end of this section. The Wilson coefficient functions evolve from the initial scale μ_0 down to the renormalization scale μ according to their renormalization group equation (RGE)

$$\mu \frac{d}{d\mu} \vec{C}(\mu) = \hat{\gamma}^T(g) \vec{C}(\mu) \,, \tag{2.73}$$

where $\hat{\gamma}(g)$ is the ADM corresponding to $\vec{Q}$. Neglecting the running of the electromagnetic coupling constant the general solution of this equation reads

$$\vec{C}(\mu) = \hat{U}(\mu, \mu_0) \vec{C}(\mu_0) \,, \tag{2.74}$$

with

$$\hat{U}(\mu, \mu_0) = T_g \exp \int_{g(\mu_0)}^{g(\mu)} dg' \frac{\hat{\gamma}^T(g')}{\beta(g')} \,, \tag{2.75}$$

$$\hat{\gamma}(g) = \sum_{i=0}^{\infty} \left(\frac{g^2}{16\pi^2} \right)^{i+1} \hat{\gamma}^{(i)} \,, \quad \text{and} \quad \beta(g) = -g \sum_{i=0}^{\infty} \left(\frac{g^2}{16\pi^2} \right)^{i+1} \beta_i \,. \tag{2.76}$$

Here $\vec{C}(\mu_0)$ are the initial conditions of the evolution and T_g denotes ordering of the coupling constants $g(\mu)$ in such a way that their value increases from right to left. $\beta(g)$ is the QCD β function.

Keeping the first three terms in the expansions of $\hat{\gamma}(g)$ and $\beta(g)$ as given in Eq. (2.76), we find for the evolution matrix $\hat{U}(\mu, \mu_0)$ in NNLO approximation

$$\hat{U}(\mu, \mu_0) = \hat{K}(\mu) \hat{U}^{(0)}(\mu, \mu_0) \hat{K}^{-1}(\mu_0) \,, \tag{2.77}$$

where

$$\begin{aligned}\hat{K}(\mu) &= \hat{1} + \frac{\alpha_s(\mu)}{4\pi}\hat{J}^{(1)} + \left(\frac{\alpha_s(\mu)}{4\pi}\right)^2 \hat{J}^{(2)}\,,\\ \hat{K}^{-1}(\mu_0) &= \hat{1} - \frac{\alpha_s(\mu_0)}{4\pi}\hat{J}^{(1)} - \left(\frac{\alpha_s(\mu_0)}{4\pi}\right)^2 \left(\hat{J}^{(2)} - \left(\hat{J}^{(1)}\right)^2\right)\,,\end{aligned} \tag{2.78}$$

and

$$\hat{U}^{(0)}(\mu,\mu_0) = \hat{V}\,\mathrm{diag}\,(\eta^{a_i})\,\hat{V}^{-1}\,, \tag{2.79}$$

denotes the LO evolution matrix, which depends on the matrix $\hat{V}$ and the so-called magic numbers a_i that are obtained via diagonalizing $\hat{\gamma}^{(0)\,T}$

$$\left(\hat{V}^{-1}\hat{\gamma}^{(0)\,T}\hat{V}\right)_{ij} = 2\beta_0 a_i \delta_{ij}\,. \tag{2.80}$$

In order to give the explicit expressions for the matrices $\hat{J}^{(1)}$ and $\hat{J}^{(2)}$ we define

$$\hat{J}^{(i)} = \hat{V}^{-1}\hat{S}^{(i)}\hat{V}\,, \quad \text{and} \quad \hat{G}^{(i)} = \hat{V}^{-1}\hat{\gamma}^{(i)\,T}\hat{V}\,, \tag{2.81}$$

for $i = 1, 2$. The entries of the matrix kernels $\hat{S}^{(1)}$ and $\hat{S}^{(2)}$ are given by

$$\begin{aligned}S^{(1)}_{ij} &= \frac{\beta_1}{\beta_0}a_i\delta_{ij} - \frac{G^{(1)}_{ij}}{2\beta_0\left(1+a_i-a_j\right)}\,,\\ S^{(2)}_{ij} &= \frac{\beta_2}{2\beta_0}a_i\delta_{ij} + \sum_k \frac{1+a_i-a_k}{2+a_i-a_j}\left(S^{(1)}_{ik}S^{(1)}_{kj} - \frac{\beta_1}{\beta_0}S^{(1)}_{ij}\delta_{jk}\right) - \frac{G^{(2)}_{ij}}{2\beta_0\left(2+a_i-a_j\right)}\,,\end{aligned} \tag{2.82}$$

where the first line recalls the classical NLO result derived more than ten years ago [85], and the second one represents the corresponding NNLO expression, for which our findings perfectly agree with [86].

In order to derive the explicit expressions for the matrix kernels $\hat{S}^{(1)}$ and $\hat{S}^{(2)}$ as given in Eq. (2.82), we follow [85,87] and compute the partial derivative of Eqs. (2.75) and (2.77) with respect to g. After some algebra, one finds the following differential equation for $\hat{K}(g)$:

$$\frac{\partial\hat{K}(g)}{\partial g} + \frac{1}{g}\left[\frac{\hat{\gamma}^{(0)\,T}}{\beta_0}, \hat{K}(g)\right] = \left(\frac{\hat{\gamma}^{T}(g)}{\beta(g)} + \frac{1}{g}\frac{\hat{\gamma}^{(0)\,T}}{\beta_0}\right)\hat{K}(g)\,. \tag{2.83}$$

Inserting Eqs. (2.78) into the last equation we obtain

$$\begin{aligned}\hat{J}^{(1)} + \left[\frac{\hat{\gamma}^{(0)\,T}}{2\beta_0}, \hat{J}^{(1)}\right] &= -\frac{\hat{\gamma}^{(1)\,T}}{2\beta_0} + \frac{\beta_1}{2\beta_0^2}\hat{\gamma}^{(0)\,T}\,,\\ \hat{J}^{(2)} + \left[\frac{\hat{\gamma}^{(0)\,T}}{4\beta_0}, \hat{J}^{(2)}\right] &= -\frac{\hat{\gamma}^{(2)\,T}}{4\beta_0} + \frac{\beta_1}{4\beta_0^2}\hat{\gamma}^{(1)\,T} + \left(\frac{\beta_2}{4\beta_0^2} - \frac{\beta_1^2}{4\beta_0^3}\right)\hat{\gamma}^{(0)\,T}\\ &\quad - \left(\frac{\hat{\gamma}^{(1)\,T}}{4\beta_0} - \frac{\beta_1}{4\beta_0^2}\hat{\gamma}^{(0)\,T}\right)\hat{J}^{(1)}\end{aligned} \tag{2.84}$$

for the parts proportional to g and g^3 respectively. After diagonalizing these equations with the help of Eq. (2.80), we find

$$
\begin{aligned}
S_{ij}^{(1)} &= \frac{\beta_1}{\beta_0} a_i \delta_{ij} - \frac{G_{ij}^{(1)}}{2\beta_0 \left(1 + a_i - a_j\right)} \, , \\
S_{ij}^{(2)} &= \left(\frac{\beta_2}{2\beta_0} - \frac{\beta_1^2}{2\beta_0^2} \right) a_i \delta_{ij} + \sum_k \frac{2\beta_1 a_i \delta_{ik} - G_{ik}^{(1)}}{2\beta_0 \left(2 + a_i - a_j\right)} S_{kj}^{(1)} + \frac{\beta_1 G_{ij}^{(1)} - \beta_0 G_{ij}^{(2)}}{2\beta_0^2 \left(2 + a_i - a_j\right)} \, .
\end{aligned}
\tag{2.85}
$$

Finally, solving the first equation for $G_{ij}^{(1)}$ and inserting the result into the second equation, one obtains the expression for the elements of $\hat{S}^{(2)}$ as given in Eqs. (2.82).

2.3.2 Matching

An amplitude for a properly chosen non-leptonic quark decay is calculated perturbatively in the full theory including all possible diagrams such as W-boson exchange, box, and QCD and electroweak penguin diagrams as well as gluon corrections to all these building blocks. The result including LO, NLO and NNLO QCD corrections is given schematically as follows:

$$
\mathcal{A}_{\rm full} = \langle \vec{Q} \rangle^{(0)\,T} \left(\vec{A}^{(0)} + \frac{\alpha_s(\mu_0)}{4\pi} \vec{A}^{(1)} + \left(\frac{\alpha_s(\mu_0)}{4\pi} \right)^2 \vec{A}^{(2)} \right) \, , \tag{2.86}
$$

where $\langle \vec{Q} \rangle^{(0)}$ denotes the tree-level matrix elements of $\vec{Q}$.

The second step involves the calculation of the decay amplitude in the QCD effective theory. It generally requires the computation of the operator insertions into current-current and QCD penguin diagrams of the effective theory together with gluon corrections to these insertions. Including LO, NLO and NNLO QCD corrections one finds

$$
\mathcal{A}_{\rm eff} = \langle \vec{Q} \rangle^{(0)\,T} \left(\vec{1} + \frac{\alpha_s(\mu_0)}{4\pi} \hat{r}^{(1)\,T} + \left(\frac{\alpha_s(\mu_0)}{4\pi} \right)^2 \hat{r}^{(2)\,T} \right) \vec{C}(\mu_0) \, , \tag{2.87}
$$

where the quantities $\hat{r}^{(1)}$ and $\hat{r}^{(2)}$ codify the one- and two-loop matrix elements of $\vec{Q}$, respectively.

The matching procedure between full and effective theory establishes the initial conditions $\vec{C}(\mu_0)$ for the Wilson coefficients. Comparing Eqs. (2.86) and (2.87), the matching condition $\mathcal{A}_{\rm full} = \mathcal{A}_{\rm eff}$ translates into the following identity [88]:

$$
\begin{aligned}
\vec{C}(\mu_0) &= \vec{A}^{(0)} + \frac{\alpha_s(\mu_0)}{4\pi} \left(\vec{A}^{(1)} - \hat{r}^{(1)\,T} \vec{A}^{(0)} \right) \\
&\quad + \left(\frac{\alpha_s(\mu_0)}{4\pi} \right)^2 \left(\vec{A}^{(2)} - \hat{r}^{(1)\,T} \left[\vec{A}^{(1)} - \hat{r}^{(1)\,T} \vec{A}^{(0)} \right] - \hat{r}^{(2)\,T} \vec{A}^{(0)} \right) \, .
\end{aligned}
\tag{2.88}
$$

Combining Eqs. (2.73), (2.77), (2.78) and (2.88) we finally obtain

$$\vec{C}(\mu) = \hat{K}(\mu)\hat{U}^{(0)}(\mu,\mu_0)\Bigg(\vec{A}^{(0)} + \frac{\alpha_s(\mu_0)}{4\pi}\left[\vec{A}^{(1)} - \hat{R}^{(1)}\vec{A}^{(0)}\right] + \left(\frac{\alpha_s(\mu_0)}{4\pi}\right)^2\left[\vec{A}^{(2)} - \hat{R}^{(1)}\vec{A}^{(1)} - \left(\hat{R}^{(2)} - \left(\hat{R}^{(1)}\right)^2\right)\vec{A}^{(0)}\right]\Bigg) \tag{2.89}$$

where

$$\hat{R}^{(1)} = \hat{r}^{(1)\,T} + \hat{J}^{(1)}\,, \quad \text{and} \quad \hat{R}^{(2)} = \hat{r}^{(2)\,T} + \hat{J}^{(2)} + \hat{r}^{(1)\,T}\hat{J}^{(1)}\,, \tag{2.90}$$

are certain combinations of $\hat{r}^{(1)\,T}$, $\hat{r}^{(2)\,T}$, $\hat{J}^{(1)}$ and $\hat{J}^{(2)}$, which will play a special role in the following section.

2.3.3 Renormalization Scheme Dependence

Next we would like to elaborate on the question of renormalization scheme dependencies in explicit terms, to gain an insight on how the scheme dependencies arise beyond the LO, how various quantities transform under a change of scheme and how these scheme dependencies cancel in physical observables. In this respect we will extend the existing NLO QCD results [23, 85] to the NNLO level.

It is well-known that beyond LO various quantities such as the Wilson coefficients or the anomalous dimensions depend on the scheme adopted for the renormalization of the operators present in the effective theory. This scheme dependencies arise because the requirement that all UV divergences are removed by a suitable renormalization of parameters, fields as well as operators, does not fix the finite parts of the associated renormalization constants. Indeed, these constants can be defined in many different ways corresponding to distinct renormalization schemes, which are always related by a finite renormalization. In the framework of dimensional regularization one example of how such a scheme dependence may occur is the treatment of γ_5 in $n = 4 - 2\epsilon$ dimensions. In this context two well-known choices of scheme are the so-called Naive Dimensional Regularization (NDR) scheme [89] with γ_5 taken to be fully anticommuting and the 't Hooft-Veltman scheme [90–93] which comprises a γ_5 that does not have simple commutation properties with respect to the other Dirac matrices. Another example is the scheme dependence related to the exact form of the local operators used to describe the interactions in the low-energy effective theory. In general, a particular choice of the operator basis is not unique, and quantities such as Wilson coefficients or anomalous dimensions corresponding to different choices of operators can always be transformed into each other by a suitable finite renormalization. We will discuss the latter issue in great detail in one of the following sections.

In order to show that physical quantities and especially decay amplitudes do not depend on the renormalization scheme and the particular form of the operators, we have to demonstrate how these dependencies cancel out in the effective Hamiltonian introduced in

Eq. (2.72) with $\vec{C}(\mu)$ given by Eq. (2.89). We first recall that, upon renormalization, the bare operators $\vec{Q}_B$ and Wilson coefficients $\vec{C}_B(\mu)$ of Eq. (2.72) transform as

$$\vec{Q}_B = \hat{Z}\,\vec{Q}\,, \quad \text{and} \quad \vec{C}_B(\mu) = \hat{Z}^T\vec{C}(\mu) \tag{2.91}$$

respectively. In terms of the renormalization constant matrix $\hat{Z}$ the ADM defined via Eq. (2.73), is then given by

$$\hat{\gamma}(g) = \hat{Z}\,\mu\frac{d}{d\mu}\hat{Z}^{-1}\,. \tag{2.92}$$

Next, we shall denote the results obtained in two different renormalization schemes by $\hat{\gamma}_0^{(i)}$, $\hat{r}_0^{(i)}$ and $\hat{\gamma}_a^{(i)}$, $\hat{r}_a^{(i)}$, with $i = 1, 2$. Furthermore, let us assume without loss of generality that the first scheme, which we shall call reference scheme hereafter, is distinguished from the other ones by the subsidiary condition $\hat{r}_0^{(1)} = \hat{r}_0^{(2)} = 0$.

It should be clear that for any given scheme a we can always switch to the reference scheme by the following finite renormalization:

$$\hat{Z}_0 = \left(\hat{1} - \frac{\alpha_s(\mu)}{4\pi}\hat{r}_a^{(1)} - \left(\frac{\alpha_s(\mu)}{4\pi}\right)^2\left(\hat{r}_a^{(2)} - \left(\hat{r}_a^{(1)}\right)^2\right)\right)\hat{Z}_a\,. \tag{2.93}$$

The corresponding transformations of the $O(\alpha_s^2)$ and $O(\alpha_s^3)$ anomalous dimensions is easily obtained using Eqs. (2.92). At NLO we reproduce the well-known result [23, 85]

$$\hat{\gamma}_0^{(1)} = \hat{\gamma}_a^{(1)} - \left[\hat{r}_a^{(1)}, \hat{\gamma}^{(0)}\right] - 2\beta_0\hat{r}_a^{(1)}\,, \tag{2.94}$$

whereas at NNLO we find

$$\hat{\gamma}_0^{(2)} = \hat{\gamma}_a^{(2)} - \left[\hat{r}_a^{(2)}, \hat{\gamma}^{(0)}\right] - \left[\hat{r}_a^{(1)}, \hat{\gamma}_a^{(1)}\right] + \hat{r}_a^{(1)}\left[\hat{r}_a^{(1)}, \hat{\gamma}^{(0)}\right] - 4\beta_0\hat{r}_a^{(2)} - 2\beta_1\hat{r}_a^{(1)} + 2\beta_0\left(\hat{r}_a^{(1)}\right)^2. \tag{2.95}$$

Obviously, the combinations $\hat{\gamma}_0^{(1)}$ and $\hat{\gamma}_0^{(2)}$, are the same for any given scheme a.

With Eqs. (2.94) and (2.95) at hand, it is now straightforward to show that the matrices $\hat{R}^{(1)}$ and $\hat{R}^{(2)}$ introduced in Eqs. (2.90) are independent of the renormalization scheme and the form of the operators considered. The actual proof will be given in the following scetion. Next, $\vec{A}^{(0)}$, $\vec{A}^{(1)}$ and $\vec{A}^{(2)}$, obtained from the calculation in the full theory, clearly do not depend on the particular choice adopted for the renormalization of operators. In consequence, the factor to the right of $\hat{U}^{(0)}(\mu, \mu_0)$ in $\vec{C}(\mu)$, as given in Eq. (2.89), which is related to the upper end of the evolution, is independent of the renormalization scheme. The same is true for the LO evolution matrix $\hat{U}^{(0)}(\mu, \mu_0)$. However, $\vec{C}(\mu)$ still depends on the renormalization scheme through $\hat{K}(\mu)$ and consequently on $\hat{J}^{(1)}$ and $\hat{J}^{(2)}$, entering the Wilson coefficients to the left of $\hat{U}^{(0)}(\mu, \mu_0)$. As is evident from Eqs. (2.78) and (2.87), this dependence on the lower end of the evolution is canceled by the corresponding one of the matrix elements $\langle\vec{Q}^T(\mu)\rangle$, so that the effective Hamiltonian and hence also the resulting physical amplitudes are scheme independent as it has to be.

2.3.4 Scheme Independence

In order to proof the scheme independence of the matrices $\hat{R}^{(1)}$ and $\hat{R}^{(2)}$ introduced in Eqs. (2.90), we start from the anomalous dimensions in the reference scheme $\hat{\gamma}_0^{(1)}$ and $\hat{\gamma}_0^{(2)}$. These matrices can be accessed from any arbitrary scheme a using Eqs. (2.94) and (2.95). Let us transpose the latter equations and eliminate $\hat{\gamma}_a^{(1)\,T}$ and $\hat{\gamma}_a^{(2)\,T}$ by means of Eqs. (2.84). Finally, dropping the unnecessary subscript a, we obtain

$$\begin{aligned}
\hat{\gamma}_0^{(1)\,T} &= \frac{\beta_1}{\beta_0}\hat{\gamma}^{(0)\,T} - \left[\hat{\gamma}^{(0)\,T}, \hat{R}^{(1)}\right] - 2\beta_0 \hat{R}^{(1)}\,, \\
\hat{\gamma}_0^{(2)\,T} &= \frac{\beta_2}{\beta_0}\hat{\gamma}^{(0)\,T} - \left[\hat{\gamma}^{(0)\,T}, \hat{R}^{(2)}\right] - \frac{\beta_1}{\beta_0}\left[\hat{\gamma}^{(0)\,T}, \hat{R}^{(1)}\right] + \left[\hat{\gamma}^{(0)\,T}, \hat{R}^{(1)}\right]\hat{R}^{(1)} \\
&\quad - 4\beta_0 \hat{R}^{(2)} - 2\beta_1 \hat{R}^{(1)} + 2\beta_0 \big(\hat{R}^{(1)}\big)^2\,,
\end{aligned} \tag{2.96}$$

which proves the scheme independence of $\hat{R}^{(1)}$ and $\hat{R}^{(2)}$.

It is important to emphasize that the renormalization scheme dependencies discussed here refers to the renormalization of operators only, and has to be distinguished from the renormalization scheme dependence of α_s. The issue of the latter scheme dependence in the context of the operator product expansion and renormalization group techniques is discussed in [84] and will not be repeated here.

2.3.5 Including QED Corrections

In this section we want to give the formulas relevant to resum QED logarithms up to NLO. If we neglect contributions of $O(\alpha^2)$ to the anomalous dimensions we can write

$$\hat{\gamma} = \frac{\alpha_s}{4\pi}\hat{\gamma}_s^{(0)} + \left(\frac{\alpha_s}{4\pi}\right)^2 \hat{\gamma}_s^{(0)} + \left(\frac{\alpha_s}{4\pi}\right)^3 \hat{\gamma}_s^{(0)} + \frac{\alpha}{4\pi}\hat{\gamma}_s^{(0)} + \frac{\alpha}{4\pi}\frac{\alpha_s}{4\pi}\hat{\gamma}_s^{(0)}. \tag{2.97}$$

Now we have a renormalization group equation with multiple coupling constants. Therefore we will keep the μ dependence explicitly in the integral equation for the evolution matrix

$$\hat{U}(\mu,\mu_0) = T_\mu \exp \int_{\mu_0}^{\mu} d\mu' \hat{\gamma}^T(\mu') \tag{2.98}$$

and compute the derivative of Eqs. (2.77) and (2.98) with respect to μ. For $\hat{K} = \hat{K}(g(\mu), e(\mu))$ we find the following differential equation:

$$\frac{\partial \hat{K}(g,e)}{\partial g} + \frac{\beta_e}{\beta}\frac{\partial \hat{K}(g,e)}{\partial e} + \frac{1}{g}\left[\frac{\hat{\gamma}^{(0)\,T}}{\beta_0}, \hat{K}(g,e)\right] = \left(\frac{\hat{\gamma}^T(g)}{\beta(g)} + \frac{1}{g}\frac{\hat{\gamma}^{(0)\,T}}{\beta_0}\right)\hat{K}(g,e)\,. \tag{2.99}$$

Since α varies very slowly for $m_b \le \mu \le M_W$ we will in the following neglect the running of the electromagnetic coupling. This corresponds to setting β_e/β to zero.

To proceed further we expand the matrices $\hat{K}$ and $\hat{K}^{-1}$ in powers of α and α_s

$$\begin{aligned}
\hat{K} &= \left(\hat{1} + \frac{\alpha}{4\pi} J_{se}\right) \left(\frac{\alpha_s(\mu)}{4\pi}\hat{J}^{(1)} + \left(\frac{\alpha_s(\mu)}{4\pi}\right)^2 \hat{J}^{(2)}\right) \left(\hat{1} + \frac{\alpha}{\alpha_s(\mu)} J_e\right) \\
\hat{K}^{-1} &= \left(\hat{1} - \frac{\alpha}{\alpha_s(\mu_0)} J_e\right) \left(\hat{1} - \frac{\alpha_s(\mu_0)}{4\pi}\hat{J}^{(1)} - \left(\frac{\alpha_s(\mu_0)}{4\pi}\right)^2 \left(\hat{J}^{(2)} - \left(\hat{J}^{(1)}\right)^2\right)\right) \\
&\qquad \times \left(\hat{1} - \frac{\alpha}{4\pi} J_{se}\right).
\end{aligned} \tag{2.100}$$

In order to get explicit expressions for the matrices J_e and J_{se} we define

$$\hat{J}_e^{(1)} = \hat{V}\hat{S}_e^{(1)}\hat{V}^{-1}, \qquad \hat{J}_{se}^{(1)} = \hat{V}\hat{S}_{es}^{(1)}\hat{V}^{-1} \tag{2.101}$$

and

$$\hat{G}_e = \hat{\gamma}_e, \qquad \hat{G}_{se} = \hat{\gamma}_{se}. \tag{2.102}$$

The matrix kernels are then given by

$$\begin{aligned}
S^1_{e_{ij}} &= \frac{G^0_{e_{ij}}}{2\beta_0\left(1 + a_j - a_i\right)}, \\
S^1_{se_{ij}} &= \frac{1}{2\beta_0(a_j - a_i)}\left[G^1_{se} + \left[G^0_e, S^1\right] - \frac{\beta_{se}}{\beta_0}G^0_s - \frac{\beta_1}{\beta_0}G^0_e\right]_{ij},
\end{aligned} \tag{2.103}$$

which agrees with the findings of Ref. [94]. Note that the matrices S_e and S_{se} can develop singularities for $a_i = a_j$ or $a_i = a_j + 1$. However these singularites will cancel in the expression for the evolution matrix if all contributions are taken into account.

We now expand the Wilson coefficients at a scale μ in powers of α and α_s

$$\begin{aligned}
\vec{C}(\mu) =& \vec{C}^{(0)}(\mu) + \frac{\alpha_s(\mu)}{4\pi}\vec{C}^{(1)}(\mu) + \left(\frac{\alpha_s(\mu)}{4\pi}\right)^2 \vec{C}^{(2)}(\mu) \\
&+ \frac{\alpha}{\alpha_s(\mu)}\vec{C}_e^{(0)}(\mu) + \frac{\alpha}{4\pi}\vec{C}_q^{(1)}(\mu)
\end{aligned} \tag{2.104}$$

to rewrite the general solution of the RGE equations (2.74) in terms of its individual contributions:

$$\begin{aligned}
&\vec{C}^{(0)}(\mu) = \hat{U}^{(0)}(\mu,\mu_0)\vec{C}^{(0)}(\mu_0), \\
&\vec{C}^{(1)}(\mu) = \eta\hat{U}^{(0)}(\mu,\mu_0)\,\vec{C}^{(1)}(\mu_0) + \hat{U}^{(1)}(\mu,\mu_0)\,\vec{C}^{(0)}(\mu_0), \\
&\vec{C}^{(2)}(\mu) = \eta^2\hat{U}^{(0)}(\mu,\mu_0)\,\vec{C}^{(2)}(\mu_0) + \eta\hat{U}^{(1)}(\mu,\mu_0)\,\vec{C}^{(1)}(\mu_0) + \hat{U}^{(2)}(\mu,\mu_0)\,\vec{C}^{(0)}(\mu_0), \\
&\vec{C}_e^{(0)}(\mu) = \hat{U}_e^{(0)}(\mu,\mu_0)\vec{C}^{(0)}(\mu_0), \\
&\vec{C}_e^{(1)}(\mu) = \eta\hat{U}_e^{(0)}(\mu,\mu_0)\,\vec{C}^{(1)}(\mu_0) + \hat{U}^{(0)}(\mu,\mu_0)\,\vec{C}_e^{(1)}(\mu_0) + \hat{U}_e^{(1)}(\mu,\mu_0)\,\vec{C}^{(0)}(\mu_0),
\end{aligned} \tag{2.105}$$

where we expanded the evolution matrix

$$\begin{aligned} U(\mu,\mu_0) = U^{(0)}(\mu,\mu_0) + \frac{\alpha_s(\mu)}{4\pi} U^{(1)}(\mu,\mu_0) + \left(\frac{\alpha_s(\mu)}{4\pi}\right)^2 U^{(2)}(\mu,\mu_0) \\ + \frac{\alpha}{\alpha_s(\mu)} U_e^{(0)}(\mu,\mu_0) + \frac{\alpha}{4\pi} U_e^{(1)}(\mu,\mu_0) \end{aligned} \tag{2.106}$$

in the coupling constants and find the following contributions to the individual evolution matrices:

$$\begin{aligned} U^{(1)}(\mu,\mu_0) &= J^{(1)} U^{(0)}(\mu,\mu_0) - \eta U^{(0)}(\mu,\mu_0) J^{(1)}\,, \\ U^{(2)}(\mu,\mu_0) &= J^{(2)} U^{(0)}(\mu,\mu_0) - \eta J^{(1)} U^{(0)}(\mu,\mu_0) J^{(1)} - \eta^2 U^{(0)}(\mu,\mu_0) \left(J^{(2)} - \left(J^{(1)}\right)^2\right)\,, \\ U_e^{(0)}(\mu,\mu_0) &= J_e U^{(0)}(\mu,\mu_0) - \eta^{-1} U^{(0)}(\mu,\mu_0) J_e\,, \\ U_e^{(1)}(\mu,\mu_0) &= J_s J_e U^{(0)}(\mu,\mu_0) + J_{se} U^{(0)}(\mu,\mu_0) - \eta^{-1} J_s U^{(0)}(\mu,\mu_0) J_e \\ &\quad + U^{(0)}(\mu,\mu_0) J_e J_s - U^{(0)}(\mu,\mu_0) J_{se} - \eta J_e U^{(0)}(\mu,\mu_0) J_s\,. \end{aligned} \tag{2.107}$$

Chapter 3

The Method

3.1 Extracting the Divergences

In the renormalization of QCD and QED at higher orders the standard method of extracting the UV divergence structure of a Feynman integral is to perform the calculation with massless propagators. However, if one uses massless propagators to compute three-point or higher Green's functions one might generate spurious IR infinities which, in dimensional regularization, cannot be distinguished from the UV divergences one seeks. There exist several methods [95,96] to overcome this problem, but they are generally quite involved and not suitable to the automated evaluation of a large number of diagrams. In the approach of [65] the so-called IR rearrangement is performed by introducing an artificial mass. For the calculation of the renormalization constants this means that we can safely apply Taylor expansion in the external momenta after introducing a non-zero auxiliary mass M for each internal propagator, including those of the massless vector particles. The auxiliary mass regulates all IR divergences and the renormalization constants can be extracted from the UV divergences of massive, one-scale tadpole diagrams that are known up to the four-loop level [97–100].

3.1.1 Infrared Divergences and External Momenta

Following references [25,65], the starting point of our procedure is the exact decomposition of a propagator:

$$\frac{1}{(k+p)^2 - m^2} = \frac{1}{k^2 - M^2} - \frac{p^2 + 2k \cdot p - m^2 + M^2}{k^2 - M^2} \frac{1}{(k+p)^2 - m^2} \,. \tag{3.1}$$

Here k is a linear combination of the integration momenta, p stands for a linear combination of the external momenta, and m denotes the mass of the propagating particle. If we assume that the dimensionality of the operators in our effective theory is bounded from above, and we apply recursively the above decomposition a sufficient number of times, we will reach the point where the overall degree of divergence of a certain diagram would become negative if any of its propagators were replaced by the last term in the decomposition. We are then allowed to drop the last term in the propagator decomposition, as it does not affect the UV divergent part of the Green's function after subtraction of all subdivergences.

As already mentioned in Section 2, another side effect of our IR regularization is that we have to consider insertions of non-physical effective operators in our calculation. Let us explain this point in more detail. Non-physical counterterms generally arise in QCD calculations, but the projections of their matrix elements on physical operators vanish unless the underlying symmetry is broken at some stage. Due to the exact nature of the decomposition Eq. (3.1), the UV poles of the diagrams obtained by our method are correct after the subtraction of all subdivergences. However, the UV poles related to subdivergences and their subtraction terms both depend on the finite parts of certain lower loop diagrams, which in our approach are not necessarily correct and do not comply with the usual Slavnov-Taylor identities. For instance, the introduction of the IR regulator invalidates the argument that guarantees vanishing on-shell matrix elements for the non-physical operators. One therefore expects non-negligible contributions to the counterterms from all possible operators with appropriate dimension. Consequently, all EOM-vanishing operators, gauge-invariant or not, and in general even BRST-exact operators must be included in the operator basis. The "incorrect" subdivergences are present in both counterterm and irreducible diagrams, but they cancel in their sum, provided the calculation is carried out in exactly the same way. The operator renormalization constants calculated in this way are correct for all the operators in the complete basis.

3.1.2 Truncating the Expansion

This algorithm can be also simplified by the following observation [65]. The terms containing powers of the auxiliary mass squared in the numerators contribute only to UV divergences that are proportional to those powers of M^2. The latter are local after the subtraction of all subdivergences, and must precisely cancel similar terms originating from integrals with no auxiliary mass in the numerators. Since the decomposition of Eq. (3.1) is exact, no dependence on M^2 can remain after performing the whole calculation. This observation allows one to avoid calculating integrals that contain an artificial mass in the numerator. Instead of calculating them, one can just replace them by local counterterms proportional to M^2 which cancel the corresponding subdivergences in the integrals with no M^2 in the propagator numerators. Nevertheless, the final result for the UV divergent parts of the Green's functions are precisely the same as if the full propagators were used.

The counterterms proportional to M^2 in general do not preserve the symmetry of the underlying theory, specifically they do not have to be gauge-invariant. Fortunately, the number of these counterterms is usually rather small, because their dimension must be two units less than the maximal dimension of the operators belonging to the effective theory. For instance, in QCD only a single possible gauge-variant operator exists that fulfills the above requirement. It looks like a gluon mass counterterm,

$$M^2 G^a_\mu G^{a\mu}\,, \tag{3.2}$$

and cancels gauge-variant pieces of integrals with no M^2 in the numerators. To ensure that our renormalization procedure with the fictitious gluon and photon mass is valid, we have checked explicitly the full $\overline{\text{MS}}$ renormalization of QCD and QED up to the three-loop level, finding perfect agreement with the results given in the literature [67–70]. In our case, beside the term in Eq. (3.2), we also have M^2 counterterms of dimension-three and four, some of which explicitly break gauge invariance:

$$\frac{M^2}{g^2} m_b \bar{s}_L b_R\,, \quad \frac{iM^2}{g^2}\bar{s}_L \not{\partial} b_L\,, \quad \frac{M^2 e}{g^2}\bar{s}_L \not{A} b_L\,, \quad \frac{M^2}{g}\bar{s}_L \not{G} b_L\,, \tag{3.3}$$

where A_μ denotes the photon field.

3.2 The Calculation

The large number of diagrams which occurs at higher orders makes it necessary to generate the diagrams automatically. For the evaluation of the ADM presented here all diagrams have been generated by the MATHEMATICA [101] package *FeynArts* [102], which provides the possibility to implement the Feynman rules for different Lagrangians in a simple way. We have adapted it to include the effective vertices induced by the operators Q_1–Q_{32}. We have processed the *FeynArts* output using two independent programs. In one case the output is converted into a format recognizable by the language FORM [103]. The group theory for each graph as well as the projection onto all possible form factors is performed before the integrals are evaluated. The very computation of the integrals is done with the program package `MATAD` [104], which is able to deal with vacuum diagrams at one-, two- and three-loop level where several of the internal lines may have a common mass. The calculation of the tadpole integrals in `MATAD` is based on the so-called integration-by-parts technique [105, 106]. The second program is entirely a MATHEMATICA code, which for the three-loop integrals uses the algorithm described in detail in [65].

3.2.1 Tensor Decomposition

In this section we will discuss how the reduction of tensor to scalar integral was performed in this work. We will give a prescription how to do this reduction for l-loop vacuum tensor integrals with one common mass scale, while trying to keep as near to the actual implementation of such a procedure to a computer algebra program as possible.

In general we will encounter the following l-loop tensor integrals, which can be denoted by:

$$T^{a_1 a_2 \ldots a_l}_{n_1 n_2 \ldots n_l n_{11} \ldots n_{1l} \ldots n_{l-1l}} = m^{-l \cdot D - \sum a_i + 2\sum n_i} \pi^{-l\, D/2} \int \frac{\prod_i d^D q_i \; q_{i\, \mu_{i,1}} \cdots q_{i\, \mu_{i,a_i}}}{\prod_i (q_i^2 + m^2)^{n_i} \prod_{i<j} ((q_i - q_j)^2 + m^2)^{n_{ij}}}. \tag{3.4}$$

The integral is massless, has no external momenta, and is symmetric under an exchange of indices

$$\mu_{i,j} \leftrightarrow \mu_{i,k}, \tag{3.5}$$

and will be proportional to a sum of symmetrized products of metric tensors. This symmetrized product of metric tensors can be most easily denoted by the number of metric tensors which contain indices of two given loop momenta. For example the symmetrized product of two metric tensors that both contain an index of the first and second loop momenta reads:

$$g_{\mu_{1,1}\,\mu_{2,1}} g_{\mu_{1,2}\,\mu_{2,2}} + g_{\mu_{1,1}\,\mu_{2,2}} g_{\mu_{1,2}\,\mu_{2,1}} \equiv \tag{3.6}$$

$$g\left[b_1 = 0, \ldots, b_l = 0, b_{12} = 2, \ldots, b_{1l} = 0, \ldots, b_{l-1l}\right] \tag{3.7}$$

The result of the general tensor integral (3.4) can then be written as a sum of the metric tensor products times some constant

$$T^{a_1\ldots a_l}_{n_1\ldots n_{l-1l}} = \sum_{b_i} F_{b_i} g\left[b_1,\ldots,b_{l-1l}\right]. \tag{3.8}$$

The constants F_{b_i} can be determined by contracting (3.8) with all products of metric tensors. Such a contraction will yield the same result for a contraction with products of metric tensors which can be related by the symmetry transformation (3.5). If we denote by $g^{(1)}\left[c_1,\ldots,c_{l-1l}\right]$ the first term of the sum of the products of the metric tensor as a representative of the corresponding symmetry we find a set of equations:

$$\begin{aligned}
&T^{a_1\ldots a_l}_{n_1\ldots n_{l-1l}} g^{(1)}\left[c_1,\ldots,c_{l-1l}\right] = \\
&m^{-l\cdot D-2\sum c_i+2\sum n_i}\pi^{-l\,D/2}\int \frac{\prod_i d^D q_i\ \prod_i (q_i,q_i)^{c_i}\prod_{i<j}(q_i,q_j)^{c_{ij}}}{\prod_i (q_i^2+m^2)^{n_i}\prod_{i<j}((q_i-q_j)^2+m^2)^{n_{ij}}} \equiv \\
&S^{c_1,\ldots,c_{l-1l}}_{n_1\ldots n_{l-1l}} = \sum_{b_i} g^{(1)}\left[c_1,\ldots,c_{l-1l}\right] g\left[b_1,\ldots,b_{l-1l}\right] F_{b_i},
\end{aligned} \tag{3.9}$$

which allows one to express the constants F_{b_i} by the inverse of the matrix

$$M^{a_i}_{c_i,b_i} = g^{(1)}\left[c_1,\ldots,c_{l-1l}\right] g\left[b_1,\ldots,b_{l-1l}\right], \tag{3.10}$$

where the indices b_i and c_i have to fulfill the following subsidiary condition:

$$2b_i + \sum_{j>i} b_{ij} = 2c_i + \sum_{j>i} c_{ij} = a_i. \tag{3.11}$$

Since these operations are independent of the particular form of the denominator, one can apply the tensor decomposition by the following replacement of loop momenta in the nominator of (3.4):

$$\prod_i q_{i\,\mu_{i,1}}\cdots q_{i\,\mu_{i,a_i}} \to \sum_{b_i,c_i}\prod_i (q_i,q_i)^{c_i}\prod_{i<j}(q_i,q_j)^{c_{ij}}\left(M^{a_i}_{c_i,b_i}\right)^{-1} g\left[b_1,\ldots,b_{l-1l}\right]. \tag{3.12}$$

3.2.2 Integrals

After expanding in the external momenta, going to euclidian space-time, and performing tensor decomposition, one is left with one-, two-, and three-loop integrals with one common mass. These integrals are shown in Fig. 3.1 and read:

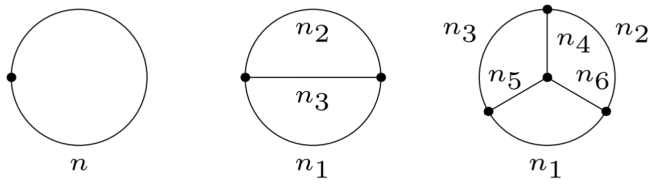

Figure 3.1: Scalar one-, two-, and three-loop integrals with one common mass. Each line denotes an arbitrary number of propagators of a given internal momenta combination.

$$I_n^{(1)} = m^{-D+2n}\,\pi^{-\frac{D}{2}}\int d^Dq\frac{1}{(q^2+m^2)^n} = \frac{\Gamma\left(n-\frac{D}{2}\right)}{\Gamma(n)},$$

$$I^{(2)}_{n_1n_2n_3} = m^{-2D+2\Sigma n_i}\,\pi^{-D}\int d^Dq_1\,d^Dq_2\frac{1}{(q_1^2+m^2)^{n_1}(q_2^2+m^2)^{n_2}((q_1-q_2)^2+m^2)^{n_3}},$$

$$I^{(3)}_{n_1n_2n_3n_4n_5n_6} = m^{-3D+2\Sigma n_i}\,\pi^{-\frac{3D}{2}}$$
$$\int\frac{d^Dq_1\,d^Dq_2\,d^Dq_3}{(q_1^2+m^2)^{n_1}(q_2^2+m^2)^{n_2}(q_3^2+m^2)^{n_3}((q_2-q_3)^2+m^2)^{n_4}((q_3-q_1)^2+m^2)^{n_5}((q_1-q_2)^2+m^2)^{n_6}}. \tag{3.13}$$

The two-loop integral reduces to a product of one-loop integrals in case of non-positive indices n_1, n_2, or, n_3, while for positive indices all integrals can be reduced with the help of the relation [107]

$$\begin{aligned} I^{(2)}_{(n_1+1)n_2n_3} =& \frac{1}{3n_1}\Big\{(3n_1-D)I^{(2)}_{n_1n_2n_3} \\ &+ n_2\left(I^{(2)}_{(n_1-1)(n_2+1)n_3} - I^{(2)}_{n_1(n_2+1)(n_3-1)}\right) \\ &+ n_3\left(I^{(2)}_{(n_1-1)n_2(n_3+1)} - I^{(2)}_{n_1(n_2-1)(n_3+1)}\right)\Big\} \end{aligned} \tag{3.14}$$

to

$$I^{(2)}_{111} = \frac{(\Gamma(1+\epsilon))^2}{(1-\epsilon)(1-2\epsilon)}\left(\frac{27}{2}s_2 - \frac{3}{2\epsilon^2}\right) + O(\epsilon), \tag{3.15}$$

where s_2 denotes the Clausen function.

As we are only interested in the UV divergent part of the three-loop vacuum integrals, we can study their behavior by considering the large energy behavior of two-point two-loop subdiagrams.

Let us exemplify this for the integral $I^{(3)}_{111111}$, where we consider the subdiagram

$$I^{(2)}_{11111}(q^2,m^2) = m^{-2D+10}\,\pi^{-D}$$
$$\int\frac{d^Dq_1\,d^Dq_2}{(q_1^2+m^2)(q_2^2+m^2)((q_1-q_2)^2+m^2)((q-q_1)^2+m^2)((q-q_2)^2+m^2)}. \tag{3.16}$$

and its momentum behavior at large q^2 [96]

$$I^{(2)}_{11111}(q^2, m^2) \to \left(\frac{m^2}{q^2}\right)^{5-D} \left(6\zeta_3 + O\left(\frac{m^2}{q^2}\right) + O(\epsilon)\right) \qquad \text{for} \quad q^2 \gg m^2\,. \tag{3.17}$$

Integrating this subdiagram we find the divergent parts of the integral

$$I^{(3)}_{111111} = 2\frac{\zeta_3}{\epsilon}. \tag{3.18}$$

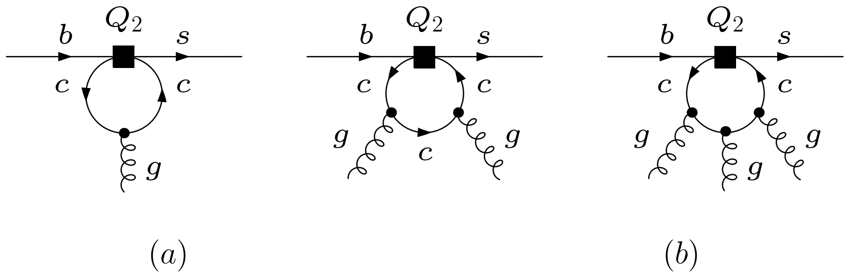

Figure 3.2: (a) Penguin insertion of Q_2. It will induce a mixing of Q_2 into Q_{12} in an off-shell calculation. Attaching an external quark to the gluon would immediately give the mixing of Q_2 into Q_4.(b) along with (a) is needed to renormalize the subdivergences which arise in the two-loop calculation.

3.3 Contributions of EOM-vanishing and BRST-exact Operators

In this section we shall study the contribution of EOM-vanishing and BRST-exact operators to our calculation. Given the complexity of this calculation we restrict ourself to some selected cases. We start with the contribution of EOM-vanishing operators to the $O(\alpha_s)$ and $O(\alpha_s^2)$ mixing of the current-current and QCD penguin operators.

3.3.1 Contribution of EOM-vanishing Operators to the QCD Mixing of Q_1–Q_6

Let us recall the definition (2.47) of

$$Q_{12} = \frac{1}{g}\bar{s}_L\gamma^\mu T^a b_L D^\nu G^a_{\mu\nu} + Q_4\,. \tag{3.19}$$

Its contribution to the QCD mixing of Q_1–Q_6 is twofold. The first comes due to the EOM structure, since Q_{12} consists of a term which is proportional to Q_4 and another term which is chosen such that the operator will vanish after applying the equation of motion for the gluon. A contribution to $Z_{i,11}$ will then give a corresponding contribution to $Z_{i,4}$, and the QCD penguin in Fig. 3.2 is contributing to the mixing of say Q_2 into Q_4. Secondly a two loop QCD calculation for the mixing of the current-current and QCD penguin operators generates subdivergences with external gluons. The two possible contributions are shown in Fig. 3.2.

At one-loop level only Q_{11} and Q_{12} are needed as nonphysical counterterms for Q_1–Q_6, as can be seen in Eq. (B.4). Since

$$Q_{11} = \frac{e}{g^2}\bar{s}_L\gamma^\mu b_L\partial^\nu F_{\mu\nu} + \frac{e^2}{g^2}(\bar{s}_L\gamma_\mu b_L)\sum\nolimits_f Q_f(\bar{f}\gamma^\mu f)\,, \tag{3.20}$$

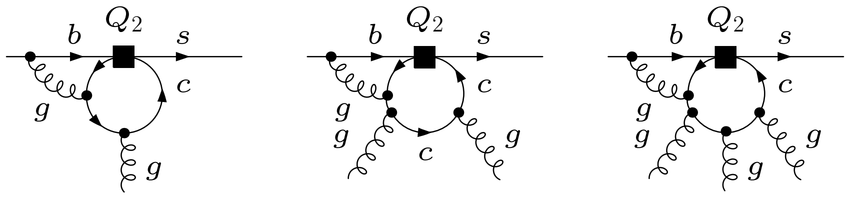

Figure 3.3: Some of the two-loop 1PI diagrams which mix Q_2 into $N_1^{(1)}$ and $N_1^{(2)}$–$N_{10}^{(2)}$.

does not contribute to a pure QCD calculation all possible subdivergences containing gluons can be subtracted using Q_{12}.

In case of a QED calculation Q_{11} will play a similar role as does Q_{12} in QCD. In particular it will induce a mixing into the electroweak penguin operator Q_3^Q.

The situation gets more difficult on the three-loop level. In order to remove the UV poles related to the two-loop subdiagrams with insertions of Q_1–Q_6 depicted in Fig. 3.3, another ten EOM-vanishing operators Q_{13}–Q_{21}, Q_{23}–Q_{24} need to be considered.

It is important to remark that the EOM-vanishing operators introduced in Eqs. (2.47) and (2.48) arise as counterterms independently of what kind of IR regularization is adopted in the computation of the anomalous dimensions of Q_1–Q_6. However, if the regularization respects the underlying symmetry, and all the diagrams are calculated without expansion in the external momenta, non-physical operators have vanishing matrix elements [77,79,81–83]. In this case the EOM-vanishing operators given in Eqs. (2.47) and (2.48) play no role in the calculation of the mixing of physical operators. If the gauge symmetry is broken this is no longer the case, as diagrams with insertions of non-physical operators will generally have non-vanishing projection on the physical operators. Since our IR regularization implies a massive gluon propagator, non-physical counterterms play a crucial role at intermediate stages of the anomalous dimensions calculation.

3.3.2 Contribution of BRST-exact Operators to the QCD Mixing of Q_1–Q_6

In contrast to the case of the two-loop mixing of the magnetic operators considered in [25,46], it is a priori not clear if BRST-exact operators do arise as counterterms of Q_1–Q_6. Since the BRST variation raises both ghost number and mass dimension by one unit, it is evident that any BRST-exact operator that potentially could mix with Q_1–Q_6 has to be a BRST variation of a dimension-five operator containing a single anti-ghost field. The only possibility for the latter operator having the correct chirality structure is given in the R_ξ

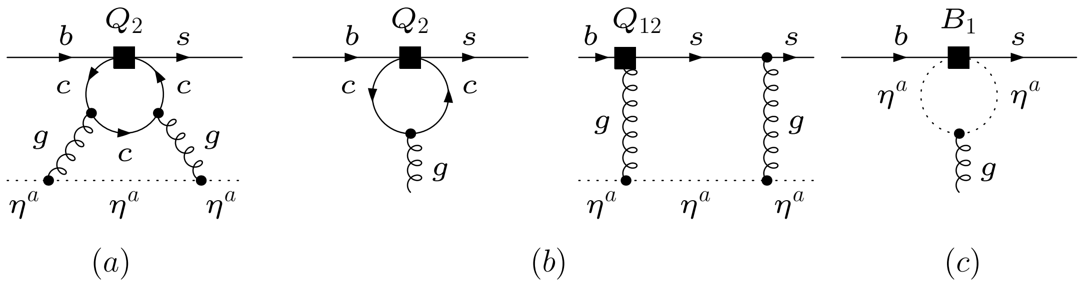

Figure 3.4: (a) A typical example of a divergent two-loop 1PI diagram which potentially could introduce a mixing of Q_2 into B_1. (b) A typical example of a counterterm contribution needed to renormalize the corresponding two-loop 1PI diagrams. (c) The one-loop matrix element of B_1 which has a non-vanishing on-shell projection on Q_4 if a non-zero ghost mass is used in the calculation.

gauge by (2.49)

$$
\begin{aligned}
B_1 &= s\left[\frac{1}{g}\left(\partial_{\mu_1}\bar{\eta}^a\right)\left(\bar{s}_L\gamma^{\mu_1}T^a b_L\right)\right] \\
&= -\frac{1}{g}\left[\frac{1}{\xi}\partial_{\mu_1}\partial^{\mu_2}G^a_{\mu_2} + g f^{abc}\left(\partial_{\mu_1}\bar{\eta}^b\right)\eta^c\right]\left(\bar{s}_L\gamma^{\mu_1}T^a b_L\right) \ ,
\end{aligned}
\tag{3.21}
$$

where s denotes the BRST operator, η^a and $\bar{\eta}^a$ are the ghost and anti-ghost fields, f^{abc} are the totally antisymmetric structure constants of $SU(3)_C$ and ξ is the covariant gauge-parameter.

Although there is no obvious reason why B_1 should not appear as a counterterm of Q_1–Q_6, it turns out that up to three loops B_1 does not play a role in the mixing of physical operators considered in this work. The key observation thereby is that the overall contribution from the two-loop 1PI diagrams depicted in Fig. 3.4 (a) is canceled by the corresponding counterterm contribution as shown in Fig. 3.4 (b), so that the associated renormalization constant is exactly zero at $O(\alpha_s^2)$. Therefore B_1 does not contribute to the mixing of Q_1–Q_6 into Q_4, although its one-loop $O(\alpha_s)$ matrix element displayed in Fig. 3.4 (c) does not vanish if it is computed using a non-vanishing ghost mass to regulate IR divergences.

3.4 Anomalous Dimension Matrix

In this section we will present our results for the anomalous dimensions describing the mixing of the four-quark operators Q_1–Q_6 up to $O(\alpha_s^3)$ for an arbitrary number of quark flavours denoted by N_f. In addition we will also give the anomalous dimension for the physical operators, Q_1–Q_6, Q_3^Q–Q_6^Q, and Q_7–Q_{10}, up to $O(\alpha_s\alpha)$ and $O(\alpha_s^2)$.

Let us recall the expression (2.70) where the anomalous dimension matrices is expressed in terms of the operator renormalization constants. For the physical operators there is no finite renormalization in the $\overline{\text{MS}}$ scheme and we can write up to $O(\alpha_s^3)$ and $O(\alpha_s\alpha)$:

$$
\begin{aligned}
\hat{\gamma}^{(0)} &= 2\hat{Z}^{(1,1)}\,, \\
\hat{\gamma}^{(1)} &= 4\hat{Z}^{(2,1)} - 2\hat{Z}^{(1,1)}\hat{Z}^{(1,0)}\,, \\
\hat{\gamma}^{(2)} &= 6\hat{Z}^{(3,1)} - 4\hat{Z}^{(2,1)}\hat{Z}^{(1,0)} - 2\hat{Z}^{(1,1)}\hat{Z}^{(2,0)} \\
\hat{\gamma_e} &= 2\hat{Z_e}^{(1,1)}\,, \\
\hat{\gamma_{es}} &= 4\hat{Z_{es}}^{(2,1)} - 2\hat{Z_e}^{(1,1)}\hat{Z_s}^{(1,0)} - 2\hat{Z_s}^{(1,1)}\hat{Z_e}^{(1,0)}\,.
\end{aligned}
\tag{3.22}
$$

The relevant matrices $\hat{Z}^{(1,0)}$, $\hat{Z}^{(1,1)}$, $\hat{Z}^{(2,0)}$ and $\hat{Z}^{(2,1)}$ are found by calculating various one- and two-loop diagrams with a single insertion of Q_1–Q_6, Q_3^Q–Q_6^Q, Q_7–Q_{10}, $E_1^{(1)}$–$E_4^{(1)}$, and $E_1^{(2)}$–$E_4^{(2)}$, whereas the matrix $\hat{Z}^{(3,1)}$ requires the computation of three-loop diagrams with insertions of Q_1–Q_6 as shown in Fig. 2.2. The pole and constants parts of these one-, two- and three-loop diagrams are evaluated using the method we have described in detail [46]. We perform the calculation off-shell in an arbitrary R_ξ gauge which allows us to explicitly check the gauge-parameter independence of the mixing among physical operators.

Having summarized the general formalism and our method, we will now present our results. First we will give the mixing of Q_1–Q_6 up to order α_s^3 for an arbitrary number of flavours N_f. For completeness we start with the regularization- and renormalization-scheme independent matrix $\hat{\gamma}^{(0)}$, which is given by

$$
\hat{\gamma}^{(0)} = \begin{pmatrix}
-4 & \frac{8}{3} & 0 & -\frac{2}{9} & 0 & 0 \\
12 & 0 & 0 & \frac{4}{3} & 0 & 0 \\
0 & 0 & 0 & -\frac{52}{3} & 0 & 2 \\
0 & 0 & -\frac{40}{9} & -\frac{160}{9}+\frac{4}{3}N_f & \frac{4}{9} & \frac{5}{6} \\
0 & 0 & 0 & -\frac{256}{3} & 0 & 20 \\
0 & 0 & -\frac{256}{9} & -\frac{544}{9}+\frac{40}{3}N_f & \frac{40}{9} & -\frac{2}{3}
\end{pmatrix}\,.
\tag{3.23}
$$

While the matrix $\hat{\gamma}^{(0)}$ is renormalization-scheme-independent, $\hat{\gamma}^{(1)}$ and $\hat{\gamma}^{(2)}$ are not. In the $\overline{\text{MS}}$ scheme supplemented by the definition of evanescent operators given in Eqs. (2.50), (2.51) and (2.52) we obtain

$$
\hat{\gamma}^{(1)} = \begin{pmatrix}
-\frac{145}{3}+\frac{16}{9}N_f & -26+\frac{40}{27}N_f & -\frac{1412}{243} & -\frac{1369}{243} & \frac{134}{243} & -\frac{35}{162} \\
-45+\frac{20}{3}N_f & -\frac{28}{3} & -\frac{416}{81} & \frac{1280}{81} & \frac{56}{81} & \frac{35}{27} \\
0 & 0 & -\frac{4468}{81} & -\frac{29129}{81}-\frac{52}{9}N_f & \frac{400}{81} & \frac{3493}{108}-\frac{2}{9}N_f \\
0 & 0 & -\frac{13678}{243}+\frac{368}{81}N_f & -\frac{79409}{243}+\frac{1334}{81}N_f & \frac{509}{486}-\frac{8}{81}N_f & \frac{13499}{648}-\frac{5}{27}N_f \\
0 & 0 & -\frac{244480}{81}-\frac{160}{9}N_f & -\frac{79409}{243}-\frac{1334}{81}N_f & \frac{23116}{81}+\frac{16}{9}N_f & \frac{3886}{27}+\frac{148}{9}N_f \\
0 & 0 & \frac{77600}{243}-\frac{1264}{81}N_f & -\frac{28808}{243}-\frac{164}{81}N_f & -\frac{20324}{243}+\frac{400}{81}N_f & -\frac{21211}{162}+\frac{622}{27}N_f
\end{pmatrix}, \tag{3.24}
$$

and

$$
\hat{\gamma}^{(2)} = \begin{pmatrix}
-\frac{1927}{2}+\frac{257}{9}N_f+\frac{40}{9}N_f^2+\left(224+\frac{160}{3}N_f\right)\zeta_3 & \frac{475}{9}+\frac{362}{27}N_f-\frac{40}{27}N_f^2-\left(\frac{896}{3}+\frac{320}{9}N_f\right)\zeta_3 \\
\frac{307}{2}+\frac{361}{3}N_f-\frac{20}{3}N_f^2-\left(1344+160N_f\right)\zeta_3 & \frac{1298}{3}-\frac{76}{3}N_f-224\zeta_3 \\
0 & 0 \\
0 & 0 \\
0 & 0 \\
0 & 0
\end{pmatrix.
$$

$$
\begin{matrix}
\frac{269107}{13122}-\frac{2288}{729}N_f-\frac{1360}{81}\zeta_3 & -\frac{2425817}{13122}+\frac{30815}{4374}N_f-\frac{776}{81}\zeta_3 \\
\frac{69797}{2187}+\frac{904}{243}N_f+\frac{2720}{27}\zeta_3 & \frac{1457549}{8748}-\frac{22067}{729}N_f-\frac{2768}{27}\zeta_3 \\
-\frac{4203068}{2187}+\frac{14012}{243}N_f-\frac{608}{27}\zeta_3 & -\frac{18422762}{2187}+\frac{888605}{2916}N_f+\frac{272}{27}N_f^2+\left(\frac{39824}{27}+160N_f\right)\zeta_3 \\
-\frac{5875184}{6561}+\frac{217892}{2187}N_f+\frac{472}{81}N_f^2+\left(\frac{27520}{81}+\frac{1360}{9}N_f\right)\zeta_3 & -\frac{70274587}{13122}+\frac{8860733}{17496}N_f-\frac{4010}{729}N_f^2+\left(\frac{16592}{81}+\frac{2512}{27}N_f\right)\zeta_3 \\
-\frac{194951552}{2187}+\frac{358672}{81}N_f-\frac{2144}{81}N_f^2+\frac{87040}{27}\zeta_3 & -\frac{130500332}{2187}-\frac{2949616}{729}N_f+\frac{3088}{27}N_f^2+\left(\frac{238016}{27}+640N_f\right)\zeta_3 \\
\frac{162733912}{6561}-\frac{2535466}{2187}N_f+\frac{17920}{243}N_f^2+\left(\frac{174208}{81}+\frac{12160}{9}N_f\right)\zeta_3 & \frac{13286236}{6561}-\frac{1826023}{4374}N_f-\frac{159548}{729}N_f^2-\left(\frac{24832}{81}+\frac{9440}{27}N_f\right)\zeta_3
\end{matrix} \tag{3.25}
$$

$$
\begin{pmatrix}
-\frac{343783}{52488}+\frac{392}{729}N_f+\frac{124}{81}\zeta_3 & -\frac{37573}{69984}+\frac{35}{972}N_f+\frac{100}{27}\zeta_3 \\
-\frac{37889}{8748}-\frac{28}{243}N_f-\frac{248}{27}\zeta_3 & \frac{366919}{11664}-\frac{35}{162}N_f-\frac{110}{9}\zeta_3 \\
\frac{674281}{4374}-\frac{1352}{243}N_f-\frac{496}{27}\zeta_3 & \frac{9284531}{11664}-\frac{2798}{81}N_f-\frac{26}{27}N_f^2-\left(\frac{1921}{9}+20N_f\right)\zeta_3 \\
\frac{2951809}{52488}-\frac{31175}{8748}N_f-\frac{52}{81}N_f^2-\left(\frac{3154}{81}+\frac{136}{9}N_f\right)\zeta_3 & \frac{3227801}{8748}-\frac{105293}{11664}N_f-\frac{65}{54}N_f^2+\left(\frac{200}{27}-\frac{220}{9}N_f\right)\zeta_3 \\
\frac{14732222}{2187}-\frac{27428}{81}N_f+\frac{272}{81}N_f^2-\frac{13984}{27}\zeta_3 & \frac{16521659}{2916}+\frac{8081}{54}N_f-\frac{316}{27}N_f^2-\left(\frac{22420}{9}+200N_f\right)\zeta_3 \\
-\frac{22191107}{13122}+\frac{395783}{4374}N_f-\frac{1720}{243}N_f^2-\left(\frac{33832}{81}+\frac{1360}{9}N_f\right)\zeta_3 & -\frac{32043361}{8748}+\frac{3353393}{5832}N_f-\frac{533}{81}N_f^2+\left(\frac{9248}{27}-\frac{1120}{9}N_f\right)\zeta_3
\end{pmatrix}.
$$

As far as the one- and two-loop self-mixing of the four-quark operators Q_1–Q_6, namely $\hat{\gamma}^{(0)}$ and $\hat{\gamma}^{(1)}$ are concerned, our results agree with those of [24], and therefore also with previous results [22, 23] that were obtained in a different operator basis [84]. We will come back to this point later. On the other hand, the three-loop self-mixing of Q_1–Q_6 described by $\hat{\gamma}^{(2)}$, is entirely new and has never been given before. As it is characteristic for three-loop anomalous dimensions the entries of $\hat{\gamma}^{(2)}$ contain terms proportional to the Riemann zeta function ζ_3.

Let us now turn to the mixing of the complete physical operator basis Q_1–Q_6, Q_3^Q–Q_6^Q, and Q_7–Q_{10}. Keeping the application to B-decays in mind we will give the results for $N_f = 5$ active flavours and start for completeness with the regularization- and renormalization-scheme independent matrix $\hat{\gamma}^{(0)}$ and $\hat{\gamma}_e$ which are given by

$$\hat{\gamma}^{(0)} = \begin{pmatrix}
-4 & \frac{8}{3} & 0 & -\frac{2}{9} & 0 & 0 & 0 & 0 & 0 & 0 & 0 & 0 & -\frac{32}{27} & 0 \\
12 & 0 & 0 & \frac{4}{3} & 0 & 0 & 0 & 0 & 0 & 0 & 0 & 0 & -\frac{8}{9} & 0 \\
0 & 0 & 0 & -\frac{52}{3} & 0 & 2 & 0 & 0 & 0 & 0 & 0 & 0 & -\frac{16}{9} & 0 \\
0 & 0 & -\frac{40}{9} & -\frac{100}{9} & \frac{4}{9} & \frac{5}{6} & 0 & 0 & 0 & 0 & 0 & 0 & \frac{32}{27} & 0 \\
0 & 0 & 0 & -\frac{256}{3} & 0 & 20 & 0 & 0 & 0 & 0 & 0 & 0 & -\frac{112}{9} & 0 \\
0 & 0 & -\frac{256}{9} & \frac{56}{9} & \frac{40}{9} & -\frac{2}{3} & 0 & 0 & 0 & 0 & 0 & 0 & \frac{512}{27} & 0 \\
0 & 0 & 0 & -\frac{8}{9} & 0 & 0 & 0 & -20 & 0 & 2 & 0 & 0 & -\frac{272}{27} & 0 \\
0 & 0 & 0 & \frac{16}{27} & 0 & 0 & -\frac{40}{9} & -\frac{52}{3} & \frac{4}{9} & \frac{5}{6} & 0 & 0 & -\frac{32}{81} & 0 \\
0 & 0 & 0 & -\frac{128}{9} & 0 & 0 & 0 & -128 & 0 & 20 & 0 & 0 & -\frac{2768}{27} & 0 \\
0 & 0 & 0 & \frac{184}{27} & 0 & 0 & -\frac{256}{9} & -\frac{160}{3} & \frac{40}{9} & -\frac{2}{3} & 0 & 0 & -\frac{512}{81} & 0 \\
0 & 0 & 0 & 0 & 0 & 0 & 0 & 0 & 0 & 0 & -\frac{14}{3} & 0 & 0 & 0 \\
0 & 0 & 0 & 0 & 0 & 0 & 0 & 0 & 0 & 0 & -\frac{32}{9} & -6 & 0 & 0 \\
0 & 0 & 0 & 0 & 0 & 0 & 0 & 0 & 0 & 0 & 0 & 0 & -\frac{46}{3} & 0 \\
0 & 0 & 0 & 0 & 0 & 0 & 0 & 0 & 0 & 0 & 0 & 0 & 0 & -\frac{46}{3}
\end{pmatrix}, \tag{3.26}$$

and

$$
\hat{\gamma}_e = \begin{pmatrix}
-\frac{8}{3} & 0 & 0 & 0 & 0 & 0 & \frac{32}{27} & 0 & 0 & 0 & 0 & 0 & 0 & 0 \\
0 & -\frac{8}{3} & 0 & 0 & 0 & 0 & \frac{8}{9} & 0 & 0 & 0 & 0 & 0 & 0 & 0 \\
0 & 0 & 0 & 0 & 0 & 0 & \frac{76}{9} & 0 & -\frac{2}{3} & 0 & 0 & 0 & 0 & 0 \\
0 & 0 & 0 & 0 & 0 & 0 & -\frac{32}{27} & \frac{20}{3} & 0 & -\frac{2}{3} & 0 & 0 & 0 & 0 \\
0 & 0 & 0 & 0 & 0 & 0 & \frac{496}{9} & 0 & -\frac{20}{3} & 0 & 0 & 0 & 0 & 0 \\
0 & 0 & 0 & 0 & 0 & 0 & -\frac{512}{27} & \frac{128}{3} & 0 & -\frac{20}{3} & 0 & 0 & 0 & 0 \\
0 & 0 & \frac{40}{27} & 0 & -\frac{4}{27} & 0 & \frac{332}{27} & 0 & -\frac{2}{9} & 0 & 0 & 0 & 0 & 0 \\
0 & 0 & 0 & \frac{40}{27} & 0 & -\frac{4}{27} & \frac{32}{81} & \frac{20}{9} & 0 & -\frac{2}{9} & 0 & 0 & 0 & 0 \\
0 & 0 & \frac{256}{27} & 0 & -\frac{40}{27} & 0 & \frac{3152}{27} & 0 & -\frac{20}{9} & 0 & 0 & 0 & 0 & 0 \\
0 & 0 & 0 & \frac{256}{27} & 0 & -\frac{40}{27} & \frac{512}{81} & \frac{128}{9} & 0 & -\frac{20}{9} & 0 & 0 & 0 & 0 \\
0 & 0 & 0 & 0 & 0 & 0 & 0 & 0 & 0 & 0 & \frac{16}{9} & -\frac{8}{3} & 0 & 0 \\
0 & 0 & 0 & 0 & 0 & 0 & 0 & 0 & 0 & 0 & 0 & \frac{8}{9} & 0 & 0 \\
0 & 0 & 0 & 0 & 0 & 0 & 0 & 0 & 0 & 0 & 0 & 0 & -\frac{88}{9} & -4 \\
0 & 0 & 0 & 0 & 0 & 0 & 0 & 0 & 0 & 0 & 0 & 0 & -4 & -\frac{160}{9}
\end{pmatrix}, \tag{3.27}
$$

where the electroweak penguin operators have been placed between the QCD penguin operators and the magnetic operators. Our results agree with the ones given in the literature [28, 94, 108], except for the QED mixing of Q_9 and Q_{10} which has never been calculated before. This last mentioned mixing will be an essential ingredient to the study of electroweak effects in $B \to X_s \ell^+ \ell^-$. The order α_s^2 contributions to the anomalous dimension matrix are given by

$$
\begin{aligned}
\hat{\gamma}^{(1)} = & \left(\begin{matrix}
-\frac{355}{9} & -\frac{502}{27} & -\frac{1412}{243} & -\frac{1369}{243} & \frac{134}{243} & -\frac{35}{162} \\
-\frac{35}{3} & -\frac{28}{3} & -\frac{416}{81} & \frac{1280}{81} & \frac{56}{81} & \frac{35}{27} \\
0 & 0 & -\frac{4468}{81} & -\frac{31469}{81} & \frac{400}{81} & \frac{3373}{108} \\
0 & 0 & -\frac{8158}{243} & -\frac{59399}{243} & \frac{269}{486} & \frac{12899}{648} \\
0 & 0 & -\frac{251680}{81} & -\frac{128648}{81} & \frac{23836}{81} & \frac{6106}{27} \\
0 & 0 & \frac{58640}{243} & -\frac{26348}{243} & -\frac{14324}{243} & -\frac{2551}{162} \\
0 & 0 & \frac{832}{243} & -\frac{4000}{243} & -\frac{112}{243} & -\frac{70}{81} \\
0 & 0 & \frac{3376}{729} & \frac{6344}{729} & -\frac{280}{729} & \frac{55}{486} \\
0 & 0 & \frac{2272}{243} & -\frac{72088}{243} & -\frac{688}{243} & -\frac{1240}{81} \\
0 & 0 & \frac{45424}{729} & \frac{84236}{729} & -\frac{3880}{729} & \frac{1220}{243} \\
0 & 0 & 0 & 0 & 0 & 0 \\
0 & 0 & 0 & 0 & 0 & 0 \\
0 & 0 & 0 & 0 & 0 & 0 \\
0 & 0 & 0 & 0 & 0 & 0
\end{matrix} \right. \\
& \left. \begin{matrix}
0 & 0 & 0 & 0 & -\frac{232}{243} & \frac{167}{162} & -\frac{2272}{729} & 0 \\
0 & 0 & 0 & 0 & \frac{464}{81} & \frac{76}{27} & \frac{1952}{243} & 0 \\
0 & 0 & 0 & 0 & \frac{64}{81} & \frac{368}{27} & -\frac{6752}{243} & 0 \\
0 & 0 & 0 & 0 & -\frac{200}{243} & -\frac{1409}{162} & -\frac{2192}{729} & 0 \\
0 & 0 & 0 & 0 & -\frac{6464}{81} & \frac{13052}{27} & -\frac{84032}{243} & 0 \\
0 & 0 & 0 & 0 & -\frac{11408}{243} & -\frac{2740}{81} & -\frac{37856}{729} & 0 \\
-\frac{404}{9} & -\frac{3077}{9} & \frac{32}{9} & \frac{1031}{36} & -\frac{64}{243} & -\frac{368}{81} & -\frac{24352}{729} & 0 \\
-\frac{2698}{81} & -\frac{8035}{27} & -\frac{49}{162} & \frac{4493}{216} & \frac{776}{729} & \frac{743}{486} & \frac{54608}{2187} & 0 \\
-\frac{19072}{9} & -\frac{14096}{9} & \frac{1708}{9} & \frac{1622}{9} & \frac{6464}{243} & -\frac{7220}{81} & -\frac{227008}{729} & 0 \\
\frac{32288}{81} & -\frac{15976}{27} & -\frac{6692}{81} & -\frac{2437}{54} & \frac{63824}{729} & \frac{6700}{243} & \frac{551648}{2187} & 0 \\
0 & 0 & 0 & 0 & \frac{2600}{27} & 0 & 0 & 0 \\
0 & 0 & 0 & 0 & -\frac{2192}{81} & \frac{1975}{27} & 0 & 0 \\
0 & 0 & 0 & 0 & 0 & 0 & -\frac{232}{3} & 0 \\
0 & 0 & 0 & 0 & 0 & 0 & 0 & -\frac{232}{3}
\end{matrix} \right) ,
\end{aligned}
\tag{3.28}
$$

where the mixing of the electroweak penguin operators Q_3^Q–Q_6^Q are given for the first time in the basis of Sections 2.2.1 and 2.2.2. The self-mixing of the current-current, QCD penguin, and electroweak penguin operators is given in Refs. [22, 23], while the mixing of Q_1–Q_6

into Q_7–Q_8 is given in Refs. [109, 110], and of Q_1–Q_6 into Q_9–Q_{10} in Ref. [111]. We agree with all these findings. The mixing of the electoweak penguin operators into Q_7–Q_{10} is a new result, while the mixing of Q_7 and Q_8 confirms for the first time the findings of [25]. Now let us turn to the complete order $\alpha_s\alpha$ mixing

$$\hat{\gamma_{se}}^{(1)} = \left(\begin{array}{cccccccccccccc}
\frac{169}{9} & \frac{100}{27} & 0 & \frac{254}{729} & 0 & 0 & \frac{2272}{729} & \frac{122}{81} & 0 & \frac{49}{81} & -\frac{928}{729} & \frac{118}{243} & -\frac{11680}{2187} & -\frac{416}{81} \\
\frac{50}{3} & -\frac{8}{3} & 0 & \frac{1076}{243} & 0 & 0 & -\frac{1952}{243} & -\frac{748}{27} & 0 & \frac{82}{27} & -\frac{232}{243} & -\frac{92}{81} & -\frac{2920}{729} & -\frac{104}{27} \\
0 & 0 & 0 & \frac{11116}{243} & 0 & -\frac{14}{3} & -\frac{23488}{243} & \frac{6280}{27} & \frac{112}{9} & -\frac{538}{27} & -\frac{32}{243} & \frac{32}{81} & -\frac{39752}{729} & -\frac{136}{27} \\
0 & 0 & \frac{280}{27} & \frac{18763}{729} & -\frac{28}{27} & -\frac{35}{18} & \frac{31568}{729} & \frac{9481}{81} & -\frac{92}{27} & -\frac{1012}{81} & \frac{64}{729} & \frac{260}{243} & \frac{1024}{2187} & -\frac{448}{81} \\
0 & 0 & 0 & \frac{111136}{243} & 0 & -\frac{140}{3} & -\frac{233920}{243} & \frac{68848}{27} & \frac{1120}{9} & -\frac{5056}{27} & -\frac{23480}{243} & \frac{2096}{81} & -\frac{381344}{729} & -\frac{15616}{27} \\
0 & 0 & \frac{2944}{27} & \frac{193312}{729} & -\frac{280}{27} & -\frac{175}{9} & \frac{352352}{729} & \frac{116680}{81} & -\frac{752}{27} & -\frac{10147}{81} & -\frac{6464}{729} & \frac{3548}{243} & \frac{24832}{2187} & -\frac{7936}{81} \\
0 & 0 & -\frac{2240}{81} & \frac{39392}{729} & \frac{224}{81} & -\frac{92}{27} & -\frac{5888}{729} & \frac{13916}{81} & \frac{112}{27} & -\frac{812}{81} & -\frac{544}{729} & \frac{544}{243} & -\frac{90424}{2187} & -\frac{152}{81} \\
0 & 0 & \frac{2176}{243} & \frac{84890}{2187} & -\frac{184}{243} & -\frac{224}{81} & -\frac{2552}{2187} & \frac{15638}{243} & -\frac{176}{81} & -\frac{2881}{486} & -\frac{64}{2187} & -\frac{260}{729} & -\frac{1024}{6561} & \frac{448}{243} \\
0 & 0 & -\frac{23552}{81} & \frac{399776}{729} & \frac{2240}{81} & -\frac{752}{27} & -\frac{90944}{729} & \frac{90128}{81} & \frac{1120}{27} & -\frac{1748}{81} & -\frac{28936}{729} & \frac{3664}{243} & -\frac{910048}{2187} & -\frac{8000}{81} \\
0 & 0 & \frac{23296}{243} & \frac{933776}{2187} & -\frac{1504}{243} & -\frac{2030}{81} & \frac{1312}{2187} & \frac{102488}{243} & -\frac{1592}{81} & -\frac{6008}{243} & \frac{6464}{2187} & -\frac{15212}{729} & -\frac{24832}{6561} & \frac{7936}{243} \\
0 & 0 & 0 & 0 & 0 & 0 & 0 & 0 & 0 & 0 & -\frac{124}{27} & -\frac{52}{9} & 0 & 0 \\
0 & 0 & 0 & 0 & 0 & 0 & 0 & 0 & 0 & 0 & \frac{128}{81} & \frac{92}{27} & 0 & 0 \\
0 & 0 & 0 & 0 & 0 & 0 & 0 & 0 & 0 & 0 & 0 & 0 & -\frac{308}{9} & 16 \\
0 & 0 & 0 & 0 & 0 & 0 & 0 & 0 & 0 & 0 & 0 & 0 & 16 & -\frac{308}{9}
\end{array}\right). \tag{3.29}$$

It is given for the first time in the new basis. The mixing of the four quark operators has been calculated in the so-called "standard" basis in Refs. [23, 94] while the mixing of the current-current and the QCD penguin operators into the magnetic operators has been given only in Ref. [28]. We agree with their findings. The results for the mixing of the electroweak penguin operators into the magnetic ones, the complete mixing into Q_9 and Q_{10}, and the mixing of Q_7–Q_8 are entirely new.

The order α_s^3 contribution to the mixing of Q_1–Q_6 into Q_7–Q_8 has been calculated for the first time in Ref. [24]. We confirm their findings. The self-mixing of Q_1-Q_6, and the mixing into Q_9 and Q_{10} are given for the first time. The self-mixing is given in Eq. (3.25) for an arbitrary number of flavours. The order α_s^3 mixing into Q_7–Q_{10} reads for five flavours:

$$\hat{\gamma}^{(2)} = \begin{pmatrix} \cdot & \cdot & \cdot & \cdot & \cdot & \cdot & -\frac{13234}{2187} & \frac{13957}{2916} & -\frac{1359190}{19683}+\frac{6976}{243}\zeta_3 & 0 \\ \cdot & \cdot & \cdot & \cdot & \cdot & \cdot & \frac{20204}{729} & \frac{14881}{972} & -\frac{229696}{6561}-\frac{3584}{81}\zeta_3 & 0 \\ 0 & 0 & \cdot & \cdot & \cdot & \cdot & \frac{92224}{729} & \frac{66068}{243} & -\frac{1290092}{6561}+\frac{3200}{81}\zeta_3 & 0 \\ 0 & 0 & \cdot & \cdot & \cdot & \cdot & -\frac{184190}{2187} & -\frac{1417901}{5832} & -\frac{819971}{19683}-\frac{19936}{243}\zeta_3 & 0 \\ 0 & 0 & \cdot & \cdot & \cdot & \cdot & \frac{1571264}{729} & \frac{3076372}{243} & -\frac{16821944}{6561}+\frac{30464}{81}\zeta_3 & 0 \\ 0 & 0 & \cdot & \cdot & \cdot & \cdot & -\frac{1792768}{2187} & -\frac{3029846}{729} & -\frac{17787368}{19683}-\frac{286720}{243}\zeta_3 & 0 \\ 0 & 0 & 0 & 0 & 0 & 0 & ? & 0 & 0 & 0 \\ 0 & 0 & 0 & 0 & 0 & 0 & ? & ? & 0 & 0 \\ 0 & 0 & 0 & 0 & 0 & 0 & 0 & 0 & -\frac{9769}{27} & 0 \\ 0 & 0 & 0 & 0 & 0 & 0 & 0 & 0 & 0 & -\frac{9769}{27} \end{pmatrix} . \tag{3.30}$$

3.5 Transformation to the "Standard" Basis

In $n = 4$ dimensions, a change of the physical operators is always equivalent to a simple linear transformation

$$\vec{Q}' = \hat{R}\vec{Q}\,, \tag{3.31}$$

parameterized by a rotation matrix $\hat{R}$, which as long as $\hat{R}$ is μ-independent, affects the renormalization constants and the ADM in a trivial way:

$$\hat{Z}' = \hat{R}\hat{Z}\hat{R}^{-1}\,, \quad \text{and} \quad \hat{\gamma}' = \hat{R}\hat{\gamma}\hat{R}^{-1}\,. \tag{3.32}$$

In the framework of dimensional regularization, the transformation corresponding to the change of basis turns out to be more complicated, as it generally involves evanescent operators as well. This feature basically reflects the fact that in order to formulate consistently the dimensional regularization of a theory containing Fermionic degrees of freedom, the Dirac algebra has to be infinite-dimensional, which implies that evanescent operators are necessary to form a complete basis in $n = 4 - 2\epsilon$ dimensions. In consequence, specifying the evanescent operators is necessary to make precise the definition of the $\overline{\text{MS}}$ scheme in the effective theory beyond leading order, as can been seen for instance in Eqs. (3.22). Clearly, EOM-vanishing operators are irrelevant to the present discussion.

As long as the change of basis does not mix physical and evanescent operators, the ADM still changes in a trivial way. In particular, a linear transformation of evanescent operators does not affect the physical ADM at all. However, when the change of basis involves a mixing of evanescent into physical operators or vice versa, the situation turns out to be more complicated [24]. Indeed, as we will explain in a moment, the new ADM is still given by Eq. (3.32), but the presence of evanescent operators induces a finite renormalization constant for the physical operators in the new basis. In order to restore the standard $\overline{\text{MS}}$ scheme definitions, a change of scheme is therefore required.

Let us first consider a change of basis that consists of adding some evanescent operators to the physical ones:

$$\vec{Q}' = \vec{Q} + \hat{W}\vec{E}\,, \tag{3.33}$$

parameterized by the matrix $\hat{W}$. In this case the new ADM is still given by Eq. (3.32) because of the absence of mixing of evanescent into physical operators in the original basis. However, after the above transformation, the renormalization matrix corresponding to the physical operators in the new basis will contain a finite, non-vanishing contribution

$$\hat{Z}'^{(1,0)}_{QQ} = \hat{W}\hat{Z}^{(1,0)}_{EQ}\,, \tag{3.34}$$

where the subscript Q and E denotes an element of the physical and evanescent operators, respectively. In order to re-impose the standard $\overline{\text{MS}}$ conditions, the latter contribution must be removed by a change of scheme, implemented by Eq. (2.93).

The situation is very similar for a change of basis that consists of adding multiples of ϵ times physical operators to the evanescent ones:

$$\vec{E}' = \vec{E} + \epsilon\,\hat{U}\vec{Q}\,, \tag{3.35}$$

parameterized by the matrix $\hat{U}$. In this case the ADM is unchanged because of its finiteness. However, the renormalization matrix of the physical operators in the new basis will contain a finite, non-vanishing contribution as well:

$$\hat{Z}'^{(1,0)}_{QQ} = -\hat{Z}^{(1,1)}_{QE}\hat{U} \,. \tag{3.36}$$

Needless to say, the above contribution must again be removed by a suitable change of scheme, in order to abide by the standard $\overline{\text{MS}}$ renormalization conditions.

We therefore conclude in full generality that a change of basis in dimensional regularization is equivalent to a rotation plus a change of scheme. If we discount possible μ-dependent rotations of the operator basis, it should be clear from the discussion above that the most general change of basis comprises the three linear transformations of Eqs. (3.31), (3.33), and (3.35), as well as a rotation of the evanescent operators, which will be parameterized by the matrix $\hat{M}$ in what follows. In total we thus have

$$\vec{Q}' = \hat{R}\left(\vec{Q} + \hat{W}\vec{E}\right) \,, \quad \text{and} \quad \vec{E}' = \hat{M}\left(\epsilon\,\hat{U}\vec{Q} + \left[\hat{1} + \epsilon\,\hat{U}\hat{W}\right]\vec{E}\right) \,. \tag{3.37}$$

The corresponding residual finite renormalization can be derived with simple algebra. Up to second order in α_s we find

$$\begin{aligned}
\hat{Z}'^{(1,0)}_{QQ} &= \hat{R}\left[\hat{W}\hat{Z}^{(1,0)}_{EQ} - \left(\hat{Z}^{(1,1)}_{QE} + \hat{W}\hat{Z}^{(1,1)}_{EE} - \frac{1}{2}\hat{\gamma}^{(0)}\hat{W}\right)\hat{U}\right]\hat{R}^{-1} \,, \\
\hat{Z}'^{(2,0)}_{QQ} &= \hat{R}\left[\hat{W}\hat{Z}^{(2,0)}_{EQ} - \left(\hat{Z}^{(2,1)}_{QE} + \hat{W}\hat{Z}^{(2,1)}_{EE} - \frac{1}{4}\hat{\gamma}^{(1)}\hat{W} - \frac{1}{2}\hat{Z}^{(1,1)}_{QE}\hat{Z}^{(1,0)}_{EQ}\hat{W}\right.\right. \\
&\qquad \left.\left. -\frac{1}{2}\hat{W}\hat{Z}^{(1,1)}_{EE}\hat{Z}^{(1,0)}_{EQ}\hat{W} - \frac{1}{4}\hat{W}\hat{Z}^{(1,0)}_{EQ}\hat{\gamma}^{(0)}\hat{W} + \frac{1}{2}\beta_0\hat{W}\hat{Z}^{(1,0)}_{EQ}\hat{W}\right)\hat{U}\right]\hat{R}^{-1} \,.
\end{aligned} \tag{3.38}$$

With these expressions at hand, it is now straightforward to deduce how the ADM transforms under the change of basis as given in Eq. (3.37). Up to the NNLO order we obtain

$$\begin{aligned}
\hat{\gamma}'^{(0)} &= \hat{R}\hat{\gamma}^{(0)}\hat{R}^{-1} \,, \\
\hat{\gamma}'^{(1)} &= \hat{R}\hat{\gamma}^{(1)}\hat{R}^{-1} - \left[\hat{Z}'^{(1,0)}_{QQ}, \hat{\gamma}'^{(0)}\right] - 2\beta_0\hat{Z}'^{(1,0)}_{QQ} \,, \\
\hat{\gamma}'^{(2)} &= \hat{R}\hat{\gamma}^{(2)}\hat{R}^{-1} - \left[\hat{Z}'^{(2,0)}_{QQ}, \hat{\gamma}'^{(0)}\right] - \left[\hat{Z}'^{(1,0)}_{QQ}, \hat{\gamma}'^{(1)}\right] + \left[\hat{Z}'^{(1,0)}_{QQ}, \hat{\gamma}'^{(0)}\right]\hat{Z}'^{(1,0)}_{QQ} \\
&\quad - 4\beta_0\hat{Z}'^{(2,0)}_{QQ} - 2\beta_1\hat{Z}'^{(1,0)}_{QQ} + 2\beta_0\big(\hat{Z}'^{(1,0)}_{QQ}\big)^2 \,.
\end{aligned} \tag{3.39}$$

After these general considerations, let us discuss in some detail how the anomalous dimensions given in Eqs. (3.23), (3.24) and (3.25) are transformed in going to the basis of physical operators [22, 23, 84]

$$
\begin{aligned}
Q'_1 &= (\bar{s}^\alpha_L \gamma_{\mu_1} c^\beta_L)(\bar{c}^\beta_L \gamma^{\mu_1} b^\alpha_L)\,,\\
Q'_2 &= (\bar{s}^\alpha_L \gamma_{\mu_1} c^\alpha_L)(\bar{c}^\beta_L \gamma^{\mu_1} b^\beta_L)\,,\\
Q'_3 &= (\bar{s}^\alpha_L \gamma_{\mu_1} b^\alpha_L)\textstyle\sum_q(\bar{q}^\beta_L \gamma^{\mu_1} q^\beta_L)\,,\\
Q'_4 &= (\bar{s}^\alpha_L \gamma_{\mu_1} b^\beta_L)\textstyle\sum_q(\bar{q}^\beta_L \gamma^{\mu_1} q^\alpha_L)\,,\\
Q'_5 &= (\bar{s}^\alpha_L \gamma_{\mu_1} b^\alpha_L)\textstyle\sum_q(\bar{q}^\beta_R \gamma^{\mu_1} q^\beta_R)\,,\\
Q'_6 &= (\bar{s}^\alpha_L \gamma_{\mu_1} b^\beta_L)\textstyle\sum_q(\bar{q}^\beta_R \gamma^{\mu_1} q^\alpha_R)\,,
\end{aligned}
\tag{3.40}
$$

which we shall call "standard" basis from now on. In the above definitions α and β denote colour indices.

The one- and two-loop evanescent operators that accompany the "standard" basis can be found by imposing the requirements given in [22]. At the one-loop level they are

$$
\begin{aligned}
E'^{(1)}_1 &= (\bar{s}^\alpha_L \gamma_{\mu_1\mu_2\mu_3} c^\beta_L)(\bar{c}^\beta_L \gamma^{\mu_1\mu_2\mu_3} b^\alpha_L) - (16-4\epsilon)\,Q'_1\,,\\
E'^{(1)}_2 &= (\bar{s}^\alpha_L \gamma_{\mu_1\mu_2\mu_3} c^\alpha_L)(\bar{c}^\beta_L \gamma^{\mu_1\mu_2\mu_3} b^\beta_L) - (16-4\epsilon)\,Q'_2\,,\\
E'^{(1)}_3 &= (\bar{s}^\alpha_L \gamma_{\mu_1\mu_2\mu_3} b^\alpha_L)\textstyle\sum_q(\bar{q}^\beta_L \gamma^{\mu_1\mu_2\mu_3} q^\beta_L) - (16-4\epsilon)\,Q'_3\,,\\
E'^{(1)}_4 &= (\bar{s}^\alpha_L \gamma_{\mu_1\mu_2\mu_3} b^\beta_L)\textstyle\sum_q(\bar{q}^\beta_L \gamma^{\mu_1\mu_2\mu_3} q^\alpha_L) - (16-4\epsilon)\,Q'_4\,,\\
E'^{(1)}_5 &= (\bar{s}^\alpha_L \gamma_{\mu_1\mu_2\mu_3} b^\alpha_L)\textstyle\sum_q(\bar{q}^\beta_R \gamma^{\mu_1\mu_2\mu_3} q^\beta_R) - (4+4\epsilon)\,Q'_5\,,\\
E'^{(1)}_6 &= (\bar{s}^\alpha_L \gamma_{\mu_1\mu_2\mu_3} b^\beta_L)\textstyle\sum_q(\bar{q}^\beta_R \gamma^{\mu_1\mu_2\mu_3} q^\alpha_R) - (4+4\epsilon)\,Q'_6\,.
\end{aligned}
\tag{3.41}
$$

Following the same procedure, we find the following two-loop evanescent operators:

$$
\begin{aligned}
E'^{(2)}_1 &= (\bar{s}^\alpha_L \gamma_{\mu_1\mu_2\mu_3\mu_4\mu_5} c^\beta_L)(\bar{c}^\beta_L \gamma^{\mu_1\mu_2\mu_3\mu_4\mu_5} b^\alpha_L) - (256-224\epsilon)\,Q'_1\,,\\
E'^{(2)}_2 &= (\bar{s}^\alpha_L \gamma_{\mu_1\mu_2\mu_3\mu_4\mu_5} c^\alpha_L)(\bar{c}^\beta_L \gamma^{\mu_1\mu_2\mu_3\mu_4\mu_5} b^\beta_L) - (256-224\epsilon)\,Q'_2\,,\\
E'^{(2)}_3 &= (\bar{s}^\alpha_L \gamma_{\mu_1\mu_2\mu_3\mu_4\mu_5} b^\alpha_L)\textstyle\sum_q(\bar{q}^\beta_L \gamma^{\mu_1\mu_2\mu_3\mu_4\mu_5} q^\beta_L) - (256-224\epsilon)\,Q'_3\,,\\
E'^{(2)}_4 &= (\bar{s}^\alpha_L \gamma_{\mu_1\mu_2\mu_3\mu_4\mu_5} b^\beta_L)\textstyle\sum_q(\bar{q}^\beta_L \gamma^{\mu_1\mu_2\mu_3\mu_4\mu_5} q^\alpha_L) - (256-224\epsilon)\,Q'_4\,,\\
E'^{(2)}_5 &= (\bar{s}^\alpha_L \gamma_{\mu_1\mu_2\mu_3\mu_4\mu_5} b^\alpha_L)\textstyle\sum_q(\bar{q}^\beta_R \gamma^{\mu_1\mu_2\mu_3\mu_4\mu_5} q^\beta_R) - (16+128\epsilon)\,Q'_5\,,\\
E'^{(2)}_6 &= (\bar{s}^\alpha_L \gamma_{\mu_1\mu_2\mu_3\mu_4\mu_5} b^\beta_L)\textstyle\sum_q(\bar{q}^\beta_R \gamma^{\mu_1\mu_2\mu_3\mu_4\mu_5} q^\alpha_R) - (16+128\epsilon)\,Q'_6\,.
\end{aligned}
\tag{3.42}
$$

It turns out that in order to transform the ADM given in Eqs. (3.23), (3.24) and (3.25) from the initial set of operators to the "standard" basis, we have to introduce four additional one-loop evanescent operators:

$$
\begin{aligned}
E_5^{(1)} &= (\bar{s}_L\gamma_{\mu_1}b_L)\textstyle\sum_q(\bar{q}\gamma^{\mu_1}\gamma_5 q) - \frac{5}{3}Q_3 + \frac{1}{6}Q_5\,, \\
E_6^{(1)} &= (\bar{s}_L\gamma_{\mu_1}T^a b_L)\textstyle\sum_q(\bar{q}\gamma^{\mu_1}\gamma_5 T^a q) - \frac{5}{3}Q_4 + \frac{1}{6}Q_6\,, \\
E_7^{(1)} &= (\bar{s}_L\gamma_{\mu_1\mu_2\mu_3}b_L)\textstyle\sum_q(\bar{q}\gamma^{\mu_1\mu_2\mu_3}\gamma_5 q) - \frac{32}{3}Q_3 + \frac{5}{3}Q_5\,, \\
E_8^{(1)} &= (\bar{s}_L\gamma_{\mu_1\mu_2\mu_3}T^a b_L)\textstyle\sum_q(\bar{q}\gamma^{\mu_1\mu_2\mu_3}\gamma_5 T^a q) - \frac{32}{3}Q_4 + \frac{5}{3}Q_6\,,
\end{aligned}
\tag{3.43}
$$

as well as four additional two-loop evanescent operators:

$$
\begin{aligned}
E_5^{(2)} &= (\bar{s}_L\gamma_{\mu_1\mu_2\mu_3\mu_4\mu_5}b_L)\textstyle\sum_q(\bar{q}\gamma^{\mu_1\mu_2\mu_3\mu_4\mu_5}\gamma_5 q) - \frac{320}{3}Q_3 + \frac{68}{3}Q_5\,, \\
E_6^{(2)} &= (\bar{s}_L\gamma_{\mu_1\mu_2\mu_3\mu_4\mu_5}T^a b_L)\textstyle\sum_q(\bar{q}\gamma^{\mu_1\mu_2\mu_3\mu_4\mu_5}\gamma_5 T^a q) - \frac{320}{3}Q_4 + \frac{68}{3}Q_6\,, \\
E_7^{(2)} &= (\bar{s}_L\gamma_{\mu_1\mu_2\mu_3\mu_4\mu_5\mu_6\mu_7}b_L)\textstyle\sum_q(\bar{q}\gamma^{\mu_1\mu_2\mu_3\mu_4\mu_5\mu_6\mu_7}\gamma_5 q) - \frac{4352}{3}Q_3 + \frac{1040}{3}Q_5\,, \\
E_8^{(2)} &= (\bar{s}_L\gamma_{\mu_1\mu_2\mu_3\mu_4\mu_5\mu_6\mu_7}T^a b_L)\textstyle\sum_q(\bar{q}\gamma^{\mu_1\mu_2\mu_3\mu_4\mu_5\mu_6\mu_7}T^a\gamma_5 q) - \frac{4352}{3}Q_4 + \frac{1040}{3}Q_6\,.
\end{aligned}
\tag{3.44}
$$

It should be clear that the evanescent operators $E_5^{(1)}$–$E_8^{(1)}$ and $E_5^{(2)}$–$E_8^{(2)}$ are not needed as counterterms in the initial basis of operators. However, some linear combinations of them will become parts of either the physical or the evanescent operators in the "standard" basis through the change of basis given by Eq. (3.37).

The renormalization constant matrices entering Eq. (3.38) are found from one- and two-loop matrix elements of physical and evanescent operators. We give the relevant ones, as well as the matrices characterizing the change of basis in Appendix A Our final results for the residual finite renormalization read.

$$
\hat{Z}'^{(1,0)}_{QQ} = \begin{pmatrix}
-\frac{7}{3} & -1 & 0 & 0 & 0 & 0 \\
-2 & \frac{2}{3} & 0 & 0 & 0 & 0 \\
0 & 0 & \frac{178}{27} & -\frac{34}{9} & -\frac{164}{27} & \frac{20}{9} \\
0 & 0 & 1-\frac{1}{9}N_f & -\frac{25}{3}+\frac{1}{3}N_f & -2-\frac{1}{9}N_f & 6+\frac{1}{3}N_f \\
0 & 0 & -\frac{160}{27} & \frac{16}{9} & \frac{146}{27} & -\frac{2}{9} \\
0 & 0 & -2+\frac{1}{9}N_f & 6-\frac{1}{3}N_f & 3+\frac{1}{9}N_f & -\frac{11}{3}-\frac{1}{3}N_f
\end{pmatrix}.
\tag{3.45}
$$

At this point a comment concerning the computation of the renormalization constants involving the insertions of the additional evanescent operators is in order. Transforming the three-loop anomalous dimensions from the initial to the "standard" basis requires the knowledge of one- and two-loop diagrams with insertions of $E_5^{(1)}$–$E_8^{(1)}$ and $E_5^{(2)}$–$E_8^{(2)}$, which introduces traces with γ_5 into the calculation. In this context we follow [24], and avoid anticommutation of γ_5 in any Fermionic line containing an odd number of γ_5. Moreover

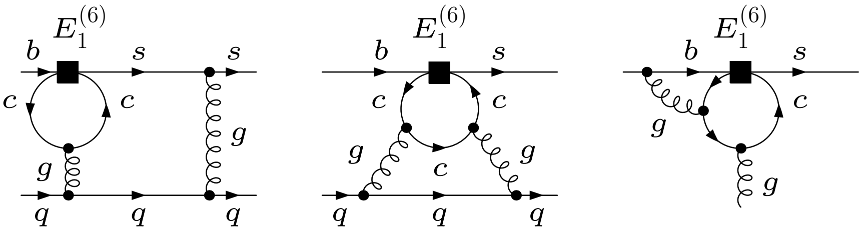

Figure 3.5: Typical examples of two-loop 1PI diagrams with an insertion of $E_1^{(6)}$ involving Dirac traces that contain γ_5.

we do not evaluate traces containing an even number of Dirac matrices and a single γ_5 in $n = 4 - 2\epsilon$ dimensions. This brings to life new evanescent structures like

$$E_{\mu_1\mu_2\mu_3\mu_4} = \mathrm{Tr}\left(\gamma_{\mu_1\mu_2\mu_3\mu_4}\gamma_5\right) - 4i\,(1 + a\epsilon)\,\epsilon_{\mu_1\mu_2\mu_3\mu_4} \tag{3.46}$$

in a natural way. Here a denotes an arbitrary parameter and $\epsilon_{\mu_1\mu_2\mu_3\mu_4}$ is the totally antisymmetric Lorentz-invariant tensor defined so that $\epsilon_{0123} = 1$. Apparently, these new evanescent structures have to be treated on the same footing as the "regular" evanescent operators introduced earlier on.

The idea of introducing more and more evanescent operators seems to make the use of an naive anticommuting γ_5 in multi-loop calculations involving chiral operators futile. Fortunately, for the problem at hand this is not the case: it turns out that the only new evanescent structure which affects the transformation of the three-loop anomalous dimensions between the initial and the "standard" basis is the one given in Eq. (3.46).

After performimg the basis transformation we agree with the ADM calculated in the standard basis:

$$\hat{\gamma}'^{(0)} = \begin{pmatrix} -2 & 6 & 0 & 0 & 0 & 0 \\ 6 & -2 & -\frac{2}{9} & \frac{2}{3} & -\frac{2}{9} & \frac{2}{3} \\ 0 & 0 & -\frac{22}{9} & \frac{22}{3} & -\frac{4}{9} & \frac{4}{3} \\ 0 & 0 & 6-\frac{2}{9}N_f & -2+\frac{2}{3}N_f & -\frac{2}{9}N_f & \frac{2}{3}N_f \\ 0 & 0 & 0 & 0 & 2 & -6 \\ 0 & 0 & -\frac{2}{9}N_f & \frac{2}{3}N_f & -\frac{2}{9}N_f & -16+\frac{2}{3}N_f \end{pmatrix}. \tag{3.47}$$

$$\hat{\gamma}'^{(1)} = \begin{pmatrix} -\frac{21}{2}-\frac{2}{9}N_f & \frac{7}{2}+\frac{2}{3}N_f & \frac{79}{9} & -\frac{7}{3} & -\frac{65}{9} & -\frac{7}{3} \\ \frac{7}{2}+\frac{2}{3}N_f & -\frac{21}{2}-\frac{2}{9}N_f & -\frac{202}{243} & \frac{1354}{81} & -\frac{1192}{243} & \frac{904}{81} \\ 0 & 0 & -\frac{5911}{486}+\frac{71}{9}N_f & \frac{5983}{162}+\frac{1}{3}N_f & -\frac{2384}{243}-\frac{71}{9}N_f & \frac{1808}{81}-\frac{1}{3}N_f \\ 0 & 0 & \frac{379}{18}+\frac{56}{243}N_f & -\frac{91}{6}+\frac{808}{81}N_f & -\frac{130}{9}-\frac{502}{243}N_f & -\frac{14}{3}+\frac{646}{81}N_f \\ 0 & 0 & -\frac{61}{9}N_f & -\frac{11}{3}N_f & \frac{71}{3}+\frac{61}{9}N_f & -99+\frac{11}{3}N_f \\ 0 & 0 & -\frac{682}{243}N_f & \frac{106}{81}N_f & -\frac{225}{2}+\frac{1676}{243}N_f & -\frac{1343}{6}+\frac{1348}{81}N_f \end{pmatrix}, \tag{3.48}$$

Chapter 4

Applications

4.1 Effective Hamiltonian for Non-leptonic B-Decays

The simplest application of the general formalism outlined in the previous sections is the case of non-leptonic B meson decays governed by the $b \to s$ transition. For simplicity we will therefore give explicit formulas for the $\Delta B = -\Delta S = 1$ decays only. However, it is straightforward to transform them to the other $|\Delta F| = 1$ cases. Neglecting contributions proportional to the small CKM factor $V_{us}^* V_{ub}$ which are of no concern to us here, the corresponding effective off-shell hamiltonian is given by

$$\mathcal{H}_{\text{eff}} = -\frac{4G_F}{\sqrt{2}} V_{ts}^* V_{tb} \left(\vec{Q}^T \vec{C}(\mu) + \vec{N}^T \vec{C}_N(\mu) + \vec{B}^T \vec{C}_B(\mu) + \vec{E}^T \vec{C}_E(\mu) \right) . \tag{4.1}$$

The specific structure of the gauge-invariant local operators $\vec{Q}$ is determined from the requirement that the hamiltonian reproduces the $\Delta B = -\Delta S = 1$ on-shell SM amplitudes at the leading order in the electroweak interactions, but to all orders in the strong coupling constants. In the process of renormalizing higher loop One-Particle-Irreducible (1PI) off-shell Green's functions with insertions of the operators $\vec{Q}$, there will in addition arise non-physical operators as counterterms, as discussed in the previous sections.

A set of physical operators $\vec{Q}$ that satisfies the requirement mentioned above consists of dimension-six operators [24, 26]

$$\begin{aligned}
Q_1 &= (\bar{s}_L \gamma_{\mu_1} T^a c_L)(\bar{c}_L \gamma^{\mu_1} T^a b_L) \,, \\
Q_2 &= (\bar{s}_L \gamma_{\mu_1} c_L)(\bar{c}_L \gamma^{\mu_1} b_L) \,, \\
Q_3 &= (\bar{s}_L \gamma_{\mu_1} b_L) \textstyle\sum_q (\bar{q} \gamma^{\mu_1} q) \,, \\
Q_4 &= (\bar{s}_L \gamma_{\mu_1} T^a b_L) \textstyle\sum_q (\bar{q} \gamma^{\mu_1} T^a q) \,, \\
Q_5 &= (\bar{s}_L \gamma_{\mu_1 \mu_2 \mu_3} b_L) \textstyle\sum_q (\bar{q} \gamma^{\mu_1 \mu_2 \mu_3} q) \,, \\
Q_6 &= (\bar{s}_L \gamma_{\mu_1 \mu_2 \mu_3} T^a b_L) \textstyle\sum_q (\bar{q} \gamma^{\mu_1 \mu_2 \mu_3} T^a q) \,,
\end{aligned} \tag{4.2}$$

and one dimension-five operator

$$Q_8 = \frac{1}{g} m_b (\bar{s}_L \sigma^{\mu_1 \mu_2} T^a b_R) G^a_{\mu_1 \mu_2} \,, \tag{4.3}$$

where we have used the abbreviations $\gamma_{\mu_1 \cdots \mu_n} = \gamma_{\mu_1} \cdots \gamma_{\mu_n}$, $\gamma^{\mu_1 \cdots \mu_n} = \gamma^{\mu_1} \cdots \gamma^{\mu_n}$ and $\sigma^{\mu_1 \mu_2} = i\,[\gamma^{\mu_1}, \gamma^{\mu_2}]/2$, and the sum over q extends over all light quark flavors. g is the strong coupling constant, q_L and q_R are the chiral quark fields, $G^a_{\mu_1 \mu_2}$ is the gluonic field strength tensor, and T^a are the generators of $SU(3)_C$, normalized so that $\mathrm{Tr}(T^a T^b) = \delta^{ab}/2$.

The physical operators given in Eqs. (4.2) and (4.3) include the current-current operators Q_1 and Q_2, the QCD penguin operators Q_3–Q_6 and the chromomagnetic moment operator Q_8. Notice that we have defined Q_1–Q_6 in such a way that problems connected with the treatment of γ_5 in $n = 4 - 2\epsilon$ dimensions do not arise [24]. Consequently, we are allowed to consistently use the NDR renormalization scheme throughout the calculation of the anomalous dimensions of the physical operators introduced above.

4.1.1 Initial Conditions for the Wilson Coefficients

Let us now turn to the initial conditions $\vec{C}(\mu_0)$ of the Wilson coefficients. Their values are found by matching the full to the effective theory amplitudes perturbatively in α_s. In the NLO and NNLO approximation this requires to calculate one- and two-loop diagrams both in the SM and the low-energy effective theory. Some of the SM two-loop 1PI diagrams one has to consider in order to find the $O(\alpha_s^2)$ corrections to $\vec{C}(\mu_0)$ are shown in Fig. 4.1. Restricting to the physical on-shell operators Q_1–Q_6 and setting $\mu_0 = M_W$ the obtained coefficients read in the NDR renormalization scheme:

$$\begin{aligned}
C_1(M_W) &= 15\frac{\alpha_s(M_W)}{4\pi} + \left(\frac{\alpha_s(M_W)}{4\pi}\right)^2 \left(\frac{7987}{72} + \frac{17}{3}\pi^2 - \widetilde{T}_0(x_t)\right) , \\
C_2(M_W) &= 1 + \left(\frac{\alpha_s(M_W)}{4\pi}\right)^2 \left(\frac{127}{18} + \frac{4}{3}\pi^2\right) , \\
C_3(M_W) &= \left(\frac{\alpha_s(M_W)}{4\pi}\right)^2 \widetilde{G}_1(x_t) , \\
C_4(M_W) &= \frac{\alpha_s(M_W)}{4\pi}\widetilde{E}_0(x_t) + \left(\frac{\alpha_s(M_W)}{4\pi}\right)^2 \widetilde{E}_1(x_t) , \\
C_5(M_W) &= \left(\frac{\alpha_s(M_W)}{4\pi}\right)^2 \left(\frac{14}{135} + \frac{2}{15}\widetilde{E}_0(x_t) - \frac{1}{10}\widetilde{G}_1(x_t)\right) , \\
C_6(M_W) &= \left(\frac{\alpha_s(M_W)}{4\pi}\right)^2 \left(\frac{7}{35} + \frac{1}{4}\widetilde{E}_0(x_t) - \frac{3}{16}\widetilde{G}_1(x_t)\right) ,
\end{aligned} \tag{4.4}$$

where $x_t = m_t^2/M_W^2$. The one-loop Inami-Lim [112] function $\widetilde{E}_0(x_t)$ characterizing the effective off-shell vertex involving a gluon reads:

$$\widetilde{E}_0(x_t) = -\frac{8 - 42x_t + 35x_t^2 - 7x_t^3}{12(x_t-1)^3} - \frac{4 - 16x_t - 9x_t^2}{6(x_t-1)^4} \ln x_t . \tag{4.5}$$

The top-quark loop contribution to the renormalization of the light quark and gluon wave functions on the SM side give rise to the one-loop function $\widetilde{T}_0(x_t)$. Subtracting the corresponding terms in the propagators in the so-called MOM scheme at $q^2 = 0$ one finds [13]:

$$\begin{aligned}
\widetilde{T}_0(x_t) &= \frac{112}{9} + 32x_t + \left(\frac{20}{3} + 16x_t\right) \ln x_t \\
&\quad - (8 + 16x_t)\sqrt{4x_t - 1}\,\mathrm{Cl}_2\left(2\arcsin\left(\frac{1}{2\sqrt{x_t}}\right)\right) ,
\end{aligned} \tag{4.6}$$

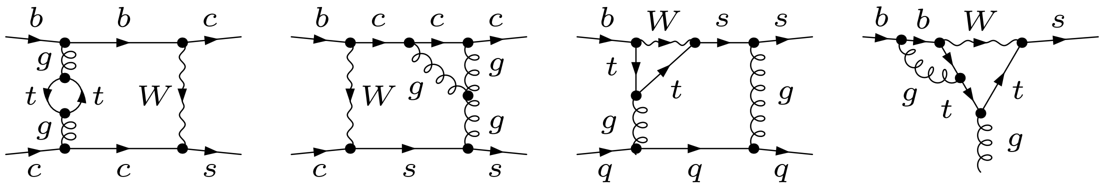

Figure 4.1: Some of the SM two-loop 1PI diagrams one has to calculate in order to find the Wilson coefficients of the four-quark operators Q_1–Q_6 at $O(\alpha_s^2)$.

with $\mathrm{Cl}_2(x) = \mathrm{Im}[\mathrm{Li}_2(e^{ix})]$ and $\mathrm{Li}_2(x) = -\int_0^x dt \ln(1-t)/t$. The remaining two-loop functions $\widetilde{E}_1(x_t)$ and $\widetilde{G}_1(x_t)$ take the following form [13]

$$\begin{aligned}
\widetilde{E}_1(x_t) = & -\frac{1120 - 12044x_t - 5121x_t^2 - 5068x_t^3 + 7289x_t^4}{648(x_t-1)^4} \\
& + \frac{380 - 7324x_t + 17702x_t^2 + 2002x_t^3 - 5981x_t^4 + 133x_t^5}{324(x_t-1)^5} \ln x_t \\
& + \frac{112 - 530x_t - 3479x_t^2 + 2783x_t^3 - 1129x_t^4 + 515x_t^5}{108(x_t-1)^5} \ln^2 x_t \\
& - \frac{40 - 190x_t - 81x_t^2 - 614x_t^3 + 515x_t^4}{54(x_t-1)^4} \mathrm{Li}_2(1-x_t) + \frac{10}{81}\pi^2 \,,
\end{aligned} \tag{4.7}$$

$$\begin{aligned}
\widetilde{G}_1(x_t) = & -\frac{554 - 2523x_t + 2919x_t^2 - 662x_t^3}{243(x_t-1)^3} \\
& + \frac{88 - 142x_t - 357x_t^2 + 100x_t^3 + 35x_t^4}{81(x_t-1)^4} \ln x_t + \frac{20 - 40x_t + 5x_t^2}{27(x_t-1)^2} \ln^2 x_t \\
& + \frac{40 - 160x_t - 30x_t^2 + 100x_t^3 - 10x_t^4}{27(x_t-1)^4} \mathrm{Li}_2(1-x_t) - \frac{20}{81}\pi^2 \,.
\end{aligned}$$

4.1.2 Renormalization Group Evolution

In this section we shall use the obtained ADM to find the explicit NNLO expressions for the Wilson coefficients

$$C_i(\mu_b) = C_i^{(0)}(\mu_b) + \frac{\alpha_s(\mu_b)}{4\pi} C_i^{(1)}(\mu_b) + \left(\frac{\alpha_s(\mu_b)}{4\pi}\right)^2 C_i^{(2)}(\mu_b) \,, \tag{4.8}$$

with $i = 1$–6, at the low-energy scale $\mu_b = O(m_b)$, which is appropriate for studying non-leptonic B meson decays. Using the general solution of the RGE given in Eq. (2.77), we arrive at

$$
\begin{aligned}
C_i^{(0)}(\mu_b) &= \sum_{j=1}^{6} c_{0,ij}^{(0)} \eta^{a_j} , \\
C_i^{(1)}(\mu_b) &= \sum_{j=1}^{6} \left(c_{0,ij}^{(1)} + c_{1,ij}^{(1)} \eta + e_{1,ij}^{(1)} \eta \widetilde{E}_0(x_t) \right) \eta^{a_j} , \\
C_i^{(2)}(\mu_b) &= \sum_{j=1}^{6} \Bigg(c_{0,ij}^{(2)} + c_{1,ij}^{(2)} \eta + c_{2,ij}^{(2)} \eta^2 + \left[e_{1,ij}^{(2)} \eta + e_{2,ij}^{(2)} \eta^2 \right] \widetilde{E}_0(x_t) \\
&\qquad + t_{2,ij}^{(2)} \eta^2 \widetilde{T}_0(x_t) + e_{1,ij}^{(1)} \eta^2 \widetilde{E}_1(x_t) + g_{2,ij}^{(2)} \eta^2 \widetilde{G}_1(x_t) \Bigg) \eta^{a_j} ,
\end{aligned}
\tag{4.9}
$$

where $\eta = \alpha_s(M_W)/\alpha_s(\mu_b)$ and

$$
\vec{a}^T = \begin{pmatrix} \frac{6}{23} & -\frac{12}{23} & 0.4086 & -0.4230 & -0.8994 & 0.1456 \end{pmatrix} \tag{4.10}
$$

$$
\hat{c}_0^{(0)} = \begin{pmatrix}
1 & -1 & 0 & 0 & 0 & 0 \\
\frac{2}{3} & \frac{1}{3} & 0 & 0 & 0 & 0 \\
\frac{2}{63} & -\frac{1}{27} & -0.0659 & 0.0595 & -0.0218 & 0.0335 \\
\frac{1}{21} & \frac{1}{9} & 0.0237 & -0.0173 & -0.1336 & -0.0316 \\
-\frac{1}{126} & \frac{1}{108} & 0.0094 & -0.0100 & 0.0010 & -0.0017 \\
-\frac{1}{84} & -\frac{1}{36} & 0.0108 & 0.0163 & 0.0103 & 0.0023
\end{pmatrix} \tag{4.11}
$$

$$
\hat{c}_0^{(1)} = \begin{pmatrix}
5.9606 & 1.0951 & 0 & 0 & 0 & 0 \\
1.9737 & -1.3650 & 0 & 0 & 0 & 0 \\
-0.5409 & 1.6332 & 1.6406 & -1.6702 & -0.2576 & -0.2250 \\
2.2203 & 2.0265 & -4.1830 & -0.7135 & -1.8215 & 0.7996 \\
0.0400 & -0.1861 & -0.1669 & 0.1887 & 0.0201 & 0.0304 \\
-0.2614 & -0.1918 & 0.4197 & 0.0295 & 0.1474 & -0.0640
\end{pmatrix} \tag{4.12}
$$

$$
\hat{c}_1^{(1)} = \begin{pmatrix}
2.0394 & 5.9049 & 0 & 0 & 0 & 0 \\
1.3596 & -1.9683 & 0 & 0 & 0 & 0 \\
0.0647 & 0.2187 & -0.4268 & -0.5165 & 0.2832 & -0.2034 \\
0.0971 & -0.6561 & 0.1534 & 0.1500 & 1.7355 & 0.1917 \\
-0.0162 & -0.0547 & 0.0606 & 0.0865 & -0.0128 & 0.0103 \\
-0.0243 & 0.1640 & 0.0700 & -0.1412 & -0.1339 & -0.0140
\end{pmatrix} \tag{4.13}
$$

$$
\hat{e}_1^{(1)} = \begin{pmatrix}
0 & 0 & 0 & 0 & 0 & 0 \\
0 & 0 & 0 & 0 & 0 & 0 \\
0 & 0 & -0.1933 & 0.1579 & 0.1428 & -0.1074 \\
0 & 0 & 0.0695 & -0.0459 & 0.8752 & 0.1012 \\
0 & 0 & 0.0274 & -0.0264 & -0.0064 & 0.0055 \\
0 & 0 & 0.0317 & 0.0432 & -0.0675 & -0.0074
\end{pmatrix} \tag{4.14}
$$

$$\hat{c}_0^{(2)} = \begin{pmatrix} 56.4723 & 22.2650 & 0 & 0 & 0 & 0 \\ 14.7825 & -11.7987 & 0 & 0 & 0 & 0 \\ 1.9906 & 19.2386 & -24.6846 & -12.9233 & -4.0085 & 2.0820 \\ 8.1141 & 42.7264 & -11.7014 & -35.4784 & -14.1041 & 4.9828 \\ -0.3660 & -1.2588 & 2.7564 & 0.6168 & 0.2854 & -0.2620 \\ -2.3243 & -3.5577 & 2.9357 & 2.4965 & 1.5568 & -0.4249 \end{pmatrix} \tag{4.15}$$

$$\hat{c}_1^{(2)} = \begin{pmatrix} 12.1560 & -6.4667 & 0 & 0 & 0 & 0 \\ 4.0252 & 8.0604 & 0 & 0 & 0 & 0 \\ -1.1032 & -9.6435 & 10.6219 & 14.5052 & 3.3472 & 1.3651 \\ 4.5281 & -11.9660 & -27.0825 & 6.19641 & 23.6695 & -4.8514 \\ 0.0816 & 1.0987 & -1.0803 & -1.6385 & -0.2612 & -0.1847 \\ -0.5332 & 1.1326 & 2.7171 & -0.2564 & -1.9149 & 0.3886 \end{pmatrix} \tag{4.16}$$

$$\hat{c}_2^{(2)} = \begin{pmatrix} 32.6228 & 49.8089 & 0 & 0 & 0 & 0 \\ 21.7486 & -16.6030 & 0 & 0 & 0 & 0 \\ 1.0357 & 1.8448 & -0.6393 & -6.6507 & 2.8568 & 0.7652 \\ 1.5535 & -5.5343 & 0.2298 & 1.9318 & 17.5067 & -0.7209 \\ -0.2589 & -0.4612 & 0.0907 & 1.1136 & -0.1290 & -0.0389 \\ -0.3884 & 1.3836 & 0.1049 & -1.8183 & -1.3504 & 0.0526 \end{pmatrix} \tag{4.17}$$

$$\hat{e}_1^{(2)} = \begin{pmatrix} 0 & 0 & 0 & 0 & 0 & 0 \\ 0 & 0 & 0 & 0 & 0 & 0 \\ 0 & 0 & 4.8111 & -4.4336 & 1.6880 & 0.7207 \\ 0 & 0 & -12.2667 & -1.8940 & 11.9366 & -2.5613 \\ 0 & 0 & -0.4893 & 0.5008 & -0.1317 & -0.0975 \\ 0 & 0 & 1.2307 & 0.0784 & -0.9657 & 0.2051 \end{pmatrix} \tag{4.18}$$

$$\hat{e}_2^{(2)} = \begin{pmatrix} 0 & 0 & 0 & 0 & 0 & 0 \\ 0 & 0 & 0 & 0 & 0 & 0 \\ 0 & 0 & -1.3169 & -0.7444 & 0.4827 & -1.2075 \\ 0 & 0 & 0.4733 & 0.2162 & 2.9582 & 1.1377 \\ 0 & 0 & 0.1869 & 0.1247 & -0.0218 & 0.0613 \\ 0 & 0 & 0.2161 & -0.2035 & -0.2282 & -0.0830 \end{pmatrix} \tag{4.19}$$

$$\hat{t}_2^{(2)} = \begin{pmatrix} -\frac{1}{3} & -\frac{2}{3} & 0 & 0 & 0 & 0 \\ -\frac{2}{9} & \frac{2}{9} & 0 & 0 & 0 & 0 \\ -\frac{2}{189} & -\frac{2}{81} & 0.0129 & 0.0497 & -0.0092 & -0.0182 \\ -\frac{1}{63} & \frac{2}{27} & -0.0046 & -0.0144 & -0.0562 & 0.0171 \\ \frac{1}{378} & \frac{1}{162} & -0.0018 & -0.0083 & 0.0004 & 0.0009 \\ \frac{1}{252} & -\frac{1}{54} & -0.0021 & 0.0136 & 0.0043 & -0.0012 \end{pmatrix} \tag{4.20}$$

$$\hat{g}_2^{(2)} = \begin{pmatrix} 0 & 0 & 0 & 0 & 0 & 0 \\ 0 & 0 & 0 & 0 & 0 & 0 \\ 0 & 0 & 0.7557 & -0.1643 & 0.0861 & 0.3224 \\ 0 & 0 & -0.2716 & 0.0477 & 0.5277 & -0.3038 \\ 0 & 0 & -0.1072 & 0.0275 & -0.0039 & -0.0164 \\ 0 & 0 & -0.1240 & -0.0449 & -0.0407 & 0.0222 \end{pmatrix} \tag{4.21}$$

As far as the LO and NLO corrections parametrized by $\hat{c}_0^{(0)}$, $\hat{c}_0^{(1)}$, $\hat{c}_1^{(1)}$ and $\hat{e}_1^{(1)}$ are concerned our results agree perfectly with the findings of [24]. Contrariwise, the resummation of NNLO logarithms is entirely new, and the corresponding matrices $\hat{c}_0^{(2)}$, $\hat{c}_1^{(2)}$, $\hat{c}_2^{(2)}$, $\hat{e}_1^{(2)}$, $\hat{e}_2^{(2)}$, $\hat{t}_2^{(2)}$ and $\hat{g}_2^{(2)}$ have never been computed before.

4.2 $B \to X_s\gamma$

Radiative B decays provide one of the most important tests for new physics and challenges to the standard model. In particular the branching ratio $B \to X_s\gamma$ with its improving experimental error of less than 15 % strongly restricts the parameter space of many new physics models. For the theory to keep up with this precision, a full NLO analysis is needed. This analysis has been formally completed last year, where all of the dominant contributions have been calculated by at least two groups independently. The last unconfirmed calculation was the three-loop mixing of Q_{1-6} into Q_7^γ, Q_8^g, and the two-loop mixing of Q_7^γ, Q_8^g; both have been checked as part of this thesis [46]. In this section we want to collect all the ingredients needed in performing a complete NLO analysis of $B \to X_s\gamma$.

The decay $B \to X_s\gamma$ is enhanced by QCD logarithms by a factor of three. This makes the use of renormalization group improved perturbation theory unavoidable. Such a calculation takes the following three steps.

- The matching calculation, which consists of integrating out the heavy degrees of freedoms, namely the top quark and the W boson. This is done by calculating the full theory and matching it on the effective theory. This calculation results in the Wilson coefficients, the coupling constants of the effective operators, at the high scale.
- Renormalization group evolution of the Wilson coefficients to the low scale, which has been discussed explicitly in section (2.3).
- Calculation of the matrix elements. Here one uses the fact that in a certain range of photon energy cutoff the inclusive $B \to X_s\gamma$ decay is up to $1/m_b^2$ well approximated by the decay on the quark level. Additional non-perturbative effects can be systematically added.

In the decay $B \to X_s\gamma$ there is the peculiarity that the mixing of the current-current and penguin type operators, Q_1–Q_6, into the magnetic type operators, Q_7 and Q_8, vanishes at the one-loop level. To do a complete LO study one has to do in some parts calculations which are typical for a NLO study. In particular the two loop mixing of Q_1–Q_6 into Q_7 and Q_8 is part of the complete LO analysis. This complication led to the fact, that the first fully correct calculation of the LO anomalous dimension for $B \to X_s\gamma$ was obtained only in 1993 in [109, 110]. The discussion of the renormalization group part is therefore a key ingredient in the understanding of the $B \to X_s\gamma$ decay.

4.2.1 Anomalous Dimension Matrix for $B \to X_s\gamma$

First we drop the semi-leptonic operators, since they are irrelevant for radiative B decays. As noted above parts of the LO anomalous dimension matrix $\gamma^{(0)}$, results form the calculation of two-loop diagrams. One therefore works in a basis where the operators Q_7 and Q_8 are not rescaled by the $1/g^2$ factor.

It might be useful to recall explicitly the relation between the ADM in our basis and the ADM in an operator basis where Q_7 and Q_8 are not rescaled by $1/g^2$. The latter is frequently used for phenomenological applications [6,7,26]. The Wilson coefficients in that basis $\widetilde{C}_i(\mu)$, are given by

$$\widetilde{C}_i(\mu) = \begin{cases} C_i(\mu)\,, & \text{for } i = 1\text{–}6\,, \\ \frac{4\pi}{\alpha_s} C_i(\mu)\,, & \text{for } i = 7,\ 10\,, \end{cases} \tag{4.22}$$

while the coefficients in the expansion in powers of α_s of the corresponding anomalous dimensions $\widetilde{\gamma}_{ij}$, take the following form:

$$\widetilde{\gamma}_{ij}^{(k-1)} = \begin{cases} \gamma_{ij}^{(k-1)}\,, & \text{for } i,j = 1\text{–}6\,, \\ \gamma_{ij}^{(k)}\,, & \text{for } i = 1\text{–}6\,, \text{ and } j = 7,\ 8\,, \\ \gamma_{ij}^{(k-1)} + 2\beta_{k-1}\delta_{ij}\,, & \text{for } i,j = 7,\ 8\,. \end{cases} \tag{4.23}$$

For the rest of this section all results are given in the basis where Q_7 and Q_8 are not rescaled by the $1/g^2$ factor. The basis then reads:

$$\begin{aligned} Q_1 &= (\bar{s}_L \gamma_\mu T^a c_L)(\bar{c}_L \gamma^\mu T^a b_L)\,, \\ Q_2 &= (\bar{s}_L \gamma_\mu c_L)(\bar{c}_L \gamma^\mu b_L)\,, \\ Q_3 &= (\bar{s}_L \gamma_\mu b_L) \sum\nolimits_q (\bar{q}\gamma^\mu q)\,, \\ Q_4 &= (\bar{s}_L \gamma_\mu T^a b_L) \sum\nolimits_q (\bar{q}\gamma^\mu T^a q)\,, \\ Q_5 &= (\bar{s}_L \gamma_\mu \gamma_\nu \gamma_\rho b_L) \sum\nolimits_q (\bar{q}\gamma^\mu \gamma^\nu \gamma^\rho q)\,, \\ Q_6 &= (\bar{s}_L \gamma_\mu \gamma_\nu \gamma_\rho T^a b_L) \sum\nolimits_q (\bar{q}\gamma^\mu \gamma^\nu \gamma^\rho T^a q)\,, \\ Q_7 &= e\, m_b (\bar{s}_L \sigma^{\mu\nu} b_R) F_{\mu\nu}\,, \\ Q_8 &= g\, m_b (\bar{s}_L \sigma^{\mu\nu} T^a b_R) G^a_{\mu\nu}\,, \end{aligned} \tag{4.24}$$

Additionally there is another not so trivial complication. Namely the parts which originate from the two-loop diagrams are in general regularization-scheme-dependent. Usually $\gamma^{(0)}$ results only from the calculation of one-loop graphs and is a scheme-independent quantity. The scheme dependence of $\gamma^{(0)}$ is therefore an interesting phenomenon and is signaled [109, 110] by the scheme dependence of the $b \to s\gamma$ and $b \to sg$ matrix elements of Q_1 to Q_6. For on-shell photons or gluons these matrix elements vanish for any 4-dimensional scheme and the HV scheme, while in the NDR scheme they are proportional to the tree-level matrix element of Q_7 and Q_8:

$$\langle Q_i \rangle_{\text{one-loop}} = y_i^{(j)} \langle Q_j \rangle_{\text{tree}} \quad \text{j} = \{7, 8\}, \tag{4.25}$$

where

$$y^{(7)} = (0, 0, -\frac{1}{3}, -\frac{4}{9}, -\frac{20}{3}, -\frac{80}{9}) \tag{4.26}$$

and

$$y^{(8)} = (0, 0, 1, -\frac{1}{6}, 20, -\frac{10}{3}) \tag{4.27}$$

are in the operator basis of [26]. The calculation of these numbers comes only from divergent parts of one-loop integrals, so that they are independent of the model for the calculation of the matrix elements.

To solve the problem of the scheme dependence it is convenient to introduce effective Wilson coefficients $C_i^{\text{eff}}(\mu)$ [113]. The definition of the effective Wilson coefficients

$$C_i^{\text{eff}}(\mu) = \begin{cases} C_i(\mu)\,, & \text{for } i = 1\text{–}6\,, \\ \frac{4\pi}{\alpha_s} C_i(\mu) + \sum_{j=1}^{6} y_j^{(i)} C_j(\mu)\,, & \text{for } i = 7\text{–}8 \end{cases} \tag{4.28}$$

corresponds to the following rotation in the operator basis (3.32):

$$Q^{\text{eff}} = R^{\text{eff}} Q, \tag{4.29}$$

where the rotation matrix is given by

$$R^{\text{eff}} = \begin{pmatrix} & -y_1^{(7)} & -y_1^{(8)} \\ 1\!\mathrm{I}_{6\text{x}6} & \vdots & \vdots \\ & -y_6^{(7)} & -y_6^{(8)} \\ 0\dots0 & 1 & 0 \\ 0\dots0 & 0 & 1 \end{pmatrix}. \tag{4.30}$$

The definition of R^{eff} implies that the one-loop matrix elements of $b \to s\gamma$ and $b \to sg$ with an on-shell photon or gluon of the effective operators Q_i^{eff} vanish. Therefore the leading order anomalous dimension for the effective Wilson coefficients (3.32)

$$\gamma_{\text{eff}}^{(0)} = R\gamma^{(0)}R^{-1} \tag{4.31}$$

is independent of the regularization scheme and reads:

$$\hat{\gamma}^{\text{eff}(0)} = \begin{pmatrix} -4 & \frac{8}{3} & 0 & -\frac{2}{9} & 0 & 0 & -\frac{208}{243} & \frac{173}{162} \\ 12 & 0 & 0 & \frac{4}{3} & 0 & 0 & \frac{416}{81} & \frac{70}{27} \\ 0 & 0 & 0 & -\frac{52}{3} & 0 & 2 & -\frac{176}{81} & \frac{14}{27} \\ 0 & 0 & -\frac{40}{9} & -\frac{100}{9} & \frac{4}{9} & \frac{5}{6} & -\frac{152}{243} & -\frac{587}{162} \\ 0 & 0 & 0 & -\frac{256}{3} & 0 & 20 & -\frac{6272}{81} & \frac{6596}{27} \\ 0 & 0 & -\frac{256}{9} & \frac{56}{9} & \frac{40}{9} & -\frac{2}{3} & \frac{4624}{243} & \frac{4772}{81} \\ 0 & 0 & 0 & 0 & 0 & 0 & \frac{32}{3} & 0 \\ 0 & 0 & 0 & 0 & 0 & 0 & -\frac{32}{9} & \frac{28}{3} \end{pmatrix}. \tag{4.32}$$

To compute the Wilson coefficients up to NLO accuracy we also need

$$\hat{\gamma}^{\text{eff}(1)} = \begin{pmatrix} -\frac{355}{9} & -\frac{502}{27} & -\frac{1412}{243} & -\frac{1369}{243} & \frac{134}{243} & -\frac{35}{162} & -\frac{818}{243} & \frac{3779}{324} \\ -\frac{35}{3} & -\frac{28}{3} & -\frac{416}{81} & \frac{1280}{81} & \frac{56}{81} & \frac{35}{27} & \frac{508}{81} & \frac{1841}{108} \\ 0 & 0 & -\frac{4468}{81} & -\frac{31469}{81} & \frac{400}{81} & \frac{3373}{108} & \frac{22348}{243} & \frac{10178}{81} \\ 0 & 0 & -\frac{8158}{243} & -\frac{59399}{243} & \frac{269}{486} & \frac{12899}{648} & -\frac{17584}{243} & -\frac{172471}{648} \\ 0 & 0 & -\frac{251680}{81} & -\frac{128648}{81} & \frac{23836}{81} & \frac{6106}{27} & \frac{1183696}{729} & \frac{2901296}{243} \\ 0 & 0 & \frac{58640}{243} & -\frac{26348}{243} & -\frac{14324}{243} & -\frac{2551}{162} & \frac{2480344}{2187} & -\frac{3296257}{729} \\ 0 & 0 & 0 & 0 & 0 & 0 & \frac{4688}{27} & 0 \\ 0 & 0 & 0 & 0 & 0 & 0 & -\frac{2192}{81} & \frac{4063}{27} \end{pmatrix} . \tag{4.33}$$

The two loop mixing of the Q_1–Q_6 sector has been calculated in the "standard" basis in Refs. [22, 23, 81, 85]. These results have been confirmed by a calculation in the same basis we used in our calulation (4.24) in Ref. [24]. We confirm their findings.

The two loop mixing of Q_7 and Q_8 and the three loop mixing of Q_1–Q_6 into Q_7 and Q_8 have only been calculated by one group [25, 26]. We completly confirm their results [46].

4.2.2 Wilson Coefficients for $B \to X_s\gamma$

With the anomalous dimension matrix at hand one can relate the Wilson coefficients at the matching scale $\mu_W = O(M_W)$ to the scale where the matrix elements are calculated, which is $\mu_b = O(m_b)$. To calculate the Wilson coefficients at the high scale one has to match the Green's functions of the full theory to the effective theory. In [13] the matching calculation has been done separately for the top, charm, and up sectors using the 't Hooft–Feynman version of the background field gauge. The effective Lagrangian (2.41), after going on-shell and neglecting the CKM suppressed up-quark contribution, then reads

$$\mathcal{L}_{\text{eff}} = \mathcal{L}_{\text{QCD}\times\text{QED}}(u, d, s, c, b, e, \mu, \tau) + \frac{4G_F}{\sqrt{2}} \left(V_{cs}^* V_{cb} \sum_{i=1}^{8} C_i^c Q_i + V_{ts}^* V_{tb} \sum_{i=3}^{8} C_i^t Q_i \right), \tag{4.34}$$

where the Wilson coefficients can be perturbatively expanded

$$C_i^Q = C_i^{Q(0)} + \frac{\alpha_s}{4\pi} C_i^{Q(1)} + \dots \qquad Q = c \text{ or } t. \tag{4.35}$$

The only non-vanishing $C_i^{Q(0)}$, which are necessary for the LO analysis of $B \to X_s\gamma$ are

$$\begin{aligned} C_2^{c(0)} &= -1\,, \\ C_7^{c(0)} &= \frac{23}{36}\,, \\ C_8^{c(0)} &= \frac{1}{3}\,, \\ C_7^{t(0)} &= -\frac{1}{2} A_0^t(x_t) \\ C_8^{t(0)} &= -\frac{1}{2} F_0^t(x_t)\,, \end{aligned} \tag{4.36}$$

i	1	2	3	4	5	6	7	8
a_i	$\frac{14}{23}$	$\frac{16}{23}$	$\frac{6}{23}$	$-\frac{12}{23}$	0.4086	-0.423	-0.8994	0.1456
h_i	$\frac{626126}{272277}$	$-\frac{56281}{51730}$	$-\frac{3}{7}$	$-\frac{1}{14}$	-0.6494	-0.038	-0.0185	-0.0057

where $A_0^t(x_t)$ and $F_0^t(x_t)$ are the so called Inami-Lim [112] functions:

$$A_0^t(x) = \frac{-3x^3+2x^2}{2(x-1)^4}\ln x + \frac{-22x^3+153x^2-159x+46}{36(x-1)^3}, \tag{4.37}$$

$$F_0^t(x) = \frac{3x^2}{2(x-1)^4}\ln x + \frac{-5x^3+9x^2-30x+8}{12(x-1)^3}. \tag{4.38}$$

They, as $C_7^{c(0)}$ and $C_8^{c(0)}$, result from the one-loop $b \to s\gamma$ and $b \to sg$ calculation in the standard model for background gauge fields. Expanding in external momenta up to second order and in m_b the contributions can be separately matched with respect to the internal flavour.

We compute the effective Wilson coefficients at the scale μ_b with the help of the evolution matrix

$$\vec{C}^{\text{eff}(0)}(\mu_b) = \hat{U}^{(0)}(\mu_b,\mu_0)\vec{C}^{\text{eff}(0)}(\mu_0), \tag{4.39}$$

for separate charm and top contributions

$$C_7^{\text{eff}(0)}(\mu_b) = C_7^{t,\text{eff}(0)}(\mu_b) - C_7^{c,\text{eff}(0)}(\mu_b) \tag{4.40}$$

and find

$$C_7^{t,\text{eff}(0)}(\mu_b) = -\frac{1}{2}\eta^{16/23}A_0^t(x_t) - \frac{4}{3}\left(\eta^{14/23}-\eta^{16/23}\right)F_0^t(x_t) \tag{4.41}$$

$$C_7^{c,\text{eff}(0)}(\mu_b) = \frac{23}{36}\eta^{16/23} + \frac{8}{9}\left(\eta^{14/23}-\eta^{16/23}\right) - \sum_{i=1}^{8} h_i\eta^{a_i}, \tag{4.42}$$

where

$$\eta = \frac{\alpha_s(\mu_W)}{\alpha_s(\mu_b)}. \tag{4.43}$$

By plotting the scale dependence of $C_7^{\text{eff}(0)}$ in Fig. 4.2 as a sum of the separate charm and top contributions one can see the origin of the strong QCD enhancement. A change of η from 1 to 0.566, which corresponds to a scale change of μ from M_W to $\mu_b = 5$GeV, leaves $C_7^{c,\text{eff}(0)}$ nearly unaffected while there is a strong decrease in $C_7^{t,\text{eff}(0)}$. Since the top and the charm contribution tend to cancel at the scale M_W the decrease of the top contribution leads to an increase in $\left|C_7^{\text{eff}(0)}\right|^2$ from 0.036 to 0.094. Therfore the top contribution is the origin of the strong QCD enhancement of $B \to X_s\gamma$.

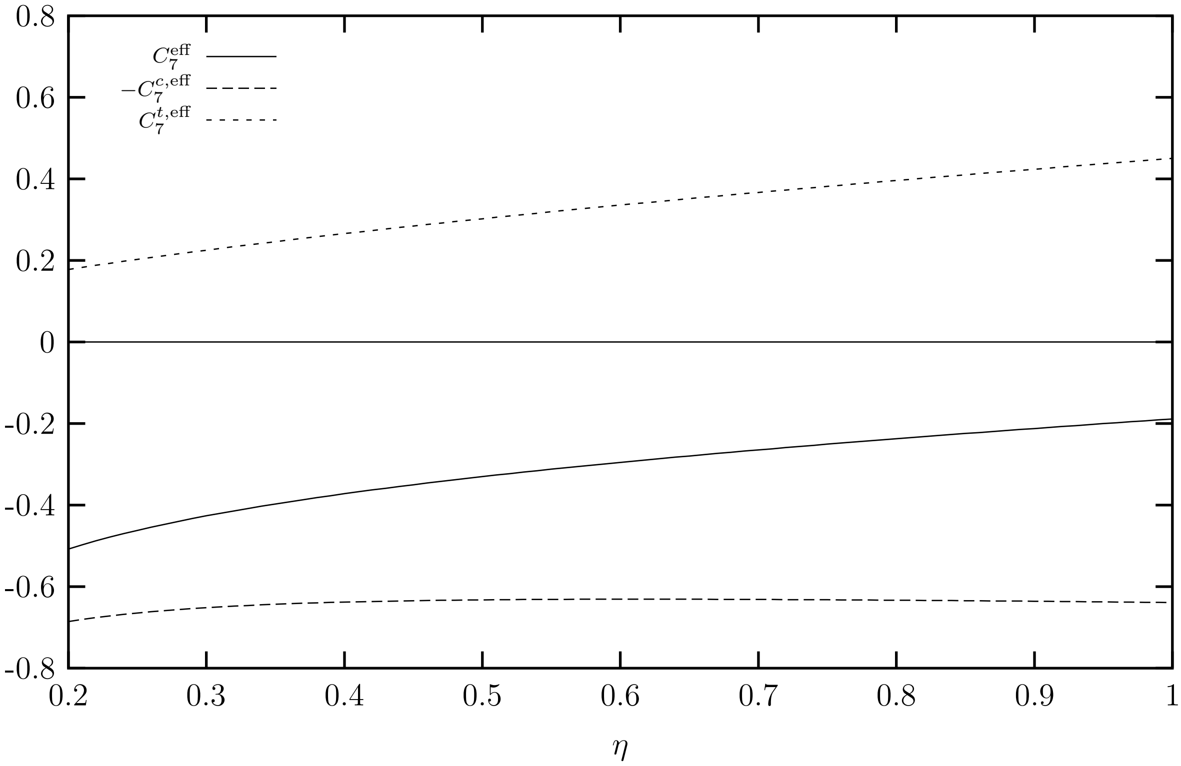

Figure 4.2: $C_7^{\mathrm{eff}(0)}(\mu)$ as a sum of the charm and top contributions. The strong QCD enhancement has its origin in the top sector $C_7^{t,\mathrm{eff}(0)}(\mu)$.

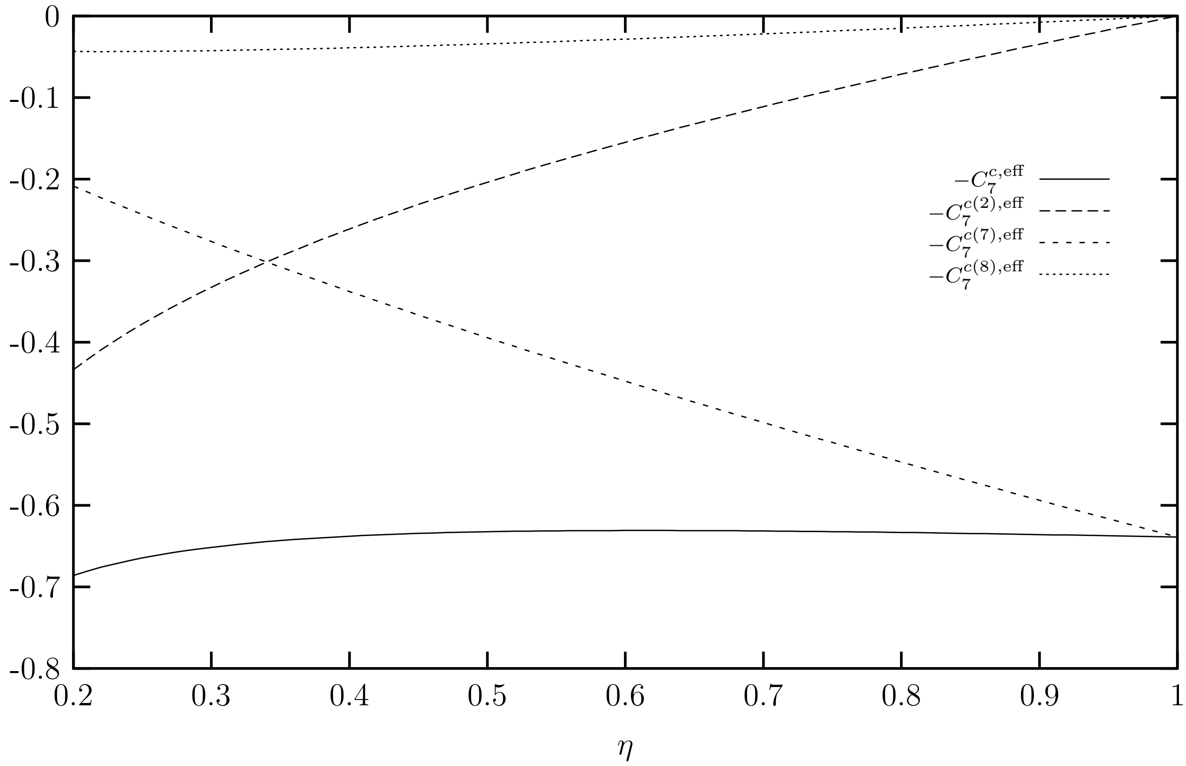

Figure 4.3: Non-accidental cancellations of QCD effects in the charm sector $C_7^{c,\mathrm{eff}(0)}(\mu)$.

The scale independence of the charm contribution can also be seen in Fig. 4.3, where $C_7^{c,\mathrm{eff}(0)}$ is given as a sum of the different contributions of Eq. (4.42). There is a strong cancellation of the η dependence coming from the different terms. Yet the cancellation is not accidental, since the different components are not separately physical.

The strong η dependence of $C_7^{t,\mathrm{eff}(0)}$ is given by the global η factor in Eq. (4.41). The anomalous dimension of $m_b(\mu)$ that stands in front of the operator Q_7 is responsible of 12/23 of 16/23 of the power of η and thus gives the main contribution to the η dependence. Using an m_b which is renormalized at $\mu_0 \sim M_W$ for the top contribution would take the logarithmic QCD effects approximately into account. This was noted in Ref. [6], where the authors conjecture that this feature will also be valid up to NNLO, and thus propose to renormalize m_b in Q_7 at m_t or M_W in the top contribution to the decay amplitude. We will follow this approach in our analysis.

The reason for the different optimal renormalization in the charm and top sector is the different origin of m_b in both sectors [6].

i	1	2	3	4	5	6	7	8
e_i	5.7064	-3.8412	0	0	-1.9043	-0.1008	0.1216	0.0183
f_i	-10.6142	6.5489	4.5508	0.7519	2.004	0.7476	-0.5385	0.0914
g_i	9.2746	-6.9366	-0.874	0.4218	-2.7231	0.4083	0.1465	0.0205
l_i	6.5833	-4.4692	-0.8571	0.2857	-2.0343	0.1232	0.1279	-0.0064

Let us now compute the effective Wilson coefficients at the scale μ:

$$\begin{aligned} C_7^{\mathrm{teff}(1)}(\mu) = & -\frac{1}{2}\eta^{\frac{39}{23}} A_1^t(x_t) + \frac{18604}{4761}\left(\eta^{\frac{16}{23}} - \eta^{\frac{39}{23}}\right) A_0^t(x_t) \\ & + \left(-\frac{148832}{14283}\eta^{\frac{16}{23}} + \frac{3349442}{357075}\eta^{\frac{39}{23}} + \frac{3582208}{357075}\eta^{\frac{14}{23}} - \frac{128434}{14283}\eta^{\frac{37}{23}}\right) F_0^t(x_t) \\ & + \frac{4}{3}\left(\eta^{\frac{39}{23}} - \eta^{\frac{37}{23}}\right) F_1^t(x_t) + \sum_{i=1}^{8} e_i \eta^{a_i+1} E_0^t(x_t) \end{aligned} \tag{4.44}$$

$$C_7^{\mathrm{ceff}(1)}(\mu) = -\sum_{i=1}^{8}\left(f_i + g_i\eta + l_i\eta\ln\frac{\mu_0}{M_W}\right), \tag{4.45}$$

where we have used the matching conditions of Ref. [13]:

$$\begin{aligned} C_1^{c(1)} &= -15 - 6\ln\frac{\mu_0^2}{\mu_W^2} \\ C_4^{c(1)} &= \frac{7}{9} - \frac{2}{3}\ln\frac{\mu_0^2}{\mu_W^2} \\ C_7^{c(1)} &= -\frac{713}{243} - \frac{4}{81}\ln\frac{\mu_0^2}{\mu_W^2} \\ C_8^{c(1)} &= -\frac{91}{324} + \frac{4}{27}\ln\frac{\mu_0^2}{\mu_W^2} \\ C_4^{t(1)} &= E_0^t(x_t) \\ C_7^{t(1)} &= -\frac{1}{2}A_1^t(x_t) \\ C_7^{t(1)} &= -\frac{1}{2}F_1^t(x_t). \end{aligned} \tag{4.46}$$

4.2.3 Inclusive Decay and Partonic Contribution

With the preceeding method we have the coupling constants of the operators, the Wilson coefficients, at the scale of the decay at hand. Still one has to insert the effective Lagrangian into the external states to relate it to physical observables. Neglecting QCD effects only Q_7 would contribute and in the case of $B \to X_s\gamma$ the following matrix element has to be calculated:

$$\langle \gamma X_s | Q_7 | B \rangle. \tag{4.47}$$

This is an hadronic matrix element and can not be calculated in perturbation theory. One approach to this problem is to consider the inclusive decay by summing over all X_s final states and use the fact that the decay itself should be a short distance phenomenon compared to the scales of confinement if the b quark mass m_b is large compared to Λ_{QCD}. By this it is hoped that the individual contribution of the external states drop out and the decay is well approximated by the partonic level.

On the partonic level at LO only Q_7 would contribute to $B \to X_s\gamma$. If we assume that this is also the only operator in the effective Lagrangian we can do the analyses in analogy to the analysis [114, 115] of the inclusive semileptonic decay $\bar{B} \to X_u e\bar{\nu}$. The differential decay rate is then given by the squared matrix element

$$\mathrm{d}\Gamma = \sum_{X_s} \mathrm{d}\,[\mathrm{PS}]\,(2\pi)^4\,\delta^{(4)}\,(p_B - p_{X_s} - q)\,\langle B|i\mathcal{L}_{\mathrm{eff}}^{\dagger}|X_s\gamma\rangle\langle X_s\gamma|i\mathcal{L}_{\mathrm{eff}}|B\rangle, \tag{4.48}$$

where $\mathrm{d}\,[\mathrm{PS}]$ denotes the phase space differential and $\mathcal{L}_{\mathrm{eff}}$ consists only out of Q_7. The photonic contribution of Q_7 to (4.48) can be calculated perturbatively and the nonperturbative contribution is given by

$$W(q) = \sum_{X_s} (2\pi)^4\,\delta^{(4)}\,(p_B - p_{X_s} - q)\,\langle B|O^{\dagger}|X_s\rangle\langle X_s|O|B\rangle, \tag{4.49}$$

where the operator O is the Fermionic part of Q_7.

Using the optical theorem one can relate $W(q)$ to the absorptive part of the forward scattering amplitude

$$W(q) = 2\Im\langle B|T\left\{O^{\dagger}, O\right\}|B\rangle. \tag{4.50}$$

Here $T\,(\dots)$ denotes the time-ordered product.

As was observed by Chay, Georgi and Grinstein, the energy which flows into X_s scales with m_b and thus the strange quark is far off shell in the time ordered product in (4.50), except for a small region where $P_X^2 \sim m_s^2$. The compared to Λ_{QCD} large momentum flow allows for a operator product expansion (OPE) of the time ordered product in (4.50).

In general such an OPE has the following form:

$$T\left\{O^{\dagger}O\right\} \sim \Gamma_b\left(\bar{b}b\right) + \frac{z_2}{mb^2}\left(\bar{b}g\sigma\cdot Gb\right) + \sum \frac{z_{qi}}{m_b^3}\left(\bar{b}\Gamma_i q\right)\left(\bar{q}\Gamma_i b\right) + dots. \tag{4.51}$$

The Wilson coefficients Γ_b and z_k can be calculated by a matching calculation between (4.51) and (4.50). The matrix elements of (4.51) still contain the nonperturbative physics, but one can still use HQET to further analyse them. If we expand the matrix element of the dimension-three operator using the HQET-two-component-spinor field h(x) we find

$$\langle B|\bar{b}b|B\rangle = 1 + \frac{1}{2m_b^2}\langle B|\bar{h}\,(iD)^2\,h|B\rangle + \dots. \tag{4.52}$$

By inspection of (4.50), (4.51), and (4.52) we find that the leading term of the decay rate is given by the Partonic level, while the nonperturbative $1/m_b^2$ corrections can be written in terms of the matrix elements

$$\lambda_1 = \frac{\langle B|\bar{h}\,(iD)^2\,h|B\rangle}{2m_B} \qquad\qquad \lambda_2 = \frac{1}{6}\frac{\langle B|\bar{h}\,\left(\bar{b}g\sigma\cdot Gb\right)\,h|B\rangle}{2m_B}. \tag{4.53}$$

The standard HQET parameters $\lambda_{1,2}$ can be extracted from experiment. The value of $\lambda_2 \simeq 0.12\mathrm{GeV}^2$ is given by the $B-B^*$ mass difference, while $\lambda_1 = -(0.27\pm0.10\pm0.04)\mathrm{GeV}^2$ has been determined in [116–118] from the semileptonic B-decay spectra.

The correction to the partonic decay rate, which could be calculated in perturbation theory by [32, 119] are given by

$$\mathrm{d}\Gamma = \mathrm{d}\Gamma^{\mathrm{parton}}\left(1+\frac{1}{2}\frac{\lambda_1}{\mathrm{m_b^2}}-\frac{9}{2}\frac{\lambda_2}{\mathrm{m_b^2}}+\ldots\right). \tag{4.54}$$

If operators other than Q_7 contribute to $\mathcal{L}_{\mathrm{eff}}$ the separation of the b-quark annihilation and the photon emission is not anymore small compared to Λ_{QCD} and the operator product expansion (4.51) may not be applied. Yet the leading contribution is still given by the quark level, and the fact that some perturbative contributions are small implies the unimportance of the corresponding nonperturbative corrections. The discussion of the non-perturbative effects is outlined in Ref. [120] and we will follow their discussion for the remainder of this section.

The contribution of Q_8 to the branching ratio has been studied in Ref. [121]. With the help of fragmentation functions the only important non-perturbative contributions were found for low photon energies E_γ much below the current experimental cutoff of 2.0 GeV. Since the perturbative contribution of Q_8 to the decay rate is less than 3%, neglecting the non-perturbative contributions will be a good approximation for the current experimental cutoff.

The perturbative contributions $Q_3, \ldots, Q_6$ are even smaller than the one of Q_8. The contributions of u, d, and s quarks might generate virtual vector mesons which could convert to a real photon. In the factorization approximation such a production can only be produced by $\bar{q}\gamma_\mu\gamma_\nu q$ type currents. Deviations of the factorization approximation should be suppressed either by α_s or by Λ_{QCD} [122, 123]. Given the smallness of the Wilson coefficients this is sufficient to make them negligible.

The b-quark contributions in $(\bar{s}\Gamma b)(\bar{b}\Gamma b)$ can be treated again with an operator product expansion since the b-quark loops are localized at distances much smaller than $\Lambda_{\mathrm{QCD}}^{-1}$. Again, given the smallness of the Wilson coefficients, the non-perturbative corrections are negligible.

Charm Loop Contributions

The only remaining contribution originates from the charm loops. We will first discuss the contributions of real intermediate $c\bar{c}$ states.

First let us note that, for a photon cutoff larger than 1.6GeV, the invariant mass of the final X_s state is smaller than $m_{\eta_c} + m_K$. Thus the $c\bar{c}$ state might only exist before the photon emission via a cascade decay:

$$\begin{array}{rcl} \bar{B} & \to & Y_{c\bar{c}} X_s^{(1)} \\ & & \quad\searrow \\ & & \qquad X^{(2)}\gamma. \end{array} \tag{4.55}$$

For $Y_{c\bar{c}} = \psi$ experimental data for both components of the cascade decay are available. For a low cutoff energy E_0 the ψ contributions would dominate the branching ratio, while it gets reduced to a few percent for $E_0 = 1.6$GeV and will be negligible for $E_0 = 2.0$GeV [120]. Henceforth we will proceed by taking the ψ contributions as background. Concerning the experimental side the current extrapolation by [120] misiak] from the experimental cutoff of $E_0 = 2.0$GeV to the theoretical preferred one of $E_0 = 1.6$GeV does only partially include such contributions. The ones which are included have only a 1.7% effect on the branching ratio. Thus it is consistent to treat the intermediate ψ contribution as background.

Similar arguments hold for a ψ' intermediate state, while higher $c\bar{c}$ states have negligible branching ratios. The contributions of intermediate ψ' will also be subtracted.

Virtual $c\bar{c}$ states will lead to $1/m_c^2$ corrections as was first pointed out in Ref. [33], where by the 'gluon-photon penguin' type mechanisms a $1/m_c^2$ series of operators is generated in the effective Lagrangian. By calculating the gluon-photon penguin diagram with an insertion of Q_2 for a soft gluon, which may originate from the decaying $\bar{B}$ meson, and keeping the first term in the gluon momentum an effective photon-gluon operator is generated

$$Q_{g\gamma} = \frac{eQ_c}{48\pi^2 m_c^2} \bar{s}\gamma_\mu(1-\gamma_5) g G_{\nu\lambda} b\, \epsilon^{\mu\nu\rho\sigma} \partial^\lambda F_{\rho\sigma}. \tag{4.56}$$

This will, by the interference with Q_7, generate a correction term to (4.50)

$$\Delta T = -\frac{G_F^2 m_b^5}{192\pi^3} V_{cs}^* V_{cb}^2 \frac{\alpha}{9\pi} \frac{C_2\, C_7}{m_c^2} \bar{b} g\sigma \cdot G b. \tag{4.57}$$

With the help of (4.53) and using $V_{cs}^* V_{cb} \simeq V_{ts}^* V_{tb}$ one finds the correction to the decay rate

$$\frac{\Delta\Gamma(B \to X_s\gamma)}{\Gamma(B \to X_s\gamma)} = -\frac{C_2}{C_7}\lambda_2 \simeq 0.03. \tag{4.58}$$

Higher terms in the gluon momentum k will lead to an expansion in

$$(q \cdot k)/m_c^2 \simeq \frac{\Lambda_{\mathrm{QCD}} m_b}{m_c^2} \simeq 0.6, \tag{4.59}$$

q being the photon momentum, for the gluon is soft and the photon is onshell. This further expansion will generate an infinite number of additional operators involving all powers of the gluon momentum [35,36]. Only the contribution of the first operator can be calculated, while the higher corrections are given by unknown matrix elements of higher dimensional operators. Given that the expansion parameter in (4.59) is $O(1)$ the result in (4.58) might receive large incalculable corrections. Yet it has been shown in Refs. [35–37] that the Taylor expansion in $(q \cdot k)/m_c^2$ involves small coefficients, which implies that the summed contribution of the higher dimensional operators is not too important.

4.2.4 Partonic Decay Rate

In the previous section we have seen that the partonic decay width

$$\Gamma\left[b \to X_s^{\text{parton}}\gamma\right]^\delta = \Gamma\left[b \to s\gamma\right] + \Gamma\left[b \to s\gamma g\right]^\delta + \Gamma\left[b \to s\bar{q}q\right]^\delta + \ldots, \tag{4.60}$$

approximates the decay $B \to X_s\gamma$ well for a certain range of the photon cutoff

$$E_\gamma > (1-\delta)\, E_\gamma^{\max} = (1-\delta)\,\frac{m_b}{2}. \tag{4.61}$$

The decay rate can be written as follows:

$$\Gamma\left[b \to X_s^{\text{parton}}\gamma\right]^\delta = \frac{G_F^2\alpha}{32\pi^2}\left|V_{ts}^* V_{tb}\right| m_{b,\text{pole}}^3 m_{b,\overline{\text{MS}}}^2\,(m_b)\left(|D|^2 + B\,(\delta)\right). \tag{4.62}$$

To find the contribution to $|D|^2$, apart from the effective theory calculations, the partonic matrix elements have to be calculated. The two-loop matrix elements $\langle s\gamma\, |Q1,2|\, b\rangle$ were presented for the first time in Refs. [19,20] and have been confirmed and extended to include also the two-loop matrix elements of the QCD penguin operators in Refs. [7,21]. The one-loop matrix element $\langle s\gamma\, |Q_8|\, b\rangle$ was also found in Refs. [7,19,20]. The resulting expression reproduces the expected μ-dependence of the matrix elements [113] and reads:

$$D = C_7^{(0)\text{eff}}(\mu_b) + \frac{\alpha_s(\mu_b)}{4\pi}\left(C_7^{(1)\text{eff}}(\mu_b) + \sum_{i=1}^{8} C_i^{(0)\text{eff}}(\mu_b)\left[r_i + \gamma_{i7}^{(0)\text{eff}}\ln\frac{m_b}{\mu_b}\right]\right). \tag{4.63}$$

The one-loop matrix element $\langle s\gamma|Q_7|b\rangle$ as well as the bremsstrahlung, the leading order matrix elements $\langle s\gamma g|Q_i|b\rangle$; they have been given in Refs. [14,18,124]. The matrix elements read[1]:

[1]The value of r_7 is fixed by the requirement that $\phi_{77}(\delta)$ vanishes in the limit $\delta \to 1$. This corresponds to a choice where the contribution from the $B(\delta)$ term is small.

$$
\begin{aligned}
r_1 &= \frac{833}{729} - \frac{1}{3}[a(z)+b(z)] + \frac{40}{243} i\pi, \\
r_2 &= -\frac{1666}{243} + 2[a(z)+b(z)] - \frac{80}{81} i\pi, \\
r_3 &= \frac{2392}{243} + \frac{8\pi}{3\sqrt{3}} + \frac{32}{9} X_b - a(1) + 2b(1) + \frac{56}{81} i\pi, \\
r_4 &= -\frac{761}{729} - \frac{4\pi}{9\sqrt{3}} - \frac{16}{27} X_b + \frac{1}{6} a(1) + \frac{5}{3} b(1) + 2b(z) - \frac{148}{243} i\pi, \\
r_5 &= \frac{56680}{243} + \frac{32\pi}{3\sqrt{3}} + \frac{128}{9} X_b - 16a(1) + 32b(1) + \frac{896}{81} i\pi, \\
r_6 &= \frac{5710}{729} - \frac{16\pi}{9\sqrt{3}} - \frac{64}{27} X_b - \frac{10}{3} a(1) + \frac{44}{3} b(1) + 12a(z) + 20b(z) - \frac{2296}{243} i\pi, \\
r_7 &= \frac{32}{9} - \frac{8}{9}\pi^2 \\
r_8 &= \frac{44}{9} - \frac{8}{27}\pi^2 + \frac{8}{9} i\pi\,. \qquad (4.64)
\end{aligned}
$$

On the parton level the only δ dependent part is

$$
B(E_0) = \frac{\alpha_s(\mu_b)}{\pi} \sum_{\substack{i,j=1,\ldots,8 \\ i\le j}} C_i^{(0)\mathrm{eff}}(\mu_b)\; C_j^{(0)\mathrm{eff}}(\mu_b)\; \phi_{ij}(\delta) \; + \; \beta_{q\bar{q}}(E_0); \qquad (4.65)
$$

here the functions ϕ_{ij} originate from the gluon bremsstrahlung [14, 18, 124]. They can be found for example in Ref. [6]. The contributions from $b \to s q\bar{q}\gamma$ are denoted by $\beta_{q\bar{q}}(E_0)$, where q stands for u, d or s quarks. Their contribution is either suppressed by the smallness of the QCD penguin Wilson coefficients, or by $\left|\frac{V_{us}^* V_{ub}}{V_{ts}^* V_{tb}}\right|$. Additional suppression occurs for high-energy photons [124].

4.2.5 Branching Ratio

In the previous sections we have discussed the NLO QCD contributions to the decay rate of $B \to X_s\gamma$, and have seen that the leading QCD logarithms can be taken into account by renormalizing $m_b(\mu)$ in Q_7 at μ. We will now give a NLO formula for the branching ratio where we split the charm and the top contributions in an analogous manner. The $B \to X_s\gamma$ branching ratio can be written as follows[2]:

$$
\mathrm{BR}[\bar{B} \to X_s\gamma]_{E_\gamma > E_0}^{\text{subtracted } \psi,\, \psi'} = \mathrm{BR}[\bar{B} \to X_c e\bar{\nu}]_{\mathrm{exp}} \left|\frac{V_{ts}^* V_{tb}}{V_{cb}}\right|^2 \frac{6\alpha_{\mathrm{em}}}{\pi\, C} \left[P(E_0) + N(E_0)\right]. \qquad (4.66)
$$

[2] ψ and ψ' have been subtracted. See the previous dicussion of the nonperturbative effects

Here the constant C

$$C = \left|\frac{V_{ub}}{V_{cb}}\right|^2 \frac{\Gamma[\bar{B} \to X_c e\bar{\nu}]}{\Gamma[\bar{B} \to X_u e\bar{\nu}]} \tag{4.67}$$

is introduced, so that the charmless semileptonic decay can be chosen as the normalization factor. Hereby the convergence of the perturbation theory is separated from the m_c mass determination. The perturbative ratio is thus given by

$$\frac{\Gamma[b \to X_s\gamma]_{E_\gamma > E_0}}{|V_{cb}/V_{ub}|^2\, \Gamma[b \to X_u e\bar{\nu}]} = \left|\frac{V_{ts}^* V_{tb}}{V_{cb}}\right|^2 \frac{6\alpha_{\rm em}}{\pi}\, P(E_0), \tag{4.68}$$

where the $|V_{cb}/V_{ub}|^2$ is the correction factor for the normalization to the charmless decay. As suggested in Ref. [27] we set $\alpha = \alpha^{\rm onshell}$. The semileptonic phase space factor C is known up to NNLO [6]:

$$C = 0.575 \pm 0.02\,. \tag{4.69}$$

To find an expression for the perturbative ratio up to NLO we need the charmless semileptonic decay

$$\Gamma[b \to X_u e\bar{\nu}] = \frac{G_F^2 \left(m_b^{\rm pole}\right)^5}{192\pi^3} |V_{ub}|^2 \left(1 + \frac{\alpha_s}{\pi}\left(\frac{25}{6} - \frac{2}{3}\pi^2\right)\right), \tag{4.70}$$

as further input. It is proportional to $\left(m_b^{\rm pole}\right)^5$, thus the relation [6] between the pole and the $\overline{\rm MS}$ mass

$$\frac{m_b^{\rm pole}}{m_{b,\overline{\rm MS}}(\mu_b)} = 1 + \frac{\alpha_s(\mu_b)}{4\pi}\left(\frac{16}{3} - 4\ln\frac{m_b^2}{\mu_b^2}\right) \tag{4.71}$$

is also needed.

The perturbative expression can then be expanded in powers of α_s. In addition we want to keep the b-quark mass in the top contribution of Q_7 renormalized at μ_0 and write the perturbative quantity

$$P(\delta) = \left|K_c + \left(1 + \frac{\alpha_s(\mu_0)}{\pi}\right) r(\mu_0) K_t + \epsilon_{\rm ew}\right|^2 + B(\delta), \tag{4.72}$$

where

$$r(\mu_0) = \frac{m_b^{\overline{\rm MS}}(\mu_0)}{m_b^{1S}} \tag{4.73}$$

denotes the ratio of m_b renormalized at μ_0 and the bottom "1S mass". As argued in Refs. [116, 117] expressing all kinematical factors of m_b in inclusive decays in terms of the 1S mass, which is defined as half of the perturbative contribution to the Υ mass, improves the behavior of QCD perturbation theory. The NLO expression reads:

$$r_{\rm NLO}(\mu_0) = \left(\frac{\alpha_s(\mu_0)}{\alpha_s(m_b)}\right)^{\frac{12}{23}} \left\{1 + \frac{\alpha_s(m_b)}{4\pi}\left[\frac{7462}{1587}\frac{\alpha_s(\mu_0)}{\alpha_s(m_b)} - \frac{15926}{1587}\right] + \frac{2}{9}\alpha_s(m_b)^2\right\} \tag{4.74}$$

i	1	2	3	4	5	6	7	8
d_i	1.4107	-0.838	-0.4286	-0.0714	-0.6494	-0.038	-0.0185	-0.0057
$\tilde{d}_i$	-17.6507	11.346	2.4692	-0.8056	4.8898	-0.2308	-0.529	0.1994
$\tilde{d}_i^\eta$	9.2746	-6.9366	-0.874	0.4218	-2.7231	0.4083	0.1465	0.0205
$\tilde{d}_i^a$	0	0	0.8571	0.6667	0.1298	0.1951	0.1236	0.0276
$\tilde{d}_i^b$	0	0	0.8571	0.6667	0.2637	0.2906	-0.0611	-0.0171
$\tilde{d}_i^{i\pi}$	0.4702	0	-0.4268	-0.2222	-0.9042	-0.115	-0.0975	0.0115

Now we have all the ingredients to write down the complete NLO expression for K_t and K_c in (4.72). The light quark contribution reads:

$$\begin{aligned} K_c = & \sum_{k=1}^{8} \eta^{a_k} \left\{ d_k + \frac{\alpha_s(\mu_b)}{4\pi} \left[2\beta_0 a_k d_k \left(\ln \frac{m_b}{\mu_b} + \eta \ln \frac{\mu_0}{M_W} \right) \right. \right. \\ & \left. \left. + \tilde{d}_k + \tilde{d}_k^\eta\, \eta + \tilde{d}_k^a a(z) + \tilde{d}_k^b b(z) + \tilde{d}_k^{i\pi} i\pi \right] \right\} \\ & + \frac{V_{us}^* V_{ub}}{V_{ts}^* V_{tb}} \frac{\alpha_s}{4\pi} \left(\eta^{a_3} + \eta^{a_4} \right) [a(z) + b(z)]., \end{aligned} \tag{4.75}$$

while the top quark contribution can be written like the following:

$$\begin{aligned} K_t = & \left(1 - \frac{2}{9}\alpha_s(m_b)^2\right) \left(-\frac{1}{2}\eta^{4/23} A_0^t(x_t) + \left(\eta^{4/23} - \eta^{2/23}\right) F_0^t(x_t) \right) \\ & + \frac{\alpha_s(\mu_b)}{4\pi} \left\{ E_0^t(x_t) \sum_{k=1}^{8} e_k \eta^{a_k + 11/23} - \frac{4}{3}\eta^{25/23} F_1^t(x_t) - \frac{1}{2}\left(\eta^{27/23} A_1^t(x_t)\right) \right. \\ & + \eta^{4/23} A_0^t(x_t) \left(\frac{12523}{3174} - \frac{2}{9}\pi^2 - \frac{7411}{4761}\eta + \frac{1}{2}\eta \ln \frac{\mu_0^2}{m_t^2} - \frac{2}{3} \ln \frac{m_b^2}{\mu_b^2} \right) \\ & + \eta^{4/23} F_0^t(x_t) \left(-\frac{50092}{4761} + \frac{16\pi^2}{27} + \frac{1110842}{357075}\eta - \frac{4}{3}\eta \ln \frac{\mu_0^2}{m_t^2} + \frac{16}{9} \ln \frac{m_b^2}{\mu_b^2} \right) \\ & \left. + \eta^{2/23} F_0^t(x_t) \left(\frac{4}{9}\pi(\pi + i) + \frac{2745458}{357075} - \frac{38890}{14283}\eta + \frac{4}{3}\eta \ln \frac{\mu_0^2}{m_t^2} - \frac{8}{9} \ln \frac{m_b^2}{\mu_b^2} \right) \right\}. \end{aligned} \tag{4.76}$$

Our results agree with [6, 7]. Thus we confirm their result for the branching ratio

$$\mathrm{BR}(B \to X_s\gamma)_{\mathrm{th}} = (3.70 \pm 0.30) \times 10^{-4} \tag{4.77}$$

for $B \to X_s\gamma$, and put it on even stronger theoretical footing, for now all important contributions to this decay have been calculated independently by at least two groups. This is in particular important if one takes into account that the scale uncertainty is at the LO level around 25% [113].

4.3 $B \to X_s \ell^+ \ell^-$

The rare semileptonic transitions $b \to s\ell^+\ell^-$ have been observed for the first time by Belle and BaBar in 2001-2002 in the exclusive mode $B \to K\ell^+\ell^-$ [2, 38, 39, 49]. They are an important probe of the short-distance physics that governs flavor-changing transitions, and they are complementary to the less rare $b \to s\gamma$ decay. A precise measurement of the inclusive channel $B \to X_s\ell^+\ell^-$ is particularly relevant because it is amenable to a clean theoretical description, especially in the region of low leptonic invariant mass, $m_{\ell\ell}^2 = m_b^2\, \hat{s}$, below the charm resonances, $0.05 \le \hat{s} \le 0.25$.

4.3.1 Completing the NNLO QCD Calculation

The formula for the dilepton invariant mass distribution is [42]:

$$\begin{aligned}
&\frac{d\Gamma(B \to X_s\ell^+\ell^-)}{d\hat{s}} = \left(\frac{\alpha}{4\pi}\right)^2 \frac{G_F m_{b,\text{pole}}^5 \left|V_{ts}^* V_{tb}\right|^2}{48\pi^2} (1-\hat{s})^2 \\
&\times \left[4\left(1+\frac{2}{\hat{s}}\right) \left|\widetilde{C}_7^{\text{eff}}\right|^2 \left(1 + \frac{2\alpha_s}{\pi}\omega_{77}(\hat{s})\right) + (1+2\hat{s}) \left(\left|\widetilde{C}_9^{\text{eff}}\right|^2 + \left|\widetilde{C}_{10}^{\text{eff}}\right|^2 \right) \left(1 + \frac{2\alpha_s}{\pi}\omega_{99}(\hat{s})\right) \right. \\
&\left. \quad + 12\,\text{Re}\left(\widetilde{C}_7^{\text{eff}} \widetilde{C}_9^{\text{eff}*}\right) + \frac{\alpha_s}{\pi}\delta_R(\hat{s}) \right] ,
\end{aligned} \tag{4.78}$$

where the effective Wilson coefficients $\widetilde{C}^{\text{eff}}$ contain the contributions of the matrix elements which are proportional to the operators Q_7 and Q_9. On the NLO level these are the matrix elements of Q_1–Q_6, and are given in [125, 126]. The infrared divergencies which arise in the calculation of the matrix element of Q_9 cancel after adding the bremsstrahlung contributions, and the final contribution to the dilepton invariant mass contribution is taken into account by $\omega_{99}(\hat{s})$.

On the NNLO level most of the important contributions to the low $\hat{s}$ region have been calculated. The matching conditions are given in Ref. [13], while the matrix elements and the relevant bremsstrahlung contributions are given in Refs. [42, 43, 45]. The only potentially relevant NNLO terms still missing at low $\hat{s}$ have to do with the three-loop ADM of the operators in the low-energy effective Hamiltonian, and with the two-loop matrix element of one of them, Q_9.

Let us start with the contributions of the three-loop ADM to the NNLO QCD corrections. Let us recall that the renormalization scale (μ) dependence of the Wilson coefficients $\vec{C}^T(\mu) = (C_1(\mu), ...)$ of the effective operators is governed by the renormalization group equation (RGE) whose solution is schematically given by

$$\vec{C}(\mu) = \hat{U}(\mu, \mu_0, \alpha)\vec{C}(\mu_0)\,. \tag{4.79}$$

In the case at hand we are interested in the running of the Wilson coefficients from the electroweak scale $\mu_0 \approx O(M_W)$ to a scale $\mu_b = O(m_b)$. Neglecting for the moment the

i	1	2	3	4	5	6	7	8	9
a_i	$\frac{6}{23}$	$-\frac{12}{23}$	0.4086	-0.4230	-0.8994	0.1456	-1	$-\frac{24}{23}$	$\frac{3}{23}$
b_i	12.4592	0.694	-1.7339	1.2359	-0.1921	0.3997	0	0	0
c_i	-2.5918	-0.2971	-0.5949	0.1241	0.317	2.8655	0	0	0
d_i	1.321	3.1616	-0.4814	1.9362	-5.0873	0.0468	-13.582	0	0
e_i	-0.0238	0.0107	0.0023	0.0071	0.005	-0.00003	-0.0087	-0.0008	0.0342
f_i	0.001	0.013	0.0045	-0.0022	-0.0714	-0.0008	0.0299	0	0
g_i	0	0	0	0	0	0	0.0035	0	0
h_i	0.0114	-0.0107	-0.0012	-0.0057	-0.0098	0.0002	0.0122	0	0

Table 4.1: Numerical coefficients parameterizing the RGE solutions in Eqs. (4.80), (4.84), and (4.85).

electromagnetic coupling α, all QCD corrections to $\vec{C}(\mu_b)$ up to $O(\alpha_s)$ are detailed in [13], while the only $O(\alpha_s^2)$ contributions to the evolution matrix $\hat{U}$ relevant in $b \to s\ell^+\ell^-$ at NNLO concerns the mixing of Q_2 into Q_9 and Q_7. Expanding $\hat{U}$ in powers of $\alpha_s(\mu_b)/4\pi$, we denote these terms by $U_{92}^{(2)}(\mu_b, \mu_0)$ and $U_{72}^{(2)}(\mu_b, \mu_0)$. The ingredients necessary for the calculation of the latter were already available in 1999 and Ref. [13] includes it. On the other hand, the calculation of $U_{92}^{(2)}$ requires the knowledge of the three-loop self-mixing of Q_1-Q_6 and of the three-loop mixing of Q_1-Q_6 into Q_9. The relevant ADM entries have just been calculated in (3.25, 3.30). Solving the NNLO RGE (2.78–2.85), we obtain

$$U_{92}^{(2)}(\mu_b, \mu_0) = \sum_{i=1}^{7} \left[b_i \eta^{a_i} + c_i \eta^{a_i+1} + d_i \eta^{a_i+2} \right] , \tag{4.80}$$

where $\eta = \alpha_s(\mu_0)/\alpha_s(\mu_b)$. The constants a_i, b_i, c_i, d_i are given in Table 1.

Using $\alpha_s(M_Z) = 0.119$ and $m_b = 4.8$ GeV, we find $U_{92}^{(2)}(m_b, M_W) \simeq 4.1$. Unless $\eta < 0.48$, our result is within the range that was guessed in Ref. [13], $-10\,\eta < U_{92}^{(2)}(\mu_b, \mu_0) < 10\,\eta$. Our determination of $U_{92}^{(2)}$ eliminates one source of uncertainty in the NNLO calculation and increases the branching ratio by about 2%, the exact amount depending on the choice of the various renormalization scales.

Another missing ingredient of the NNLO calculation is the two-loop $O(\alpha_s^2)$ $b \to s\ell^+\ell^-$ matrix element of Q_9. This is a contribution that is necessary because Q_9 has a non-vanishing matrix element at tree-level. Fortunately, no explicit calculation is necessary here as the QCD corrections to $b \to s\ell^+\ell^-$ are identical to those to $b \to u\ell\nu$ (or $t \to b\ell\nu$), in the limit of vanishing strange (bottom) quark mass. In particular, we need the QCD corrections to the invariant lepton mass spectrum. The $O(\alpha_s^2)$ corrections to this spectrum for the decay $b \to u\ell\nu$ have been computed in [27] in terms of an expansion in $(1 - \hat{s})$, which converges well also in the low-$\hat{s}$ region of interest. The results up to third and fourth order in $(1 - \hat{s})$ are shown in Fig. 4.4 at small $\hat{s}$ in the b-quark pole mass scheme with α_s normalized at m_b.

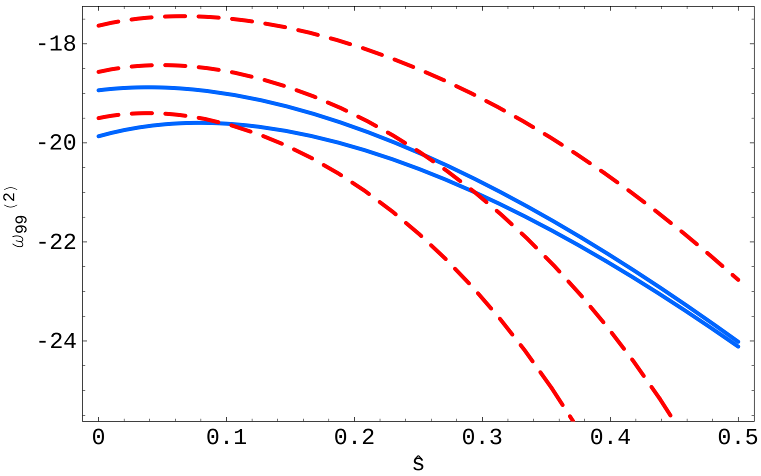

Figure 4.4: Second order perturbative corrections to the lepton invariant mass spectrum of $b \to u\ell\nu$ or $b \to s\ell^+\ell^-$ in the low-$\hat{s}$ region normalized to the tree-level spectrum and in units of $(\alpha_s/\pi)^2$. The lower (upper) solid curve corresponds to the $(1-\hat{s})$ expansion up to third (fourth) order [27], while the dashed curves correspond to the $\hat{s}$ expansion [127] (central value and linearly added errors).

The lepton mass spectrum at small $\hat{s}$ can also be obtained from the M_W^2/M_t^2 expansion of the second order QCD corrections to top decay calculated in [127]. In principle, using $M_W^2 \to m_{\ell\ell}^2$ and $M_t \to m_b$, this expansion is better suited to the low-$\hat{s}$ region. However, Ref. [127] provides only the terms up to $(M_W/M_t)^4$, obtained by Padé approximants from a q^2/M_t^2 expansion. The ensuing uncertainty is displayed in Fig. 4.4, where the errors on the various coefficients have been added linearly and the pole mass scheme is used. Although this is likely to overestimate the uncertainty in the calculation based on [127], the precision attained is sufficient for our purposes. Moreover, Fig. 4.4 shows that the two approaches [27, 127] to the calculation of the $O(\alpha_s^2)$ corrections to the lepton mass spectrum agree quite well. A simple approximation of the result is

$$
\begin{aligned}
\langle Q_9 \rangle &= \langle Q_9 \rangle^{(0)} \left[1 + \frac{\alpha_s(m_b)}{\pi} \omega_{99}^{(1)}(\hat{s}) + \left(\frac{\alpha_s(m_b)}{\pi} \right)^2 \omega_{99}^{(2)}(\hat{s}) \right] \\
\omega_{99}^{(2)}(\hat{s}) &\approx -18.57 + 6.1\,\hat{s} - (43.4 - 8.5 \ln \hat{s})\,\hat{s}^2 + 30\,\hat{s}^3,
\end{aligned} \tag{4.81}
$$

which is valid in the range $0 < \hat{s} < 0.4$, in the pole mass scheme with α_s evaluated at m_b. Using this expression in the NNLO calculation of the branching ratio of [13], we observe a reduction of about 3%, that overcompensates for the three-loop running of C_9 discussed above. In summary, the net effect of the two new contributions considered here is small.

4.3.2 Electroweak corrections

Electroweak effects in $b \to s\ell^+\ell^-$ have never been discussed in the literature. As shown in the case of radiative decays [27–31], they may be as important as the higher order QCD effects. Therefore we will study the electroweak effects in the $b \to s\ell^+\ell^-$ decay, calculating the dominant $O(\alpha)$ contributions to the running of the Wilson coefficients and estimating other potentially large effects.

For consistency with the QCD analysis, in the following we adopt the operator basis of [13], enlarged to include the electroweak penguin operators Q_3^Q–Q_6^Q. The only difference with respect to the basis used in [29,30] are g_s^2 factors in the normalization of Q_7–Q_{10}, which complicate somewhat the counting of couplings and the comparison with [29,30]. Working at first order in α and neglecting its running, we can expand the evolution matrix $\hat{U}$ of Eq. (4.79) as in (2.106). The matrices $\hat{U}^{(i)}$—pure QCD evolution—and $\hat{U}_e^{(i)}$ are functions of the ADM of the operators in question and of the QCD and mixed QED-QCD β functions. $\hat{U}_e^{(0)}$ is formally of the same order of the LO QCD evolution matrix $U^{(0)}$, while $\hat{U}_e^{(1)}$ is of order α. They can be computed using (2.101) and (2.107). Expanding also the Wilson coefficients at the weak scale and inserting (2.106) and (2.104) into (4.79) we find the expressions for the various terms at the low scale μ

$$\vec{C}(\mu) = \vec{C}_s(\mu) + \frac{\alpha}{\alpha_s(\mu)}\vec{C}_e^{(0)}(\mu) + \frac{\alpha}{4\pi}\vec{C}_e^{(1)}(\mu) + \frac{\alpha\alpha_s(\mu)}{(4\pi)^2}\vec{C}_{se}^{(1)}(\mu) + \ldots \quad . \tag{4.82}$$

$\vec{C}_s(\mu)$ results from the $O(1)$, $O(\alpha_s)$ and $O(\alpha_s^2)$ contributions to $\vec{C}(\mu_0)$ and from the QCD evolution matrices $\hat{U}^{(i)}(\mu, \mu_0)$.

The formally leading electroweak effect is the nonvanishing $O(\alpha)$ mixing described by $\hat{\gamma}_e^{(0)}$. It has been calculated in Ref. [28], except for the QED mixing of Q_9 and Q_{10} which is given by (3.27):

$$\hat{\gamma}_e^{(0)} = \begin{pmatrix} -\frac{88}{9} & -4 \\ -4 & -\frac{160}{9} \end{pmatrix}, \tag{4.83}$$

while the lowest order — $O(\alpha_s)$ in our notation — mixing between the electroweak penguin operators Q^{ew}_{7-10} and Q_9 is given by $\gamma_{i\,9}^{(0)} = (-\frac{272}{27}, -\frac{32}{81}, -\frac{2768}{27}, -\frac{512}{81})$.

Since only the mixing of Q_2 into $Q_{9,10}$ is relevant at this order, we solve the RGE and get ($C_2^{(0)}(\mu_0) = 1$)

$$C_{e,9}^{(0)}(\mu) = U_{e,9\,2}^{(0)}\, C_2^{(0)}(\mu_0) = \sum_{i=1}^{9}\left[e_i\eta^{a_i-1} + f_i\eta^{a_i}\right] \approx 0.00824 - 0.0116\eta, \tag{4.84}$$

where the approximation is valid within $\approx 2\%$ for $0.5 < \eta < 0.6$. We see that the formally leading QED contribution shifts $C_9(m_b)$ by only 0.00006 for $\eta = 0.56$. The above QED mixing between Q_9 and Q_{10} means that we also have a contribution to

$$C_{e,10}^{(0)}(\mu) = U_{e,10\,2}^{(0)}\, C_2^{(0)}(\mu_0) = \sum_{i=1}^{9}\left[g_i\eta^{a_i-1} + h_i\eta^{a_i}\right] \approx 0.02223 - 0.0325\eta, \tag{4.85}$$

which shifts $C_{10}(m_b)$ by 0.00014 for $\eta = 0.56$. The impact on the branching ratio of these $O(\alpha/\alpha_s)$ contributions is tiny.

As discussed in [29, 30, 88], next-to-leading effects of $O(\alpha\alpha_s^n L^n)$ can be larger than the leading ones. In the case of $b \to s\ell^+\ell^-$, moreover, the LO QCD contribution is accidentally small compared to the NLO QCD one. Let us therefore look at the next order, $O(\alpha\alpha_s^n L^n)$, effects. The general expression for $\vec{C}_e^{(1)}$ is (2.105)

$$\vec{C}_e^{(1)}(\mu) = \eta\, \hat{U}_e^{(0)} \vec{C}_s^{(1)}(\mu_0) + \hat{U}^{(0)} \vec{C}_e^{(1)}(\mu_0) + \hat{U}_e^{(1)} \vec{C}_s^{(0)}(\mu_0). \tag{4.86}$$

The last term in this equation requires the knowledge of the $O(\alpha\alpha_s)$ ADM, which we have given in Eq. (3.29). The expression of $C_{8,e}^{(1)}$ is given by Eqs. (4.88-90) of Ref. [128].

We also find the electroweak correction to $C_9(m_b)$ be about -0.0023 using $\eta = 0.56$ and the explicit expressions for the $\vec{C}_e^{(1)}(\mu_0)$ coefficients in our operator basis, which are given in [29, 30], while the shift in $C_{10}(m_b)$ is about -0.002.

4.3.3 Numerical Results

Similar to the study of $B \to X_s\gamma$ we will normalize the dilepton invariant mass distribution to the semileptonic decay and define

$$R^{l^+l^-}(\hat{s}) = \frac{1}{C\Gamma\left(b \to X_u e\bar{\nu}\right)} \frac{d}{d\hat{s}} \Gamma\left(b \to X_s l^+ l^-\right), \tag{4.87}$$

where the constant C

$$C = \left|\frac{V_{ub}}{V_{cb}}\right|^2 \frac{\Gamma[\bar{B} \to X_c e\bar{\nu}]}{\Gamma[\bar{B} \to X_u e\bar{\nu}]} \tag{4.88}$$

is again introduced, so that the charmless semileptonic decay can be chosen as the normalization factor. This decay rate has been calculated up to NNLO accuracy in Ref. [129]:

$$\Gamma[\bar{B} \to X_u e\bar{\nu}] = \frac{G_F^2 (m_b^{\text{pole}})^5}{192\pi^3} |V_{ub}|^2 \left[1 + \frac{\alpha_s}{\pi} p_u^{(1)} + \frac{\alpha_s^2}{\pi^2} p_u^{(2)}(z_p) + \frac{\lambda_1}{2m_b^2} - \frac{9\lambda_2}{2m_b^2}\right], \tag{4.89}$$

where the explicit expressions for $p_u^{(1/2)}$ can be found in [6, 129]. The relevant electroweak corrections are given in [130].

While in a previous analysis [45] the semileptonic decay used to normalize the dileptonic decay rate was only considered up to NLO we use the NNLO result. Furthermore we expand the whole fraction in (4.87) consistently up to NLO and NNLO order. If we vary the low energy matching scale μ_b between 2.5 GeV and 10 GeV and the high energy matching scale of the top and charm sector $\mu_0^t = 3/2\mu_0^c$ between 60 GeV and 240 GeV, and 40 GeV and 180 GeV, respectively, we find the scale dependencies shown in Fig. 4.5 for the NLO and NNLO results. Notice that the corresponding scale dependencies of the NNLO result lies within the NLO one if (4.87) is expanded consistently up to NLO and NNLO.

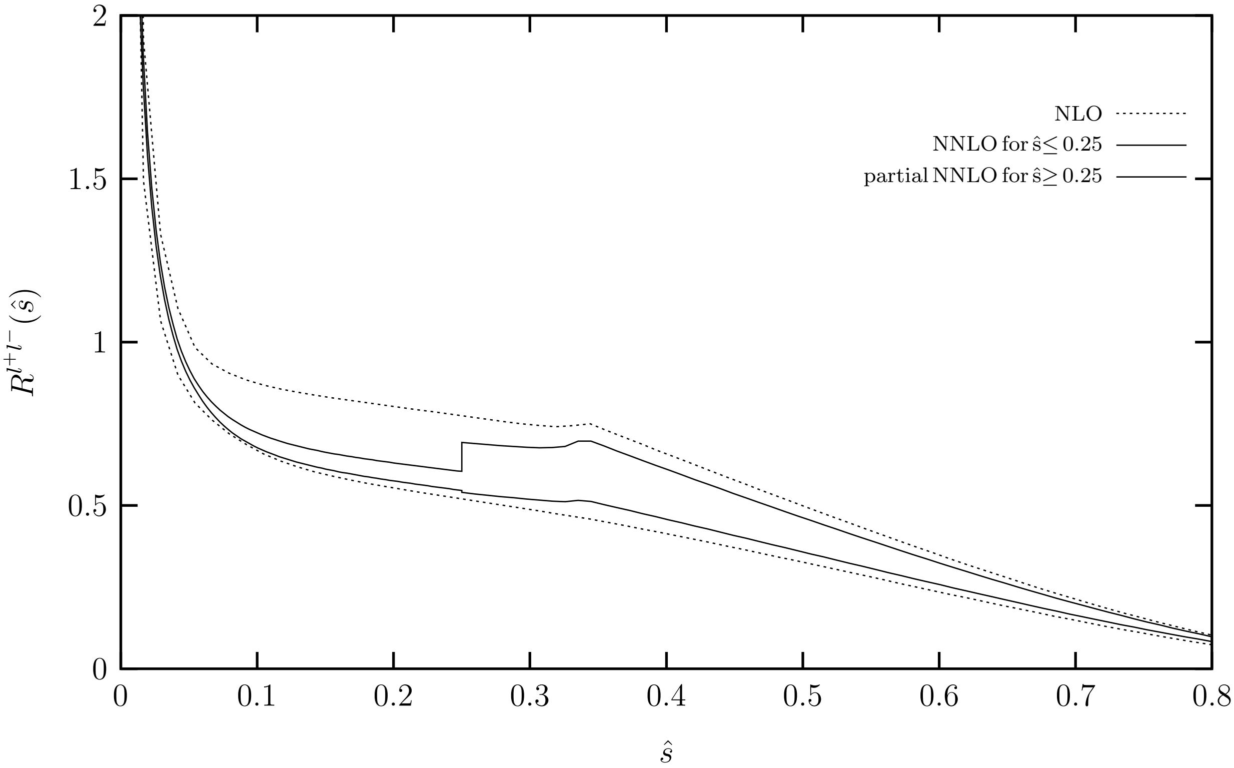

Figure 4.5: Renormalization scale dependence of $R^{l^+l^-}(\hat{s})$. The scale dependence of the NNLO result lies within the scale dependence of the NLO one

Contributions	BR $[b \to X_s l^+ l^-]$
NLO	$(1.53 \pm 0.27)10^{-6}$
partial NNLO [13]	$(1.45 \pm 0.13)10^{-6}$
partial NNLO [42–44]	$(1.413 \pm 0.044)10^{-6}$
partial NNLO [42–44] + U_{29}	$(1.435 \pm 0.037)10^{-6}$
partial NNLO [42–44] + ω_{99}	$(1.371 \pm 0.063)10^{-6}$
NNLO	$(1.401 \pm 0.048)10^{-6}$

The perturbatively calculable branching ratio is given by the integral

$$\mathrm{BR}\left[b \to X_s l^+ l^-\right] = \mathrm{BR}\left[\bar{B} \to X_c e \bar{\nu}\right] \int_{\hat{s}_l}^{\hat{s}_h} d\hat{s} R^{l^+ l^-}(\hat{s}) \tag{4.90}$$

over a given $\hat{s}$ region. For the theoretically favored low $\hat{s}$ region, where $0.05 \leq \hat{s} \leq 0.25$, we calculate the branching ratio in Table 4.3.3.

Chapter 5

Outlook and Conclusions

In this thesis we have computed NNLO QCD and NLO QED corrections to weak decays. In particular we calculated the mixing of current-current and QCD penguin operators into the operators relevant for $\Delta B = 1$ decays up to three-loop order in QCD. In addition we calculated the complete operator mixing relevant for $\Delta B = 1$ decays up to two-loop order, including QED corrections. Some of these results checked previously unconfirmed calculations, while other results are completely new.

In our calculation we used several cross-checks, following from: *i*) the locality of the UV divergences, *ii*) the independence of the ADM from the external states used in the calculation, *iii*) the completeness of our operator basis, *iv*) the gauge-parameter independence of the mixing among physical operators, and *v*) the absence of mixing of non-physical into physical operators. We have also reproduced the full $\overline{\text{MS}}$ renormalization of QCD and QED up to the three-loop level.

In particular, we agree with the previously unconfirmed

- two-loop QED mixing of Q_1–Q_6 into Q_7 and Q_8 [28],
- two-loop self-mixing of the magnetic operators Q_7 and Q_8 [25],
- three-loop mixing of Q_1–Q_6 into Q_7 and Q_8 [24].

The last two results enable us to confirm the standard model predictions [6, 7]

$$\text{BR}(B \to X_s\gamma)_{\text{th}} = (3.70 \pm 0.30) \times 10^{-4} \tag{5.1}$$

for $B \to X_s\gamma$, and put it on even stronger theoretical footing, for now all important contributions to this decay have been calculated independently by at least two groups. This is in particular important if one takes into account that the scale uncertainty is at the LO level around 25% [113].

In addition many of our results are new. In particular we have calculated for the first time the

- three-loop QCD self-mixing of Q_1–Q_6,
- three-loop QCD mixing of Q_1–Q_6 into the semileptonic operators relevant for the semileptonic $b \to s\ell^+\ell^-$ transitions, namely Q_9 and Q_{10},
- contributions relevant for a complete NNLO analysis of rare semileptonic $b \to s\ell^+\ell^-$ transitions, where we used the fact that we could extract the $O(\alpha_s^2)$ matrix element of Q_9 from the literature,
- electroweak corrections to $b \to s\ell^+\ell^-$ decay for the first time in the literature at LO and NLO,
- mixing of the semileptonic operators Q_9 and Q_{10} at order α and at order $\alpha\alpha_s$,
- two-loop QCD mixing of Q_1–Q_6 into Q_9 and Q_{10},
- two-loop QCD mixing of Q_3^Q–Q_6^Q into Q_7–Q_{10}.

We also studied formal aspects of beyond leading order calculations, and showed

- the formulas which govern the change of scheme at NNLO,
- a proof for the scheme indpendence of the matching procedure at NNLO,
- that the change of basis is nothing but a change of scheme.

The mere calculation of the three-loop QCD anomalous dimension matrix has more applications than inclusive radiative and semileptonic weak decays. We exemplified this by providing the formulas relevant to a NNLO study of non-leptonic B decays. Yet, as was the case when the two-loop mixing matrix was calculated for the first time, there will be many phenomenological applications for the standard model and some of its extensions.

Let us for example consider the short distance dominated exclusive rare decay $K^+ \to \pi^+\nu\bar{\nu}$. This facilitates a precise measurement of the unitarity triangle [131]. A NNLO analysis would reduce the theoretical error to the percent level. Such an analysis requires the three-loop self-mixing of the current-current operators, which were calculated in this work, as well as the mixing into the operator $(\bar{s}_L\gamma_\mu d_L)(\bar{\nu}_L\gamma^\mu\nu_L)$, which we will study in the future.

As mentioned already in the introduction, the main limiting factor for $B \to X_s\gamma$ lies in the perturbative QCD calculation and is related to the ambiguity in the definition of the charm quark mass in some two-loop diagrams containing the charm quark [6]. This can be improved by going to NNLO where the charm quark mass becomes well defined. Such a calculation consists of many ingredients, most notably the calculation of the three-loop matrix elements. Concerning the anomalous dimension matrix we have already computed the mixing of Q_1–Q_6, which is needed at this accuracy. In addition we plan to calculate the three-loop mixing of the magnetic operators, and in the future to compute the four-loop mixing of Q_1–Q_6 into the magnetic operators. As was shown in this thesis, this reduces to the calculation of four-loop vacuum integrals with one common mass.

Appendix A

Change to the "Standard" Operator Basis

In order to give the explicit expressions for the matrices $\hat{R}$, $\hat{W}$, $\hat{U}$ and $\hat{M}$ characterizing the change to the "standard" basis, we first have to define the primed and unprimed set of operators according to Eq. (3.37). The physical and evanescent operators in the initial basis are given by

$$\begin{aligned} \vec{Q}^T &= (Q_1, \ldots, Q_6)\,, \\ \vec{E}^T &= (E_1^{(1)}, \ldots, E_8^{(1)}, E_1^{(2)}, \ldots, E_8^{(2)})\,, \end{aligned} \tag{A.1}$$

while the "standard" basis consists of the following two sets of operators:

$$\begin{aligned} \vec{Q'}^T &= (Q'_1, \ldots, Q'_6)\,, \\ \vec{E'}^T &= (E_1'^{(1)}, \ldots, E_6'^{(1)}, E_1'^{(2)}, \ldots, E_6'^{(2)}, E_3^{(2)}, E_4^{(2)}, E_7^{(2)}, E_8^{(2)})\,. \end{aligned} \tag{A.2}$$

Needless to say, $E_3^{(2)}$, $E_4^{(2)}$, $E_7^{(2)}$ and $E_8^{(2)}$ play the role of extra, in principle unnecessary operators in the "standard" operator basis. They are just included for completeness in the above equation.

With these definitions at hand, it is just a matter of simple algebra to find the explicit expressions for the matrices $\hat{R}$, $\hat{W}$, $\hat{U}$ and $\hat{M}$. The rotation matrix $\hat{R}$, which links the physical operators, is given by

$$\hat{R} = \begin{pmatrix} 2 & \frac{1}{3} & 0 & 0 & 0 & 0 \\ 0 & 1 & 0 & 0 & 0 & 0 \\ 0 & 0 & -\frac{1}{3} & 0 & \frac{1}{12} & 0 \\ 0 & 0 & -\frac{1}{9} & -\frac{2}{3} & \frac{1}{36} & \frac{1}{6} \\ 0 & 0 & \frac{4}{3} & 0 & -\frac{1}{12} & 0 \\ 0 & 0 & \frac{4}{9} & \frac{8}{3} & -\frac{1}{36} & -\frac{1}{6} \end{pmatrix}. \tag{A.3}$$

The matrix $\hat{W}$ parametrizes a redefinition of the physical operators $\vec{Q}$ by adding some evanescent operators $\vec{E}$ to them. In the case at hand, $\hat{W}$ reads

$$\hat{W} = \begin{pmatrix} 0 & 0 & 0 & 0 & 0 & 0 & 0 & 0 & 0 & 0 & 0 & 0 & 0 & 0 & 0 & 0 \\ 0 & 0 & 0 & 0 & 0 & 0 & 0 & 0 & 0 & 0 & 0 & 0 & 0 & 0 & 0 & 0 \\ 0 & 0 & 0 & 0 & 0 & 0 & 0 & 0 & 0 & 0 & 0 & 0 & 0 & 0 & 0 & 0 \\ 0 & 0 & 0 & 0 & 0 & 0 & 0 & 0 & 0 & 0 & 0 & 0 & 0 & 0 & 0 & 0 \\ 0 & 0 & 0 & 0 & -6 & 0 & 0 & 0 & 0 & 0 & 0 & 0 & 0 & 0 & 0 & 0 \\ 0 & 0 & 0 & 0 & 0 & -6 & 0 & 0 & 0 & 0 & 0 & 0 & 0 & 0 & 0 & 0 \end{pmatrix} . \tag{A.4}$$

On the other hand, $\hat{U}$ describes a redefinition of the evanescent operators $\vec{E}$ by adding some multiples of ϵ times physical operators $\vec{Q}$ to them. The relevant matrix $\hat{U}$ takes the following form:

$$\hat{U} = \begin{pmatrix} 4 & 0 & 0 & 0 & 0 & 0 \\ 0 & 4 & 0 & 0 & 0 & 0 \\ 0 & 0 & -112 & 0 & 16 & 0 \\ 0 & 0 & 0 & -112 & 0 & 16 \\ 0 & 0 & -\frac{10}{9} & 0 & \frac{1}{9} & 0 \\ 0 & 0 & 0 & -\frac{10}{9} & 0 & \frac{1}{9} \\ 0 & 0 & -\frac{136}{9} & 0 & \frac{10}{9} & 0 \\ 0 & 0 & 0 & -\frac{136}{9} & 0 & \frac{10}{9} \\ 144 & 0 & 0 & 0 & 0 & 0 \\ 0 & 144 & 0 & 0 & 0 & 0 \\ 0 & 0 & 0 & 0 & 0 & 0 \\ 0 & 0 & 0 & 0 & 0 & 0 \\ 0 & 0 & -\frac{2224}{9} & 0 & \frac{64}{9} & 0 \\ 0 & 0 & 0 & -\frac{2224}{9} & 0 & \frac{64}{9} \\ 0 & 0 & 0 & 0 & 0 & 0 \\ 0 & 0 & 0 & 0 & 0 & 0 \end{pmatrix} . \tag{A.5}$$

Finally, the matrix $\hat{M}$ represents a simple linear transformation of the evanescent operators.

In our case we find

$$\hat{M} = \begin{pmatrix}
2 & \frac{1}{3} & 0 & 0 & 0 & 0 & 0 & 0 & 0 & 0 & 0 & 0 & 0 & 0 & 0 & 0 \\
0 & 1 & 0 & 0 & 0 & 0 & 0 & 0 & 0 & 0 & 0 & 0 & 0 & 0 & 0 & 0 \\
0 & 0 & 0 & 0 & 8 & 0 & -\frac{1}{2} & 0 & 0 & 0 & 0 & 0 & 0 & 0 & 0 & 0 \\
0 & 0 & 0 & 0 & \frac{8}{3} & 16 & -\frac{1}{6} & -1 & 0 & 0 & 0 & 0 & 0 & 0 & 0 & 0 \\
0 & 0 & 0 & 0 & -2 & 0 & \frac{1}{2} & 0 & 0 & 0 & 0 & 0 & 0 & 0 & 0 & 0 \\
0 & 0 & 0 & 0 & -\frac{2}{3} & -4 & \frac{1}{6} & 1 & 0 & 0 & 0 & 0 & 0 & 0 & 0 & 0 \\
40 & \frac{20}{3} & 0 & 0 & 0 & 0 & 0 & 0 & 2 & \frac{1}{3} & 0 & 0 & 0 & 0 & 0 & 0 \\
0 & 20 & 0 & 0 & 0 & 0 & 0 & 0 & 0 & 1 & 0 & 0 & 0 & 0 & 0 & 0 \\
0 & 0 & \frac{1}{2} & 0 & 128 & 0 & 0 & 0 & 0 & 0 & 0 & 0 & -\frac{1}{2} & 0 & 0 & 0 \\
0 & 0 & \frac{1}{6} & 1 & \frac{128}{3} & 256 & 0 & 0 & 0 & 0 & 0 & 0 & -\frac{1}{6} & -1 & 0 & 0 \\
0 & 0 & \frac{1}{2} & 0 & -8 & 0 & 0 & 0 & 0 & 0 & 0 & 0 & \frac{1}{2} & 0 & 0 & 0 \\
0 & 0 & \frac{1}{6} & 1 & -\frac{8}{3} & -16 & 0 & 0 & 0 & 0 & 0 & 0 & \frac{1}{6} & 1 & 0 & 0 \\
0 & 0 & 0 & 0 & 0 & 0 & 0 & 0 & 0 & 0 & 1 & 0 & 0 & 0 & 0 & 0 \\
0 & 0 & 0 & 0 & 0 & 0 & 0 & 0 & 0 & 0 & 0 & 1 & 0 & 0 & 0 & 0 \\
0 & 0 & 0 & 0 & 0 & 0 & 0 & 0 & 0 & 0 & 0 & 0 & 0 & 0 & 1 & 0 \\
0 & 0 & 0 & 0 & 0 & 0 & 0 & 0 & 0 & 0 & 0 & 0 & 0 & 0 & 0 & 1
\end{pmatrix} . \tag{A.6}$$

Parts of the above matrices have already been given explicitly in [24], where the change of basis from the initial to the "standard" basis has been performed including NLO QCD corrections. If we take into account that the definition of $E_5^{(1)}$–$E_8^{(1)}$ adopted in Eq. (3.43) differs slightly from the definition of $E_5^{(1)}$–$E_8^{(1)}$ used in [24], our results agree with the expressions given in the latter paper.

The renormalization constant matrices entering Eq. (3.38) are found from one- and two-loop matrix elements of physical and evanescent operators. In the following we will give only the relevant entries of the necessary renormalization constant matrices, denoting elements that do not affect the final results for the residual finite renormalizations introduced in Eq. (3.38) with a star. For the finite renormalization between evanescent operators $\vec{E}$ and physical operators $\vec{Q}$ we get

$$\hat{Z}_{EQ}^{(1,0)} = \begin{pmatrix} \star & \star & \star & \star & 0 & 0 \\ \star & \star & \star & \star & 0 & 0 \\ \star & \star & \star & \star & -\frac{1280}{3} & 320 \\ \star & \star & \star & \star & \frac{640}{9} & \frac{1280}{3} \\ 0 & 0 & \frac{160}{9} & -\frac{128}{9} & -\frac{16}{9} & \frac{4}{3} \\ 0 & 0 & -\frac{80}{27} & -\frac{476}{27}-\frac{2}{3}N_f & \frac{8}{27} & \frac{16}{9} \\ \star & \star & \star & \star & -\frac{160}{9} & \frac{40}{3} \\ \star & \star & \star & \star & \frac{80}{27} & \frac{160}{9} \\ \star & \star & \star & \star & 0 & 0 \\ \star & \star & \star & \star & 0 & 0 \\ \star & \star & \star & \star & -\frac{98560}{3} & 24640 \\ \star & \star & \star & \star & \frac{49280}{9} & \frac{98560}{3} \\ \star & \star & \star & \star & -\frac{256}{9} & \frac{64}{3} \\ \star & \star & \star & \star & \frac{128}{27} & \frac{256}{9} \\ \star & \star & \star & \star & \frac{154880}{9} & -\frac{38720}{3} \\ \star & \star & \star & \star & -\frac{77440}{27} & -\frac{154880}{9} \end{pmatrix} . \tag{A.7}$$

For the one-loop mixing of physical operators $\vec{Q}$ into evanescent operators $\vec{E}$ we obtain

$$\hat{Z}_{QE}^{(1,1)} = \begin{pmatrix} \frac{5}{12} & \frac{2}{9} & 0 & 0 & 0 & 0 & 0 & 0 & 0 & 0 & 0 & 0 & 0 & 0 & 0 & 0 \\ 1 & 0 & 0 & 0 & 0 & 0 & 0 & 0 & 0 & 0 & 0 & 0 & 0 & 0 & 0 & 0 \\ 0 & 0 & 0 & 0 & 0 & 0 & 0 & 0 & 0 & 0 & 0 & 0 & 0 & 0 & 0 & 0 \\ 0 & 0 & 0 & 0 & 0 & 0 & 0 & 0 & 0 & 0 & 0 & 0 & 0 & 0 & 0 & 0 \\ 0 & 0 & 0 & 1 & 0 & 0 & 0 & 0 & 0 & 0 & 0 & 0 & 0 & 0 & 0 & 0 \\ 0 & 0 & \frac{2}{9} & \frac{5}{12} & 0 & 0 & 0 & 0 & 0 & 0 & 0 & 0 & 0 & 0 & 0 & 0 \end{pmatrix} . \tag{A.8}$$

The one-loop mixing among evanescent operators $\vec{E}$ reads

$$
\hat{Z}_{EE}^{(1,1)} = \begin{pmatrix}
\star & \star & \star & \star & \star & \star & \star & \star & \star & \star & \star & \star & \star & \star & \star & \star \\
\star & \star & \star & \star & \star & \star & \star & \star & \star & \star & \star & \star & \star & \star & \star & \star \\
\star & \star & \star & \star & \star & \star & \star & \star & \star & \star & \star & \star & \star & \star & \star & \star \\
\star & \star & \star & \star & \star & \star & \star & \star & \star & \star & \star & \star & \star & \star & \star & \star \\
0 & 0 & 0 & \frac{1}{6} & 0 & -10 & 0 & 1 & 0 & 0 & 0 & 0 & 0 & 0 & 0 & 0 \\
0 & 0 & \frac{1}{27} & \frac{5}{72} & -\frac{20}{9} & -\frac{26}{3} & \frac{2}{9} & \frac{5}{12} & 0 & 0 & 0 & 0 & 0 & 0 & 0 & 0 \\
\star & \star & \star & \star & \star & \star & \star & \star & \star & \star & \star & \star & \star & \star & \star & \star \\
\star & \star & \star & \star & \star & \star & \star & \star & \star & \star & \star & \star & \star & \star & \star & \star \\
\star & \star & \star & \star & \star & \star & \star & \star & \star & \star & \star & \star & \star & \star & \star & \star \\
\star & \star & \star & \star & \star & \star & \star & \star & \star & \star & \star & \star & \star & \star & \star & \star \\
\star & \star & \star & \star & \star & \star & \star & \star & \star & \star & \star & \star & \star & \star & \star & \star \\
\star & \star & \star & \star & \star & \star & \star & \star & \star & \star & \star & \star & \star & \star & \star & \star \\
\star & \star & \star & \star & \star & \star & \star & \star & \star & \star & \star & \star & \star & \star & \star & \star \\
\star & \star & \star & \star & \star & \star & \star & \star & \star & \star & \star & \star & \star & \star & \star & \star \\
\star & \star & \star & \star & \star & \star & \star & \star & \star & \star & \star & \star & \star & \star & \star & \star \\
\star & \star & \star & \star & \star & \star & \star & \star & \star & \star & \star & \star & \star & \star & \star & \star
\end{pmatrix} . \tag{A.9}
$$

At the two-loop order we find for the finite renormalization between evanescent operators $\vec{E}$ and physical operators $\vec{Q}$

$$
\hat{Z}_{EQ}^{(2,0)} = \begin{pmatrix}
\star & \star & \star & \star & \star & \star \\
\star & \star & \star & \star & \star & \star \\
\star & \star & \star & \star & \star & \star \\
\star & \star & \star & \star & \star & \star \\
0 & 0 & -\frac{21632}{243}+\frac{44}{81}N_f-\frac{20}{3}aN_f & ? & \frac{266}{243}-\frac{8}{81}N_f+\frac{2}{3}aN_f & \frac{1208}{81}+\frac{2}{27}N_f \\
0 & 0 & \frac{77020}{729}-\frac{46}{243}N_f & ? & -\frac{5182}{729}+\frac{1}{243}N_f & -\frac{21019}{972}+\frac{49}{648}N_f+\frac{5}{24}aN_f \\
\star & \star & \star & \star & \star & \star \\
\star & \star & \star & \star & \star & \star \\
\star & \star & \star & \star & \star & \star \\
\star & \star & \star & \star & \star & \star \\
\star & \star & \star & \star & \star & \star \\
\star & \star & \star & \star & \star & \star \\
\star & \star & \star & \star & \star & \star \\
\star & \star & \star & \star & \star & \star \\
\star & \star & \star & \star & \star & \star \\
\star & \star & \star & \star & \star & \star
\end{pmatrix} . \tag{A.10}
$$

The two-loop mixing of physical operators $\vec{Q}$ into evanescent operators $\vec{E}$ is given by

$$\hat{Z}^{(2,1)}_{QE} = \begin{pmatrix} \frac{1531}{288}-\frac{5}{216}N_f & -\frac{1}{72}-\frac{1}{81}N_f & 0 & 0 & 0 & 0 & 0 & 0 & \frac{1}{384} & -\frac{35}{864} & \star & \star & 0 & 0 & \star & \star \\ \frac{119}{16}-\frac{1}{18}N_f & \frac{8}{9} & 0 & 0 & 0 & 0 & 0 & 0 & -\frac{35}{192} & -\frac{7}{72} & \star & \star & 0 & 0 & \star & \star \\ 0 & 0 & -\frac{7}{72} & -\frac{35}{192} & 0 & 0 & 0 & 0 & 0 & 0 & \star & \star & 0 & 0 & \star & \star \\ 0 & 0 & -\frac{35}{864} & \frac{1}{384} & 0 & 0 & 0 & 0 & 0 & 0 & \star & \star & 0 & 0 & \star & \star \\ 0 & 0 & \frac{23}{18} & \frac{51}{4}-\frac{1}{18}N_f & 0 & 0 & 0 & 0 & 0 & 0 & \star & \star & 0 & 0 & \star & \star \\ 0 & 0 & \frac{7}{6}-\frac{1}{81}N_f & \frac{317}{72}-\frac{5}{216}N_f & 0 & 0 & 0 & 0 & 0 & 0 & \star & \star & 0 & 0 & \star & \star \end{pmatrix}. \tag{A.11}$$

Finally, the two-loop mixing among evanescent operators $\vec{E}$ reads

$$\hat{Z}^{(2,1)}_{EE} = \begin{pmatrix} \star & \star & \star & \star & \star & \star & \star & \star & \star & \star & \star & \star & \star & \star & \star & \star \\ \star & \star & \star & \star & \star & \star & \star & \star & \star & \star & \star & \star & \star & \star & \star & \star \\ \star & \star & \star & \star & \star & \star & \star & \star & \star & \star & \star & \star & \star & \star & \star & \star \\ \star & \star & \star & \star & \star & \star & \star & \star & \star & \star & \star & \star & \star & \star & \star & \star \\ 0 & 0 & -\frac{145}{216} & -\frac{695}{576}+\frac{1}{108}N_f & \frac{157}{9} & \frac{1319}{12}-\frac{23}{9}N_f & -\frac{17}{6} & -\frac{133}{12}+\frac{1}{18}N_f & 0 & 0 & \frac{7}{432} & \frac{35}{1152} & \frac{7}{72} & \frac{35}{192} & \star & \star \\ 0 & 0 & -\frac{1703}{2592}+\frac{1}{486}N_f & -\frac{2035}{1152}+\frac{5}{1296}N_f & \frac{743}{54}-\frac{46}{81}N_f & \frac{2819}{36}-\frac{22}{27}N_f & -\frac{43}{54}+\frac{1}{81}N_f & -\frac{379}{72}+\frac{5}{216}N_f & 0 & 0 & \frac{35}{5184} & -\frac{1}{2304} & \frac{35}{864} & -\frac{1}{384} & \star & \star \\ \star & \star & \star & \star & \star & \star & \star & \star & \star & \star & \star & \star & \star & \star & \star & \star \\ \star & \star & \star & \star & \star & \star & \star & \star & \star & \star & \star & \star & \star & \star & \star & \star \\ \star & \star & \star & \star & \star & \star & \star & \star & \star & \star & \star & \star & \star & \star & \star & \star \\ \star & \star & \star & \star & \star & \star & \star & \star & \star & \star & \star & \star & \star & \star & \star & \star \\ \star & \star & \star & \star & \star & \star & \star & \star & \star & \star & \star & \star & \star & \star & \star & \star \\ \star & \star & \star & \star & \star & \star & \star & \star & \star & \star & \star & \star & \star & \star & \star & \star \\ \star & \star & \star & \star & \star & \star & \star & \star & \star & \star & \star & \star & \star & \star & \star & \star \\ \star & \star & \star & \star & \star & \star & \star & \star & \star & \star & \star & \star & \star & \star & \star & \star \\ \star & \star & \star & \star & \star & \star & \star & \star & \star & \star & \star & \star & \star & \star & \star & \star \\ \star & \star & \star & \star & \star & \star & \star & \star & \star & \star & \star & \star & \star & \star & \star & \star \end{pmatrix}. \tag{A.12}$$

As far as the one-loop renormalization constant matrices are concerned, let us note, that our results agree with the findings of [24], after taking into account that the definition of $E_5^{(1)}$–$E_8^{(1)}$ adopted in Eq. (3.43) differs slightly from definition of $E_5^{(1)}$–$E_8^{(1)}$ used in the latter article. On the other hand, the two-loop renormalization constant matrices involving the insertion of $E_5^{(1)}$ and $E_6^{(1)}$, are entirely new and have to our knowledge never been computed before.

Appendix B

The Complete QCD Operator Renormalization Matrix

The general structure of the operator renormalization matrix is

$$\hat{Z}^{(k,l)} = \begin{pmatrix} \hat{Z}^{(k,l)}_{PP} & \hat{Z}^{(k,l)}_{PN} & \hat{Z}^{(k,l)}_{PE} \\ \hat{Z}^{(k,l)}_{NP} & \hat{Z}^{(k,l)}_{NN} & \hat{Z}^{(k,l)}_{NE} \\ \hat{Z}^{(k,l)}_{EP} & \hat{Z}^{(k,l)}_{EN} & \hat{Z}^{(k,l)}_{EE} \end{pmatrix} , \tag{B.1}$$

where $P = 1$–10 denotes the physical operators, $N = 11$–24 the EOM-vanishing operators, and $E = 25$–32 the evanescent operators. Throughout this section we set $N_f = 5$.

The mixing of non-physical into physical operators must vanish at all orders in α_s. This is in fact only a requirement on the ADM, but we have seen in Eq. (2.70) that the one-loop renormalization matrix $\hat{Z}^{(1,1)}$ is proportional to $\hat{\gamma}^{(0)}$, and therefore at one-loop it implies the vanishing of $\hat{Z}^{(1,1)}_{NP}$ and $\hat{Z}^{(1,1)}_{EP}$. Since $\hat{\gamma}^{(0)}$ for the physical operators can be found in Eq. (3.23), it is sufficient to give here only the non-physical parts of $\hat{Z}^{(1,0)}$ and $\hat{Z}^{(1,1)}$. By definition, the only non-vanishing parts of $\hat{Z}^{(1,0)}$ are $\hat{Z}^{(1,0)}_{EP}$ and $\hat{Z}^{(1,0)}_{EN}$. We find

$$\hat{Z}^{(1,0)}_{EP} = \begin{pmatrix} 64 & \frac{32}{3} & 0 & \frac{4}{9} & 0 & 0 & 0 & 0 & \frac{64}{27} & 0 \\ 48 & -64 & 0 & -\frac{8}{3} & 0 & 0 & 0 & 0 & \frac{16}{9} & 0 \\ 0 & 0 & \frac{8960}{3} & -2432 & -\frac{1280}{3} & 320 & \frac{64}{3} & -64 & 16 & 0 \\ 0 & 0 & -\frac{4480}{9} & -\frac{9464}{3} & \frac{640}{9} & \frac{1280}{3} & \frac{256}{9} & \frac{32}{3} & -\frac{256}{3} & 0 \\ 3840 & 640 & 0 & 16 & 0 & 0 & 0 & 0 & \frac{256}{3} & 0 \\ 2880 & -3840 & 0 & -96 & 0 & 0 & 0 & 0 & 64 & 0 \\ 0 & 0 & \frac{609280}{3} & -160768 & -\frac{98560}{3} & 24640 & \frac{512}{3} & -512 & 544 & 0 \\ 0 & 0 & -\frac{304640}{9} & -\frac{630256}{3} & \frac{49280}{9} & \frac{98560}{3} & \frac{2048}{9} & \frac{256}{3} & -\frac{11264}{3} & 0 \end{pmatrix} , \tag{B.2}$$

and

$$\hat{Z}_{EN}^{(1,0)} = \begin{pmatrix} \frac{64}{27} & -\frac{4}{9} & 0 & 0 & 0 & 0 & 0 & 0 & 0 & 0 & 0 & 0 & 0 & 0 \\ \frac{16}{9} & \frac{8}{3} & 0 & 0 & 0 & 0 & 0 & 0 & 0 & 0 & 0 & 0 & 0 & 0 \\ 16 & 192 & 0 & 0 & 0 & 0 & 0 & 0 & 0 & 0 & 0 & 0 & 0 & 0 \\ -\frac{256}{3} & 168 & 0 & 0 & 0 & 0 & 0 & 0 & 0 & 0 & 0 & 0 & 0 & 0 \\ \frac{256}{3} & -16 & 0 & 0 & 0 & 0 & 0 & 0 & 0 & 0 & 0 & 0 & 0 & 0 \\ 64 & 96 & 0 & 0 & 0 & 0 & 0 & 0 & 0 & 0 & 0 & 0 & 0 & 0 \\ 544 & 8448 & 0 & 0 & 0 & 0 & 0 & 0 & 0 & 0 & 0 & 0 & 0 & 0 \\ -\frac{11264}{3} & 6992 & 0 & 0 & 0 & 0 & 0 & 0 & 0 & 0 & 0 & 0 & 0 & 0 \end{pmatrix}. \tag{B.3}$$

The 6×4 block in the upper left corner of $\hat{Z}_{EP}^{(1,0)}$ agrees with the expression for the upper 6×4 block of $\hat{c}$ given in Eq. (46) of [24].

The one-loop mixing of physical into non-physical operators is described by $\hat{Z}_{PN}^{(1,1)}$ and $\hat{Z}_{PE}^{(1,1)}$. We get

$$\hat{Z}_{PN}^{(1,1)} = \begin{pmatrix} -\frac{16}{27} & \frac{1}{9} & 0 & 0 & 0 & 0 & 0 & 0 & 0 & 0 & 0 & 0 & 0 & 0 \\ -\frac{4}{9} & -\frac{2}{3} & 0 & 0 & 0 & 0 & 0 & 0 & 0 & 0 & 0 & 0 & 0 & 0 \\ -\frac{8}{9} & -\frac{4}{3} & 0 & 0 & 0 & 0 & 0 & 0 & 0 & 0 & 0 & 0 & 0 & 0 \\ \frac{16}{27} & -\frac{28}{9} & 0 & 0 & 0 & 0 & 0 & 0 & 0 & 0 & 0 & 0 & 0 & 0 \\ -\frac{56}{9} & -\frac{64}{3} & 0 & 0 & 0 & 0 & 0 & 0 & 0 & 0 & 0 & 0 & 0 & 0 \\ \frac{256}{27} & -\frac{268}{9} & 0 & 0 & 0 & 0 & 0 & 0 & 0 & 0 & 0 & 0 & 0 & 0 \\ 0 & 0 & 0 & 0 & 0 & 0 & 0 & 0 & 0 & 0 & 0 & 0 & 0 & 0 \\ 0 & 0 & -8 & 0 & 0 & 0 & -\frac{9}{4} & 0 & 0 & 0 & 0 & 0 & 0 & 0 \\ 0 & 0 & 0 & 0 & 0 & 0 & 0 & 0 & 0 & 0 & 0 & 0 & 0 & 0 \\ 0 & 0 & 0 & 0 & 0 & 0 & 0 & 0 & 0 & 0 & 0 & 0 & 0 & 0 \end{pmatrix}, \tag{B.4}$$

and

$$\hat{Z}_{PE}^{(1,1)} = \begin{pmatrix} \frac{5}{12} & \frac{2}{9} & 0 & 0 & 0 & 0 & 0 & 0 \\ 1 & 0 & 0 & 0 & 0 & 0 & 0 & 0 \\ 0 & 0 & 0 & 0 & 0 & 0 & 0 & 0 \\ 0 & 0 & 0 & 0 & 0 & 0 & 0 & 0 \\ 0 & 0 & 0 & 1 & 0 & 0 & 0 & 0 \\ 0 & 0 & \frac{2}{9} & \frac{5}{12} & 0 & 0 & 0 & 0 \\ 0 & 0 & 0 & 0 & 0 & 0 & 0 & 0 \\ 0 & 0 & 0 & 0 & 0 & 0 & 0 & 0 \\ 0 & 0 & 0 & 0 & 0 & 0 & 0 & 0 \\ 0 & 0 & 0 & 0 & 0 & 0 & 0 & 0 \end{pmatrix}. \tag{B.5}$$

The 4×6 block in the upper left corner of $\hat{Z}_{PE}^{(1,1)}$ agrees with the expression for the 4×6 block in the upper left corner of $\hat{b}$ given in Eq. (45) of [24].

At one-loop we have moreover the mixing among EOM-vanishing operators, given by

$$\hat{Z}^{(1,1)}_{NN} = \begin{pmatrix} -\frac{23}{3} & 0 & 0 & 0 & 0 & 0 & 0 & 0 & 0 & 0 & 0 & 0 & 0 & 0 \\ 0 & -\frac{9}{2} & 0 & -\frac{4}{3} & 0 & \frac{3}{8} & -\frac{9}{8} & -\frac{9}{8} & -\frac{3}{2} & \frac{3}{16} & \frac{3}{2} & 0 & \frac{9}{4} & -\frac{9}{16} \\ 0 & 0 & -\frac{11}{3}-\frac{4}{3}\xi & 0 & 0 & 0 & 0 & 0 & 0 & 0 & 0 & 0 & 0 & 0 \\ 0 & 0 & 4 & -\frac{23}{3}-\frac{4}{3}\xi & 0 & 0 & 0 & 0 & 0 & 0 & 0 & 0 & \frac{9}{4}+\frac{3}{4}\xi & 0 \\ 0 & 0 & 0 & 0 & -\frac{23}{3} & 0 & 0 & 0 & 0 & 0 & 0 & 0 & 0 & 0 \\ 0 & 0 & -8 & 8 & -\frac{8}{9} & -\frac{17}{4} & 0 & -\frac{3}{4} & 0 & \frac{1}{8} & 0 & 0 & -\frac{9}{2} & -\frac{3}{8} \\ 0 & 0 & \frac{8}{3}\xi & 0 & 0 & 0 & -\frac{11}{3} & 0 & 0 & 0 & 0 & 0 & 0 & 0 \\ 0 & 0 & 0 & 0 & 0 & -\frac{97}{24}-\frac{3}{8}\xi & 0 & -\frac{31}{12} & \frac{13}{3} & -\frac{61}{72}-\frac{1}{8}\xi & -\frac{25}{3} & -4 & -\frac{17}{2}-\frac{17}{6}\xi & \frac{95}{48}+\frac{3}{16}\xi \\ 0 & 0 & -4-\frac{8}{3}\xi & \frac{8}{3}\xi & 0 & \frac{49}{24}+\frac{3}{8}\xi & 0 & -\frac{13}{12} & -8 & \frac{13}{72}+\frac{1}{8}\xi & \frac{1}{3} & 0 & \frac{1}{2}+\frac{1}{6}\xi & \frac{1}{48}-\frac{3}{16}\xi \\ 0 & 0 & 0 & 0 & 0 & -\frac{1}{2} & 0 & 0 & 1 & -\frac{65}{12}-\frac{3}{4}\xi & -4 & -3 & -3-\xi & 0 \\ 0 & 0 & -\frac{2}{3}\xi & -2+\frac{2}{3}\xi & \frac{2}{9} & -\frac{17}{24} & 0 & \frac{1}{12} & -\frac{7}{24} & -\frac{29}{144}+\frac{1}{8}\xi & -\frac{13}{2} & -\frac{1}{4} & -\frac{1}{4}-\frac{1}{12}\xi & \frac{29}{48}-\frac{3}{16}\xi \\ 0 & 0 & 0 & \frac{4}{3}\xi & 0 & 0 & 0 & 0 & 0 & -\frac{1}{8}\xi & 0 & -\frac{65}{12} & -\frac{3}{4}\xi & \frac{3}{16}\xi \\ 0 & 0 & 0 & 0 & 0 & 0 & 0 & 0 & 0 & 0 & 0 & 0 & -\frac{65}{12}-\frac{7}{12}\xi & 0 \\ 0 & 0 & 0 & 0 & 0 & \frac{5}{12} & 0 & -\frac{5}{12} & -\frac{5}{6} & \frac{5}{72} & \frac{10}{3} & \frac{5}{2} & \frac{5}{2}+\frac{5}{6}\xi & -\frac{45}{8}-\frac{3}{8}\xi \end{pmatrix}, \tag{B.6}$$

and the mixing among evanescent operators, which reads

$$\hat{Z}^{(1,1)}_{EE} = \begin{pmatrix} -7 & -\frac{4}{3} & 0 & 0 & \frac{5}{12} & \frac{2}{9} & 0 & 0 \\ -6 & 0 & 0 & 0 & 1 & 0 & 0 & 0 \\ 0 & 0 & -\frac{64}{3} & -14 & 0 & 0 & 0 & 1 \\ 0 & 0 & -\frac{28}{9} & \frac{13}{3} & 0 & 0 & \frac{2}{9} & \frac{5}{12} \\ 0 & 0 & 0 & 0 & \frac{13}{3} & -\frac{28}{9} & 0 & 0 \\ 0 & 0 & 0 & 0 & -14 & -\frac{64}{3} & 0 & 0 \\ 0 & 0 & \frac{1792}{3} & -784 & 0 & 0 & -64 & 38 \\ 0 & 0 & -\frac{1568}{9} & -\frac{2212}{3} & 0 & 0 & \frac{76}{9} & \frac{166}{3} \end{pmatrix}. \tag{B.7}$$

The 4×4 block in the upper left corner of $\hat{Z}^{(1,1)}_{EE}$ agrees with the expression for the 4×4 block in the upper left corner of $\hat{d}$ given in Eq. (47) of [24]. The last block $\hat{Z}^{(1,1)}_{NE}$ contains only zeros.

Now we can proceed to the two-loop renormalization matrices. The non-vanishing blocks of $\hat{Z}^{(2,0)}$ are $\hat{Z}^{(2,0)}_{EP}$ and $\hat{Z}^{(2,0)}_{EN}$, for which we give only the rows corresponding to the evanescent operators Q_{25}–Q_{28}. Our results are

$$\hat{Z}^{(2,0)}_{25-28,P} = \begin{pmatrix} \frac{3908}{9} & \frac{2656}{27} & \frac{7292}{243} & \frac{157}{243} & -\frac{722}{243} & \frac{55}{81} & \frac{1096}{243} & -\frac{761}{162} & \frac{11392}{729} & 0 \\ \frac{1760}{3} & -\frac{3584}{9} & \frac{1616}{81} & \frac{3736}{81} & -\frac{176}{81} & -\frac{110}{27} & -\frac{2192}{81} & -\frac{454}{27} & -\frac{4640}{243} & 0 \\ 0 & 0 & \frac{442528}{9} & \frac{589928}{27} & -\frac{27680}{9} & \frac{15560}{9} & \frac{9344}{9} & -\frac{18524}{3} & \frac{23456}{81} & 0 \\ 0 & 0 & -\frac{145528}{9} & \frac{860864}{81} & \frac{41276}{27} & \frac{108475}{54} & -\frac{2416}{3} & -\frac{177}{2} & -\frac{152512}{243} & 0 \end{pmatrix}, \tag{B.8}$$

and

$$\hat{Z}^{(2,0)}_{25-28,N} = \begin{pmatrix} \frac{11392}{729} & -\frac{3101}{486} & -\frac{4}{9} & -\frac{4}{27} & -\frac{376}{243} & ? & ? & ? & ? & ? & ? & ? & ? & ? \\ -\frac{4640}{243} & -\frac{949}{81} & \frac{8}{3} & \frac{8}{9} & \frac{752}{81} & ? & ? & ? & ? & ? & ? & ? & ? & ? \\ \frac{23456}{81} & -\frac{35120}{27} & \frac{3712}{3} & -\frac{64}{9} & -\frac{1088}{9} & ? & ? & ? & ? & ? & ? & ? & ? & ? \\ -\frac{152512}{243} & \frac{337192}{81} & -\frac{56}{9} & -\frac{1768}{27} & \frac{688}{9} & ? & ? & ? & ? & ? & ? & ? & ? & ? \end{pmatrix}, \tag{B.9}$$

where the question marks correspond to entries that we have not calculated. Notice that only the 4×4 block to the right of $\hat{Z}^{(2,0)}_{25-28,P}$ is needed to determine the $O(\alpha_s^3)$ mixing of Q_1–Q_6 into Q_7–Q_{10}. On the other hand the 6×4 block to the left is necessary to find the three-loop self-mixing of Q_1–Q_6 which we shall present elsewhere [47]. Finally the mixing of evanescent operators into EOM-vanishing ones, described by $\hat{Z}^{(2,0)}_{25-28,N}$, is not necessary, but given for completeness here.

Since $\hat{Z}^{(2,2)}$ is completely determined by the one-loop mixing, we give only the non-vanishing building blocks of $\hat{Z}^{(2,1)}$, namely

$$\hat{Z}^{(2,1)}_{PP} = \begin{pmatrix} \frac{317}{36} & -\frac{515}{54} & -\frac{353}{243} & -\frac{1567}{972} & \frac{67}{486} & -\frac{35}{648} & -\frac{58}{243} & \frac{167}{648} & -\frac{64}{729} & 0 \\ \frac{349}{12} & 3 & -\frac{104}{81} & \frac{338}{81} & \frac{14}{81} & \frac{35}{108} & \frac{116}{81} & \frac{19}{27} & \frac{776}{243} & 0 \\ 0 & 0 & -\frac{1117}{81} & -\frac{31469}{324} & \frac{100}{81} & \frac{3373}{432} & \frac{16}{81} & \frac{92}{27} & -\frac{1688}{243} & 0 \\ 0 & 0 & -\frac{4079}{486} & -\frac{59399}{972} & \frac{269}{1944} & \frac{12899}{2592} & -\frac{50}{243} & -\frac{1409}{648} & -\frac{548}{729} & 0 \\ 0 & 0 & -\frac{83080}{81} & -\frac{159926}{81} & \frac{8839}{81} & \frac{14573}{54} & -\frac{464}{81} & \frac{3407}{27} & -\frac{31376}{243} & 0 \\ 0 & 0 & \frac{70100}{243} & -\frac{231956}{243} & -\frac{11501}{243} & \frac{78089}{648} & -\frac{836}{243} & -\frac{1081}{81} & -\frac{21128}{729} & 0 \\ 0 & 0 & 0 & 0 & 0 & 0 & \frac{650}{27} & 0 & 0 & 0 \\ 0 & 0 & 0 & 0 & 0 & 0 & -\frac{548}{81} & \frac{1975}{108} & 0 & 0 \\ 0 & 0 & 0 & 0 & 0 & 0 & 0 & 0 & -\frac{58}{3} & 0 \\ 0 & 0 & 0 & 0 & 0 & 0 & 0 & 0 & 0 & -\frac{58}{3} \end{pmatrix}, \tag{B.10}$$

$$\hat{Z}^{(2,1)}_{PN} = \begin{pmatrix} -\frac{64}{729} & \frac{3671}{1944} & \frac{1}{9} & -\frac{1}{27} & \frac{22}{243} & -\frac{65}{2592} & -\frac{1}{96} & \frac{1}{32} & \frac{1}{72} & -\frac{1}{192} & -\frac{1}{72} & 0 & \frac{1}{48} & \frac{1}{64} \\ \frac{776}{243} & -\frac{1889}{324} & -\frac{2}{3} & \frac{2}{9} & -\frac{44}{81} & -\frac{259}{432} & \frac{1}{16} & -\frac{3}{16} & -\frac{1}{12} & \frac{1}{32} & \frac{1}{12} & 0 & -\frac{1}{8} & -\frac{3}{32} \\ -\frac{1688}{243} & \frac{1351}{162} & -\frac{16}{3} & \frac{4}{9} & \frac{20}{81} & -\frac{259}{216} & -1 & -\frac{3}{8} & -\frac{1}{6} & \frac{1}{16} & \frac{1}{6} & 0 & -\frac{1}{4} & -\frac{3}{16} \\ -\frac{548}{729} & -\frac{3559}{972} & -\frac{22}{9} & -\frac{32}{27} & -\frac{130}{243} & -\frac{625}{648} & -\frac{67}{48} & -\frac{11}{4} & -\frac{26}{9} & \frac{11}{24} & \frac{26}{9} & 0 & \frac{19}{6} & -\frac{11}{8} \\ -\frac{31376}{243} & \frac{2054}{81} & -\frac{304}{3} & \frac{32}{3} & \frac{320}{81} & -\frac{950}{27} & -\frac{35}{2} & -3 & \frac{4}{3} & \frac{1}{2} & -\frac{4}{3} & 0 & -10 & -\frac{3}{2} \\ -\frac{21128}{729} & -\frac{32669}{486} & -\frac{148}{9} & \frac{4}{9} & -\frac{1684}{243} & -\frac{12817}{648} & -\frac{35}{24} & -\frac{131}{8} & -\frac{259}{18} & \frac{131}{48} & \frac{259}{18} & 0 & \frac{125}{12} & -\frac{131}{16} \\ 0 & 0 & 0 & 0 & 0 & 0 & 0 & 0 & 0 & 0 & 0 & 0 & 0 & 0 \\ 0 & 0 & -\frac{995}{18}-\frac{7}{9}\xi & 0 & 0 & 0 & -\frac{43}{8}-\frac{27}{32}\xi & 0 & 0 & 0 & 0 & 0 & 0 & 0 \\ 0 & 0 & 0 & 0 & 0 & 0 & 0 & 0 & 0 & 0 & 0 & 0 & 0 & 0 \\ 0 & 0 & 0 & 0 & 0 & 0 & 0 & 0 & 0 & 0 & 0 & 0 & 0 & 0 \end{pmatrix}, \tag{B.11}$$

and

$$\hat{Z}^{(2,1)}_{PE} = \begin{pmatrix} \frac{4493}{864} & -\frac{49}{648} & 0 & 0 & \frac{1}{384} & -\frac{35}{864} & 0 & 0 \\ \frac{1031}{144} & \frac{8}{9} & 0 & 0 & -\frac{35}{192} & -\frac{7}{72} & 0 & 0 \\ 0 & 0 & -\frac{7}{72} & -\frac{35}{192} & 0 & 0 & 0 & 0 \\ 0 & 0 & -\frac{35}{864} & \frac{1}{384} & 0 & 0 & 0 & 0 \\ 0 & 0 & \frac{23}{18} & \frac{449}{36} & 0 & 0 & -\frac{7}{72} & -\frac{35}{192} \\ 0 & 0 & \frac{179}{162} & \frac{463}{108} & 0 & 0 & -\frac{35}{864} & \frac{1}{384} \\ 0 & 0 & 0 & 0 & 0 & 0 & 0 & 0 \\ 0 & 0 & 0 & 0 & 0 & 0 & 0 & 0 \\ 0 & 0 & 0 & 0 & 0 & 0 & 0 & 0 \\ 0 & 0 & 0 & 0 & 0 & 0 & 0 & 0 \end{pmatrix}. \tag{B.12}$$

Similarly to what happens in the case of $\hat{Z}^{(2,0)}_{PE}$ not all entries of $\hat{Z}^{(2,1)}_{PE}$ are needed to find the $O(\alpha_s^3)$ ADM of physical operators considered in this work. Needless to say, the mixing of physical into EOM-vanishing operators, described by $\hat{Z}^{(2,1)}_{PN}$, is not required to determine the mixing of physical operators at the three-loop level. However, some entries are important to verify the $O(\alpha_s^2)$ mixing of magnetic into non-physical operators, which has been discussed in part in [25].

As far as the mixing among EOM-vanishing operators is concerned, we have calculated only the first two rows of the corresponding matrix $\hat{Z}^{(2,1)}_{NN}$. We find

$$\hat{Z}^{(2,1)}_{11-12,N} = \begin{pmatrix} -\frac{58}{3} & 0 & 0 & 0 & 0 & ? & ? & ? & ? & ? & ? & ? & ? & ? \\ 0 & -\frac{149}{16} & \frac{13}{36}-\frac{7}{36}\xi & -\frac{11}{2}-\frac{7}{36}\xi & -\frac{1}{6} & ? & ? & ? & ? & ? & ? & ? & ? & ? \end{pmatrix}, \tag{B.13}$$

where the question marks stand for entries that we have not calculated.

In the case of the mixing of evanescent into other operators, we have calculated only the first four rows of the corresponding matrices $\hat{Z}^{(2,1)}_{EP}$, $\hat{Z}^{(2,1)}_{EN}$ and $\hat{Z}^{(2,1)}_{EE}$. We get

$$\hat{Z}^{(2,1)}_{25-28,P} = \begin{pmatrix} \frac{1760}{3} & -\frac{2576}{9} & -\frac{40}{81} & -\frac{814}{81} & \frac{4}{81} & \frac{5}{54} & 0 & 0 & -\frac{5824}{243} & 0 \\ 1304 & \frac{1696}{3} & \frac{80}{27} & \frac{8}{27} & -\frac{8}{27} & -\frac{5}{9} & 0 & 0 & \frac{1712}{81} & 0 \\ 0 & 0 & -56320 & -\frac{132848}{3} & 8512 & 7600 & -\frac{1088}{3} & 992 & -\frac{6992}{9} & 0 \\ 0 & 0 & \frac{109520}{9} & -\frac{127570}{3} & -\frac{16568}{9} & \frac{23255}{3} & -\frac{512}{9} & \frac{80}{3} & \frac{2432}{3} & 0 \end{pmatrix}, \tag{B.14}$$

$$\hat{Z}^{(2,1)}_{25-28,N} = \begin{pmatrix} -\frac{5824}{243} & \frac{739}{81} & 0 & \frac{8}{27} & 0 & ? & ? & ? & ? & ? & ? & ? & ? & ? \\ \frac{1712}{81} & \frac{142}{27} & 0 & -\frac{16}{9} & 0 & ? & ? & ? & ? & ? & ? & ? & ? & ? \\ -\frac{6992}{9} & \frac{2048}{3} & 256 & -128 & 0 & ? & ? & ? & ? & ? & ? & ? & ? & ? \\ \frac{2432}{3} & -\frac{1300}{3} & -\frac{128}{3} & -112 & 0 & ? & ? & ? & ? & ? & ? & ? & ? & ? \end{pmatrix}, \tag{B.15}$$

and

$$\hat{Z}^{(2,1)}_{25-28,E} = \begin{pmatrix} \frac{1615}{24} & -\frac{1021}{27} & 0 & 0 & \frac{917}{216} & \frac{142}{81} & 0 & 0 \\ \frac{599}{6} & \frac{715}{9} & 0 & 0 & \frac{277}{18} & \frac{17}{6} & 0 & 0 \\ 0 & 0 & \frac{5263}{27} & \frac{2255}{36} & 0 & 0 & -\frac{13}{9} & \frac{3041}{144} \\ 0 & 0 & -\frac{10489}{162} & \frac{57317}{108} & 0 & 0 & \frac{1961}{648} & \frac{1427}{864} \end{pmatrix}. \tag{B.16}$$

Here once again question marks denote entries that we have not computed. Clearly, the mixing of evanescent into other operators does not affect the $O(\alpha_s^3)$ mixing of physical operators at all, and thus is given here only for completeness.

At the three-loop level we have calculated only a small subset of entries of $\hat{Z}^{(3,1)}$ which are summarized below. Again $\hat{Z}^{(3,2)}$ and $\hat{Z}^{(3,3)}$ can in principle be obtained using

Eqs. (2.71). The single poles we have calculated read

$$\hat{Z}_{PP}^{(3,1)} = \begin{pmatrix} ? & ? & ? & ? & ? & ? & -\frac{15659}{6561} & -\frac{9625}{8748} & -\frac{248315}{59049}+\frac{3488}{729}\zeta_3 & 0 \\ ? & ? & ? & ? & ? & ? & \frac{13390}{2187} & \frac{5749}{5832} & -\frac{54656}{19683}-\frac{1792}{243}\zeta_3 & 0 \\ 0 & 0 & ? & ? & ? & ? & \frac{35528}{2187} & \frac{35113}{729} & -\frac{461338}{19683}+\frac{1600}{243}\zeta_3 & 0 \\ 0 & 0 & ? & ? & ? & ? & -\frac{95551}{6561} & -\frac{1356773}{34992} & -\frac{888497}{118098}-\frac{9968}{729}\zeta_3 & 0 \\ 0 & 0 & ? & ? & ? & ? & \frac{670864}{2187} & \frac{3116449}{1458} & -\frac{17938948}{19683}+\frac{15232}{243}\zeta_3 & 0 \\ 0 & 0 & ? & ? & ? & ? & -\frac{516836}{6561} & -\frac{20383751}{17496} & -\frac{27731962}{59049}-\frac{143360}{729}\zeta_3 & 0 \\ 0 & 0 & 0 & 0 & 0 & 0 & ? & 0 & 0 & 0 \\ 0 & 0 & 0 & 0 & 0 & 0 & ? & ? & 0 & 0 \\ 0 & 0 & 0 & 0 & 0 & 0 & 0 & 0 & -\frac{9769}{162} & 0 \\ 0 & 0 & 0 & 0 & 0 & 0 & 0 & 0 & 0 & -\frac{9769}{162} \end{pmatrix}, \tag{B.17}$$

and

$$\hat{Z}_{P,11-15}^{(3,1)} = \begin{pmatrix} -\frac{248315}{59049}+\frac{3488}{729}\zeta_3 & \frac{689267}{78732}-\frac{437}{243}\zeta_3 & \frac{1853}{324}+\frac{287}{1944}\xi & \frac{1955}{13122}-\frac{1}{486}\xi+\frac{80}{81}\zeta_3 & \frac{31883}{26244}+\frac{88}{243}\zeta_3 \\ -\frac{54656}{19683}-\frac{1792}{243}\zeta_3 & -\frac{2135879}{52488}+\frac{2818}{81}\zeta_3 & -\frac{521}{54}-\frac{287}{324}\xi & \frac{23722}{2187}+\frac{1}{81}\xi-\frac{160}{27}\zeta_3 & -\frac{15305}{4374}+\frac{112}{81}\zeta_3 \\ -\frac{461338}{19683}+\frac{1600}{243}\zeta_3 & \frac{5058227}{52488}+\frac{8336}{81}\zeta_3 & -\frac{247}{9}-\frac{403}{81}\xi & \frac{62024}{2187}+\frac{2}{81}\xi-\frac{320}{27}\zeta_3 & \frac{3271}{2187}-\frac{16}{81}\zeta_3 \\ -\frac{888497}{118098}-\frac{9968}{729}\zeta_3 & -\frac{4952519}{314928}+\frac{97237}{486}\zeta_3 & -\frac{8389}{162}-\frac{5899}{972}\xi & \frac{378025}{13122}+\frac{523}{486}\xi-\frac{2240}{81}\zeta_3 & -\frac{48901}{13122}+\frac{32}{243}\zeta_3 \\ -\frac{17938948}{19683}+\frac{15232}{243}\zeta_3 & \frac{50607989}{13122}+\frac{139856}{81}\zeta_3 & -\frac{61396}{81}-\frac{6410}{81}\xi & \frac{1083404}{2187}-\frac{100}{81}\xi-\frac{5120}{27}\zeta_3 & \frac{99716}{2187}-\frac{832}{81}\zeta_3 \\ -\frac{27731962}{59049}-\frac{143360}{729}\zeta_3 & \frac{38318071}{78732}+\frac{418166}{243}\zeta_3 & -\frac{34099}{243}-\frac{19915}{486}\xi & \frac{2372774}{6561}+\frac{1190}{243}\xi-\frac{21440}{81}\zeta_3 & -\frac{428893}{6561}-\frac{208}{243}\zeta_3 \\ 0 & 0 & 0 & 0 & 0 \\ 0 & 0 & ? & 0 & 0 \\ 0 & 0 & 0 & 0 & 0 \\ 0 & 0 & 0 & 0 & 0 \end{pmatrix}. \tag{B.18}$$

Bibliography

[1] R. Barate *et al.*, A Measurement of the Inclusive b → s gamma Branching Ratio, *Phys. Lett.* **B429** (1998) 169.

[2] K. Abe *et al.*, A Measurement of the Branching Fraction for the Inclusive B → X/s gamma Decays with Belle, *Phys. Lett.* **B511** (2001) 151.

[3] S. Chen *et al.*, Branching Fraction and Photon Energy Spectrum for b → s gamma, *Phys. Rev. Lett.* **87** (2001) 251807.

[4] B. Aubert *et al.*, Determination of the Branching Fraction for Inclusive Decays B → X/s gamma, (2002).

[5] C. f. c. Jessop, A World Average for B → X/s gamma, SLAC-PUB-9610.

[6] P. Gambino and M. Misiak, Quark Mass Effects in Anti-B → X/s Gamma, *Nucl. Phys.* **B611** (2001) 338.

[7] A. J. Buras, A. Czarnecki, M. Misiak, and J. Urban, Completing the NLO QCD Calculation of Anti-B → X/s Gamma, *Nucl. Phys.* **B631** (2002) 219.

[8] K. Bieri, C. Greub, and M. Steinhauser, Fermionic NNLL Corrections to b → s gamma, *Phys. Rev.* **D67** (2003) 114019.

[9] K. Adel and Y.-P. Yao, Exact Alpha-s Calculation of b → s + gamma b → s + g, *Phys. Rev.* **D49** (1994) 4945.

[10] C. Greub and T. Hurth, Two-loop Matching of the Dipole Operators for b → s gamma and b → s g, *Phys. Rev.* **D56** (1997) 2934.

[11] A. J. Buras, A. Kwiatkowski, and N. Pott, Next-to-leading Order Matching for the Magnetic Photon Penguin Operator in the B → X_s gamma Decay, *Nucl. Phys.* **B517** (1998) 353.

[12] M. Ciuchini, G. Degrassi, P. Gambino, and G. F. Giudice, Next-to-leading QCD Corrections to B → X/s gamma: Standard Model and Two-higgs Doublet Model, *Nucl. Phys.* **B527** (1998) 21.

[13] C. Bobeth, M. Misiak, and J. Urban, Photonic Penguins at Two Loops and m(t)-dependence of BR(B → X(s) l+ l-), *Nucl. Phys.* **B574** (2000) 291.

[14] A. Ali and C. Greub, Inclusive Photon Energy Spectrum in Rare B Decays, *Z. Phys.* **C49** (1991) 431.

[15] A. Ali and C. Greub, A Profile of the Final States in B → X(s) gamma and an Estimate of the Branching Ratio BR (B → K* gamma), *Phys. Lett.* **B259** (1991) 182.

[16] A. Ali and C. Greub, A Determination of the CKM Matrix Element Ratio |V(ts)| / |V(cb)| from the Rare B Decays B → K* + gamma and B → X(s) + gamma, *Z. Phys.* **C60** (1993) 433.

[17] A. Ali and C. Greub, Photon Energy Spectrum in B → X(s) + gamma and Comparison with Data, *Phys. Lett.* **B361** (1995) 146.

[18] N. Pott, Bremsstrahlung Corrections to the Decay $b \to s\gamma$, *Phys. Rev.* **D54** (1996) 938.

[19] C. Greub, T. Hurth, and D. Wyler, Virtual Corrections to the Decay $b \to s\gamma$, *Phys. Lett.* **B380** (1996) 385.

[20] C. Greub, T. Hurth, and D. Wyler, Virtual $O(\alpha_s)$ Corrections to the Inclusive Decay $b \to s\gamma$, *Phys. Rev.* **D54** (1996) 3350.

[21] A. J. Buras, A. Czarnecki, M. Misiak, and J. Urban, Two-loop Matrix Element of the Current-current Operator in the Decay b → X/s gamma, *Nucl. Phys.* **B611** (2001) 488.

[22] A. J. Buras, M. Jamin, M. E. Lautenbacher, and P. H. Weisz, Two loop Anomalous Dimension Matrix for Delta S = 1 Weak Nonleptonic Decays. 1. O(alpha-s**2), *Nucl. Phys.* **B400** (1993) 37.

[23] M. Ciuchini, E. Franco, G. Martinelli, and L. Reina, The Delta S = 1 Effective Hamiltonian Including Next-to- leading Order QCD and QED Corrections, *Nucl. Phys.* **B415** (1994) 403.

[24] K. G. Chetyrkin, M. Misiak, and M. Munz, —Delta(F)— = 1 Nonleptonic Effective Hamiltonian in a Simpler Scheme, *Nucl. Phys.* **B520** (1998) 279.

[25] M. Misiak and M. Munz, Two Loop Mixing of Dimension Five Flavor Changing Operators, *Phys. Lett.* **B344** (1995) 308.

[26] K. G. Chetyrkin, M. Misiak, and M. Munz, Weak Radiative B-meson Decay Beyond Leading Logarithms, *Phys. Lett.* **B400** (1997) 206.

[27] A. Czarnecki and W. J. Marciano, Electroweak Radiative Corrections to b → s gamma, *Phys. Rev. Lett.* **81** (1998) 277.

[28] K. Baranowski and M. Misiak, The O(alpha(em)/alpha(s)) Correction to BR(B → X/s gamma), *Phys. Lett.* **B483** (2000) 410.

[29] P. Gambino and U. Haisch, Electroweak Effects in Radiative B Decays, *JHEP* **09** (2000) 001.

[30] P. Gambino and U. Haisch, Complete Electroweak Matching for Radiative B Decays, *JHEP* **10** (2001) 020.

[31] A. L. Kagan and M. Neubert, QCD Anatomy of B → X/s gamma Decays, *Eur. Phys. J.* **C7** (1999) 5.

[32] A. F. Falk, M. E. Luke, and M. J. Savage, Nonperturbative Contributions to the Inclusive Rare Decays B → X(s) gamma and B → X(s) lepton+ lepton-, *Phys. Rev.* **D49** (1994) 3367.

[33] M. B. Voloshin, Large O(m(c)**-2) Nonperturbative Correction to the Inclusive Rate of the Decay B → X/s gamma, *Phys. Lett.* **B397** (1997) 275.

[34] A. Khodjamirian, R. Ruckl, G. Stoll, and D. Wyler, QCD Estimate of the Long-distance Effect in B → K* gamma, *Phys. Lett.* **B402** (1997) 167.

[35] Z. Ligeti, L. Randall, and M. B. Wise, Comment on Nonperturbative Effects in anti-B → X/s gamma, *Phys. Lett.* **B402** (1997) 178.

[36] A. K. Grant, A. G. Morgan, S. Nussinov, and R. D. Peccei, Comment on Nonperturbative O(1/m(c)**2) Corrections to Gamma(anti-B → X/s gamma), *Phys. Rev.* **D56** (1997) 3151.

[37] G. Buchalla, G. Isidori, and S. J. Rey, Corrections of Order Lambda(QCD)**2/m(c)**2 to Inclusive Rare B Decays, *Nucl. Phys.* **B511** (1998) 594.

[38] K. Abe *et al.*, Observation of the Decay B → K mu+ mu-, *Phys. Rev. Lett.* **88** (2002) 021801.

[39] B. Aubert *et al.*, Evidence for the Flavor Changing Neutral Current Decays B → K l+ l- and B → K* l+ l-. ((B)), (2002).

[40] J. Kaneko *et al.*, Measurement of the Electroweak Penguin Process B → X/s l+ l-. ((B)), *Phys. Rev. Lett.* **90** (2003) 021801.

[41] B. Aubert *et al.*, Measurement of the B → X(s) l+ l- Branching Fraction Using a Sum Over Exclusive Modes, (2003).

[42] H. H. Asatrian, H. M. Asatrian, C. Greub, and M. Walker, Two-loop Virtual Corrections to B $\rightarrow$ X/s l+ l- in the Standard Model, *Phys. Lett.* **B507** (2001) 162.

[43] H. H. Asatryan, H. M. Asatrian, C. Greub, and M. Walker, Calculation of Two Loop Virtual Corrections to b $\rightarrow$ s l+ l- in the Standard Model, *Phys. Rev.* **D65** (2002) 074004.

[44] H. H. Asatryan, H. M. Asatrian, C. Greub, and M. Walker, Complete Gluon Bremsstrahlung Corrections to the Process b $\rightarrow$ s l+ l-, *Phys. Rev.* **D66** (2002) 034009.

[45] A. Ghinculov, T. Hurth, G. Isidori, and Y. P. Yao, Forward-backward Asymmetry in B $\rightarrow$ X/s l+ l- at the NNLL Level, *Nucl. Phys.* **B648** (2003) 254.

[46] P. Gambino, M. Gorbahn, and U. Haisch, Anomalous Dimension Matrix for Radiative and Rare Semileptonic B Decays up to Three Loops, (2003).

[47] P. Gambino, M. Gorbahn, and U. Haisch, in preparation.

[48] T. E. Coan *et al.*, Study of Exclusive Radiative B Meson Decays, *Phys. Rev. Lett.* **84** (2000) 5283.

[49] B. Aubert *et al.*, Measurement of B $\rightarrow$ K* gamma Branching Fractions and Charge Asymmetries, *Phys. Rev. Lett.* **88** (2002) 101805.

[50] Y. Ushiroda, Radiative B Meson Decay, (2001).

[51] B. Aubert *et al.*, Search for the Exclusive Radiative Decays B $\rightarrow$ rho gamma and B0 $\rightarrow$ omega gamma, (2002).

[52] F. M. Borzumati and C. Greub, 2HDMs Predictions for anti-B $\rightarrow$ X/s gamma in NLO QCD, *Phys. Rev.* **D58** (1998) 074004.

[53] F. M. Borzumati and C. Greub, Two Higgs Doublet Model Predictions for anti-B $\rightarrow$ X/s gamma in NLO QCD. (Addendum), *Phys. Rev.* **D59** (1999) 057501.

[54] C. Bobeth, M. Misiak, and J. Urban, Matching Conditions for b $\rightarrow$ s gamma and b $\rightarrow$ s gluon in Extensions of the Standard Model, *Nucl. Phys.* **B567** (2000) 153.

[55] S. Bertolini, F. Borzumati, A. Masiero, and G. Ridolfi, Effects of Supergravity Induced Electroweak Breaking on Rare B Decays and Mixings, *Nucl. Phys.* **B353** (1991) 591.

[56] M. Ciuchini, G. Degrassi, P. Gambino, and G. F. Giudice, Next-to-leading QCD Corrections to B $\rightarrow$ X/s gamma in Supersymmetry, *Nucl. Phys.* **B534** (1998) 3.

[57] G. Degrassi, P. Gambino, and G. F. Giudice, B $\rightarrow$ X/s gamma in Supersymmetry: Large Contributions Beyond the Leading Order, *JHEP* **12** (2000) 009.

[58] M. Carena, D. Garcia, U. Nierste, and C. E. M. Wagner, b $\rightarrow$ s gamma and Supersymmetry with Large tan(beta), *Phys. Lett.* **B499** (2001) 141.

[59] P. L. Cho and M. Misiak, b $\rightarrow$ s gamma Decay in SU(2)-L x SU(2)-r x U(1) Extensions of the Standard Model, *Phys. Rev.* **D49** (1994) 5894.

[60] K. Fujikawa and A. Yamada, Test of the Chiral Structure of the top - bottom Charged Current by the Process b $\rightarrow$ s gamma, *Phys. Rev.* **D49** (1994) 5890.

[61] F. Borzumati, C. Greub, T. Hurth, and D. Wyler, Gluino Contribution to Radiative B Decays: Organization of QCD Corrections and Leading Order Results, *Phys. Rev.* **D62** (2000) 075005.

[62] S. Weinberg, The Quantum Theory of Fields. Vol. 1: Foundations, Cambridge, UK: Univ. Pr. (1995) 609 p.

[63] L. D. Faddeev and V. N. Popov, Feynman Diagrams for the Yang-Mills Field, *Phys. Lett.* **B25** (1967) 29.

[64] W. A. Bardeen, A. J. Buras, D. W. Duke, and T. Muta, Deep Inelastic Scattering Beyond the Leading Order in Asymptotically Free Gauge Theories, *Phys. Rev.* **D18** (1978) 3998.

[65] K. G. Chetyrkin, M. Misiak, and M. Munz, Beta Functions and Anomalous Dimensions up to Three Loops, *Nucl. Phys.* **B518** (1998) 473.

[66] T. Muta, Foundations of Quantum Chromodynamics. Second Edition, *World Sci. Lect. Notes Phys.* **57** (1998) 1.

[67] O. V. Tarasov and A. A. Vladimirov, Three Loop Calculations in Nonabelian Gauge Theories, JINR-E2-80-483.

[68] O. V. Tarasov, A. A. Vladimirov, and A. Y. Zharkov, The Gell-Mann-Low Function of QCD in the Three Loop Approximation, *Phys. Lett.* **B93** (1980) 429.

[69] O. V. Tarasov, Anomalous Dimensions of Quark Masses in Three Loop Approximation, JINR-P2-82-900.

[70] S. A. Larin and J. A. M. Vermaseren, The Three loop QCD Beta Function and Anomalous Dimensions, *Phys. Lett.* **B303** (1993) 334.

[71] T. Appelquist and J. Carazzone, Infrared Singularities and Massive Fields, *Phys. Rev.* **D11** (1975) 2856.

[72] E. Witten, Heavy Quark Contributions to Deep Inelastic Scattering, *Nucl. Phys.* **B104** (1976) 445.

[73] S. Weinberg, Effective Gauge Theories, *Phys. Lett.* **B91** (1980) 51.

[74] B. Grinstein, R. P. Springer, and M. B. Wise, Effective Hamiltonian for Weak Radiative B Meson Decay, *Phys. Lett.* **B202** (1988) 138.

[75] B. Grinstein, R. P. Springer, and M. B. Wise, Strong Interaction Effects in Weak Radiative anti-B Meson Decay, *Nucl. Phys.* **B339** (1990) 269.

[76] R. Grigjanis, P. J. O'Donnell, M. Sutherland, and H. Navelet, QCD Corrections to b $\to$ s Processes: An Effective Lagrangian Approach, *Phys. Rept.* **228** (1993) 93.

[77] H. Simma, Equations of Motion for Effective Lagrangians and Penguins in Rare B Decays, *Z. Phys.* **C61** (1994) 67.

[78] G. Cella, G. Curci, G. Ricciardi, and A. Vicere, QCD Corrections to Electroweak Processes in an Unconventional Scheme: Application to the b $\to$ s gamma Decay, *Nucl. Phys.* **B431** (1994) 417.

[79] J. Collins, Renoramlization, Cambridge, UK: Univ. Pr. (1985).

[80] G. Barnich, F. Brandt, and M. Henneaux, Local BRST Cohomology in Gauge Theories, *Phys. Rept.* **338** (2000) 439.

[81] A. J. Buras and P. H. Weisz, QCD Nonleading Corrections to Weak Decays in Dimensional Regularization and 't Hooft-Veltman Schemes, *Nucl. Phys.* **B333** (1990) 66.

[82] M. J. Dugan and B. Grinstein, On the Vanishing of Evanescent Operators, *Phys. Lett.* **B256** (1991) 239.

[83] S. Herrlich and U. Nierste, Evanescent Operators, Scheme Dependences and Double Insertions, *Nucl. Phys.* **B455** (1995) 39.

[84] G. Buchalla, A. J. Buras, and M. E. Lautenbacher, Weak Decays Beyond Leading Logarithms, *Rev. Mod. Phys.* **68** (1996) 1125.

[85] A. J. Buras, M. Jamin, M. E. Lautenbacher, and P. H. Weisz, Effective Hamiltonians for Delta S = 1 and Delta B = 1 Nonleptonic Decays Beyond the Leading Logarithmic Approximation, *Nucl. Phys.* **B370** (1992) 69.

[86] M. Beneke, T. Feldmann, and D. Seidel, Systematic Approach to Exclusive B $\to$ V l+ l-, V gamma Decays, *Nucl. Phys.* **B612** (2001) 25.

[87] A. J. Buras, Asymptotic Freedom in Deep Inelastic Processes in the Leading Order and Beyond, *Rev. Mod. Phys.* **52** (1980) 199.

[88] A. J. Buras, P. Gambino, and U. A. Haisch, Electroweak Penguin Contributions to Non-leptonic Delta(F) = 1 Decays at NNLO, *Nucl. Phys.* **B570** (2000) 117.

[89] M. S. Chanowitz, M. Furman, and I. Hinchliffe, The Axial Current in Dimensional Regularization, *Nucl. Phys.* **B159** (1979) 225.

[90] G. 't Hooft and M. J. G. Veltman, Regularization and Renormalization of Gauge Fields, *Nucl. Phys.* **B44** (1972) 189.

[91] P. Breitenlohner and D. Maison, Dimensional Renormalization and the Action Principle, *Commun. Math. Phys.* **52** (1977) 11.

[92] P. Breitenlohner and D. Maison, Dimensionally Renormalized Green's Functions for Theories with Massless Particles. 1, *Commun. Math. Phys.* **52** (1977) 39.

[93] P. Breitenlohner and D. Maison, Dimensionally Renormalized Green's Functions for Theories with Massless Particles. 2, *Commun. Math. Phys.* **52** (1977) 55.

[94] A. J. Buras, M. Jamin, and M. E. Lautenbacher, The Anatomy of epsilon-prime / epsilon Beyond Leading Logarithms with Improved Hadronic Matrix Elements, *Nucl. Phys.* **B408** (1993) 209.

[95] A. A. Vladimirov, Method for Computing Renormalization Group Functions in Dimensional Renormalization Scheme, *Theor. Math. Phys.* **43** (1980) 417.

[96] K. G. Chetyrkin, A. L. Kataev, and F. V. Tkachov, New Approach to Evaluation of Multiloop Feynman Integrals: The Gegenbauer Polynomial x Space Technique, *Nucl. Phys.* **B174** (1980) 345.

[97] K. G. Chetyrkin, Four and Three Loop Calculations in QCD: Theory and Applications, *Acta Phys. Polon.* **B28** (1997) 725.

[98] T. van Ritbergen, J. A. M. Vermaseren, and S. A. Larin, The Four-Loop beta Function in Quantum Chromodynamics, *Phys. Lett.* **B400** (1997) 379.

[99] J. A. M. Vermaseren, S. A. Larin, and T. van Ritbergen, The 4-loop Quark Mass Anomalous Dimension and the Invariant Quark Mass, *Phys. Lett.* **B405** (1997) 327.

[100] K. Kajantie, M. Laine, and Y. Schroder, A Simple Way to Generate High Order Vacuum Graphs, *Phys. Rev.* **D65** (2002) 045008.

[101] S. Wolfram, Mathematica.

[102] T. Hahn, Generating Feynman Diagrams and Amplitudes with FeynArts 3, *Comput. Phys. Commun.* **140** (2001) 418.

[103] J. A. M. Vermaseren, New Features of FORM, (2000).

[104] M. Steinhauser, MATAD: A Program Package for the Computation of Massive Tadpoles, *Comput. Phys. Commun.* **134** (2001) 335.

[105] F. V. Tkachov, A Theorem on Analytical Calculability of Four Loop Renormalization Group Functions, *Phys. Lett.* **B100** (1981) 65.

[106] K. G. Chetyrkin and F. V. Tkachov, Integration by Parts: The Algorithm to Calculate Beta Functions in 4 Loops, *Nucl. Phys.* **B192** (1981) 159.

[107] A. I. Davydychev and J. B. Tausk, Two Loop Selfenergy Diagrams with Different Masses and the Momentum Expansion, *Nucl. Phys.* **B397** (1993) 123.

[108] G. Buchalla, A. J. Buras, and M. K. Harlander, The Anatomy of epsilon-prime / epsilon in the Standard Model, *Nucl. Phys.* **B337** (1990) 313.

[109] M. Ciuchini, E. Franco, G. Martinelli, L. Reina, and L. Silvestrini, Scheme Independence of the Effective Hamiltonian for b → s gamma and b → s g Decays, *Phys. Lett.* **B316** (1993) 127.

[110] M. Ciuchini, E. Franco, L. Reina, and L. Silvestrini, Leading order QCD Corrections to b → s gamma and b → s g Decays in Three Regularization Schemes, *Nucl. Phys.* **B421** (1994) 41.

[111] A. J. Buras, M. E. Lautenbacher, M. Misiak, and M. Munz, Direct CP Violation in K(L) → pi0 e+ e- Beyond Leading Logarithms, *Nucl. Phys.* **B423** (1994) 349.

[112] T. Inami and C. S. Lim, Effects of Superheavy Quarks and Leptons in Low-energy Weak Processes K(L) → mu anti-mu, K+ → pi+ neutrino anti-neutrino and K0 ¡-→ anti-K0, *Prog. Theor. Phys.* **65** (1981) 297.

[113] A. J. Buras, M. Misiak, M. Munz, and S. Pokorski, Theoretical Uncertainties and Phenomenological Aspects of B → X(s) gamma Decay, *Nucl. Phys.* **B424** (1994) 374.

[114] J. Chay, H. Georgi, and B. Grinstein, Lepton Energy Distributions in Heavy Meson Decays from QCD, *Phys. Lett.* **B247** (1990) 399.

[115] A. V. Manohar and M. B. Wise, Inclusive Semileptonic B and Polarized Lambda(b) Decays from QCD, *Phys. Rev.* **D49** (1994) 1310.

[116] A. H. Hoang, Z. Ligeti, and A. V. Manohar, B Decay and the Upsilon Mass, *Phys. Rev. Lett.* **82** (1999) 277.

[117] A. H. Hoang, Z. Ligeti, and A. V. Manohar, B Decays in the Upsilon Expansion, *Phys. Rev.* **D59** (1999) 074017.

[118] C. W. Bauer and M. Trott, Reducing Theoretical Uncertainties in m(b) and lambda(1), *Phys. Rev.* **D67** (2003) 014021.

[119] I. I. Y. Bigi, B. Blok, M. A. Shifman, N. G. Uraltsev, and A. I. Vainshtein, A QCD 'Manifesto' on Inclusive Decays of Beauty and Charm, (1992).

[120] A. J. Buras and M. Misiak, Anti-B → X/s gamma After Completion of the NLO QCD Calculations, *Acta Phys. Polon.* **B33** (2002) 2597.

[121] A. Kapustin, Z. Ligeti, and H. D. Politzer, Leading Logarithms of the b Quark Mass in Inclusive B → X(s) Gamma Decay, *Phys. Lett.* **B357** (1995) 653.

[122] M. Beneke, G. Buchalla, M. Neubert, and C. T. Sachrajda, QCD Factorization for b → pi pi Decays: Strong Phases and CP Violation in the Heavy Quark Limit, *Phys. Rev. Lett.* **83** (1999) 1914.

[123] M. Beneke, G. Buchalla, M. Neubert, and C. T. Sachrajda, QCD Factorization for Exclusive, Non-leptonic B Meson Decays: General Arguments and the Case of Heavy-light Final States, *Nucl. Phys.* **B591** (2000) 313.

[124] Z. Ligeti, M. E. Luke, A. V. Manohar, and M. B. Wise, The anti-B → X/s gamma photon Spectrum, *Phys. Rev.* **D60** (1999) 034019.

[125] M. Misiak, The b → s e+ e- and b → s gamma Decays With Next- to-leading Logarithmic QCD Corrections, *Nucl. Phys.* **B393** (1993) 23.

[126] A. J. Buras and M. Munz, Effective Hamiltonian for B → X(s) e+ e- Beyond Leading Logarithms in the NDR and HV Schemes, *Phys. Rev.* **D52** (1995) 186.

[127] K. G. Chetyrkin, R. Harlander, T. Seidensticker, and M. Steinhauser, Second Order QCD Corrections to Gamma(t → W b), *Phys. Rev.* **D60** (1999) 114015.

[128] U. Haisch, The Inclusive Radiative $B \to X_s\gamma$ Decay in the Standard Model, (2002).

[129] T. van Ritbergen, The Second Order QCD Contribution to the Semileptonic b → u Decay Rate, *Phys. Lett.* **B454** (1999) 353.

[130] A. Sirlin, Large m (W), m (Z) Behavior of the O (alpha) Corrections to Semileptonic Processes Mediated by W, *Nucl. Phys.* **B196** (1982) 83.

[131] G. Buchalla and A. J. Buras, K $\rightarrow$ pi nu anti-nu and High Precision Determinations of the CKM Matrix, *Phys. Rev.* **D54** (1996) 6782.

Acknowledgements

In the first place I would like to thank my advisor, Prof. Andrzej Buras. His financial support, his helpful advice, and his straight way to approach problems in physics provided a pleasant learning experience at his chair. Especially I would like to thank Andrzej for his personal support, in particular at the time I finished this thesis.

Next I would like to thank both Dr. Paolo Gambino and Dr. Ulrich Nierste for their guidance to the field of CP violation and weak decays. I remember the many fruitful discussions we had. I also would like to thank Uli for his invitation to CERN and Fermilab and Dr. Patricia Ball for her invitation to the IPPP. I very much appreciated the kind hospitality of these groups.

I would also like to thank Ulrich Haisch. I really have enjoyed our collaboration. I am also grateful to Cyrille Barbot, Christoph Bobeth, my roommate Thorsten Ewerth, my teammate Benedikt Gaißmaier, Ulrich Haisch, and Sebastian Jäger for the stimulating discussions and the very pleasant social environment they provided. I still remember with joy the collaboration with Sebastian.

In addition I would like to thank Dr. Rouzbeh Allahverdi, Dr. Stefan Antusch, Dr. Athanasios Dedes, Jörn Kersten, Dr. Frank Krüger, Dr. Kin-ya Oda, Anton Poschenrieder, Dr. Michael Ratz, Dr. Stefan Recksiegel, Dr. Janusz Rosiek, Felix Schwab, Dr. Gerhart Seidl, Chung Lin Shan, Michael Spranger, Dr. Jörg Urban, Andreas Weiler, Elmar Wyszomirski for their lunch time conversations.

Last but not least a great thank you goes to my family. Without their support this work would not have been possible. The same is true for Anja and all of my friends.